Development of novel fluorescent and chemiluminescent protocols for quantification and functional evaluation of biomolecules

蛍光および化学発光を利用した生体分子の定量および機能性評価手法の確立

A dissertation submitted to the Graduate school of Environmental Engineering, The University of Kitakyushu, in fulfilment of the requirement for a doctoral degree

Reina Inokuchi

井口　麗和

平成 28 年 3 月

CONTENTS

CHAPTER 1

General Introduction

最近、著者の指導教官である河野智謙教授のグループが、金属含有型の人工酵素の開発に尽力している（代表的総説を参照；Kawano et al., 2015; Yokawa et al., 2011a）。上記の総説にあるように、天然の触媒性タンパク質である酵素および哺乳類から植物までの多様な生物種において確認されている低分子の機能性ペプチド群の機能と構造の相関、更には、人工的な機能性をデザインしたDNA 配列の理解へのアプローチが最近の研究の中で網羅されており、特に最新の研究事例である天然のタンパク質およびペプチド中の金属結合モチーフに発案を得た人工生体触媒（ペプチドおよび核酸）によるスーパーオキシドラジカルの生成および除去に関する技術開発が注目されている。

筆者を共著者に含む最新の総説論文（Kawano et al., 2015）において、以下にのように新規の生体触媒カテゴリーおよびコンセプトを提唱している。生体触媒の機能と化学的性質に基づく新カテゴリーおよびコンセプトについては、第2 章において詳細を述べる。中でもタンパクあるいはペプチドに遷移金属が配位することで活性中心を形成する場合は、生体触媒を無機触媒型に分類し、一方で、プロリンやグアニジンのような有機触媒が示す反応に類似した反応型を示す生体触媒を有機触媒型生体触媒ととらえる視点は重要であり、それぞれのカテゴリーを代表する事例を特異的配列のペプチドや DNA を用いた実験を通じて明示している。

筆者は、過去に卒業論文、修士論文の研究の中でヒトプリオン由来ペプチドが金属イオンと結合することで発揮するレドックス触媒活性の評価を行ってきた。本研究は、その知見にたった、生体分子への金属イオンの吸着評価法を提案するものである。以下にこれまでの研究背景を要約する。卒業研究では、プリオン・オクタリピート領域由来のペプチドを用いた、Cu 非要求性スーパーオキシド生成反応の有無、基質として添加する H_2O_2 水溶液、Tyramine 塩酸塩水溶液の、H_2O_2 水溶液添加から Tyramine 塩酸塩水溶液添加までの時間による、スーパーオキシド生成量の変化、基質濃度依存性の有無、ペプチドの繰り返し単位の長さ、開始場所による変化、ペプチドの構造による変化、SOD 様活性の

有無について研究した。これらの研究結果を用いて、プリオン・オクタリピート領域由来のペプチドを、Cu 非要求性スーパーオキシドを生成する人工酵素として、バイオセンサー等で利用することを目的とした。各実験においてのスーパーオキシド生成量の測定方法について説明した。具体的には、CLA 発光強度を指標として、スーパーオキシド生成量を測定する。CLA とは、スーパーオキシドに特異的な化学発光プローブである *Cypridina* luciferin analog（ウミホタルルシフェリン類縁体）のことであり、この CLA はスーパーオキシドと反応すると発光する性質がある。この性質を利用して、各種ペプチドや $CuSO_4$ 水溶液、H_2O_2 水溶液、Tyramine 塩酸塩水溶液を用い、反応によって生成されるスーパーオキシドの量を測定した。

本研究では、新しい生体触媒のコンセプト（第 2 章参照）に基づいた機能性生体触媒の開発に資する技術開発も視野に、触媒様の作用を示す天然のタンパク質およびペプチドを構成するアミノ酸の組成や配置、更には活性中心形成金属の配位の有無を水溶液中で反応に影響を与えない非侵襲的な手法で観察するためのプロトコル開発を中心に取り組んだ。特に蛍光法と化学発光法は、リアルタイムでの触媒性ペプチドの状態変化を感度よく観察する目的に合致しているため、本研究の主題を「蛍光および化学発光を利用した生体分子の定量および機能性評価手法の確立」とした。具体的な技術提案としては、ペプチドへの金属の結合を可視化するため、自家蛍光特性を有するテルビウム（Tb）イオンとペプチド相互作用をの蛍光消光により検出する（１）Tb 蛍光消光法および任意のペプチドに芳香族アミノ酸が含まれるものを対照とし、ペプチドが有する紫外領域での励起における自家蛍光（可視光）がペプチドと金属との相互作用により消光することを利用した（２）自家蛍光消光法の利用を提案する。Tb イオンが銅結合性ペプチドに結合し、銅結合能の評価に利用できる知見は、所属研究室での先行研究および海外での研究事例により得られた知見である（第 3 章以降で詳細を議論）。

本学位論文は、以下の構成をとる。第 1 章（本章）では、研究の概略を述べ、第 2 章では、研究のコンセプトを論じた。第 3 章から第 6 章では、4 つの異なる研究事例を報告する。最後に第 7 章において、本研究での取り組みを総括し、今後の研究展望を論じた。なお、本学位論文では、第 1 章および第 7 章を和文とし、すでに学術雑誌上において発表済あるいは、投稿済の論文に対応する第 2 章から第 6 章までの内容は、用語使用の統一性や内容の正確を期して、英文での構成とした。以下各章での議論を簡潔にのべる。また査読論文として発表済み（および投稿済み）の内容と各章との対応を表 1-1（Table 1-1）にまとめる。

Table 1-1. 個別の論文として査読付学術誌に投稿した研究内容と各章の対応。

章・タイトル	研究内容要約	発表誌・投稿誌	巻（号）：頁および審査・印刷状況（平成 28 年 2 月現在）
Capter 3 Fluorescence measurements revealed two distinct modes of metal binding by histidine-containing motifs in prion-derived peptides	プリオン蛋白のオクタリピート領域に２つの異なる金属結合モチーフが存在する（Tb 蛍光消光法・自家蛍光消光法）	Current Topics in Peptide and Protein Research	**13** : 111-118. 印刷済み
Capter 4 Fluorescent monitoring of copper-occupancy in His-ended catalytic oligo peptides	GFP 色素領域と人工酵素のキメラ分子への金属結合の評価（自家蛍光消光法）	Communicative & Integrative Biology	印刷中
Capter 5 Monitoring of copper load to cationic histidine-rich short saliva polypeptides, histatins 5 and 8, base on the quenching of copper-sensitiv intrinsic red fluorescence	ヒスタチンへの金属結合モニタリング手法の確立（Tb 蛍光消光法・自家	Bioscience, Biotechnology, and Biochemistry	投稿・ 審査済み

	蛍光消光法）		
Capter 6 Fluorometric quantification of ferulic acid concentrations based on deconvolution of intrinsic fluorescence spectra	濃度により蛍光特性が変化するフェルラ酸の蛍光法による定量の試み	Environmental Control in Biology	**54** : 57-64. 印刷済み

以下、論文構成概略。

第 1 章（CHAPTER 1）General Introduction ：本章（和文）。

第 2 章 （CHAPTER 2） Production of Superoxide Anion Radical by Artificial Metalloenzymes（英文）。触媒活性を有する金属結合型のペプチド性の生体触媒の開発に関する概念を整理した。

本研究に用いたプリオンタンパク質(PrP)とはタンパク質からなる感染性粒子のことである(Jaffray, M. et al., 2000) 。この PrP には正常型と異常型の 2 種類が存在し，異常型は正常型とは立体構造が異なる．異常型 PrP は正常型 PrP の重合体であり，モノマーである正常型が重合し異常型へと変化する過程において，正常型が自己触媒的に働き，その際に活性酸素を生成することが確認されている（Fig. 1-1）。この PrP には，触媒となる銅結合領域と基質となるチロシン残基が共存しているため，本研究を行う前に行った予備実験において，銅結合領域由来ペプチド + 過酸化水素（基質１） + チロシン残基（基質２） + 酸素（基質３）の条件で反応が起き，活性酸素が生成されることが確認されている。

第３章（CHAPTER 3） Fluorescence measurements revealed two distinct modes of metal binding by histidine-containing motifs in prion-derived peptides（英文）。プリオン由来の触媒活性を有することが明らかになっている金属結合領域に相当するペプチドへの金属（Cu、Tb）の結合を蛍光法により可視化した。ここでは、（１）Tb 蛍光消光法および（２）自家蛍光消光法の両方を適用し技術の検証をした。

プリオンタンパク（PrP）は、狂牛病やクロイツフェルトヤコブ病などの病原因子として知られるタンパク質の総称である。PrP の病原性には、正常型から異常型への変化が大きく関与し、異常型への変化の引き金として、銅イオンの結合や酸化的環境変化が重要とされる。ヒト PrP には特徴的な銅結合領域が７箇所存在しており，本研究で利用した PrP はその中でもオクタリピート領域と呼ばれる箇所のものである．このオクタリピート領域は，８個のアミノ酸からなる配列(PHGGGWGQ)が４回繰り返されている領域である．８パターンの繰り返しユニットが存在するオクタリピート領域のペプチドを用いて，活性酸素の生成活性をそれぞれ比較した結果，ヒスチジン(H, His)やプロリン(P, Pro)の位置により活性が変化することが確認された．これにより，活性酸素の生成活性を左右するのは，銅の結合活性ではないかと考察された．また，この結果は，有機素材と結合した X-X-H モチーフをもつ銅結合ペプチドは，最新の生命工学的な道具を形成可能であることを示している(Okobira, T. et al., 2011)。以上より，本研究では，（１）蛍光性金属イオンのペプチドへの結合による蛍光の消失，および（２）金属結合によるペプチド自家蛍光の消失を測定し，ヒト PrP・オクタリピート領域と金属との相互作用（結合）を可視化する方法の開発を試みた。

第４章（CHAPTER ４）Fluorescent monitoring of copper-occupancy in His-ended catalytic oligo peptides（英文）。緑色蛍光タンパク質（GFP）由来の金属結合領域に相当するペプチドへの金属（銅）の結合を蛍光法により可視化した。ここでは、自家蛍光消光法を適用し技術の検証をした。実験のアプローチは、PrP 研究に準じた。

第 5 章（CHAPTER 5）Monitoring of Copper Loading to Cationic Histidine-rich Short Salivary Polypeptides, Histatins 5 and 8, Based on the Quenching of Copper-sensitive Intrinsic Red Fluorescence（英文）。ヒト口腔内において生体防御反応に関わる微小ペプチドであるヒスタチン分子への金属（銅）の結合を蛍光法に

より可視化した。ここでは、（１）Tb 蛍光消光法および（２）自家蛍光消光法の両方を適用し技術の検証をした。

近年、100 を超える口腔内環境の維持および微生物からの防御に関わる高濃度蛋白質・ペプチド群が同定されている。中でも金属結合領域を有するオリゴペプチドであるヒスタチン（Hsts）は、金属と結合することで機能を発現すると考えられているため、銅をはじめとする金属の結合のモニタリング手法が求められている。本報告では、（１）Hst-5 および Hst-8 をモデルに、テルビウムイオン（Tb^{3+}）の蛍光の消光を指標としたペプチド上の金属結合モチーフへの Tb3+の結合の評価および（２）Hst-5 および Hst-8 が有する赤色蛍光の消光を指標とした銅イオン（Cu^{2+}）のペプチドへの結合の評価を行った。また、Hsts が示す新規の触媒活性（スーパーオキシド生成反応）が銅結合により付与されることを示した。

第 6 章（CHAPTER 6）Fluorometric quantification of ferulic acid concentrations based on deconvolution of intrinsic fluorescence spectra（英文）。植物における生体防御反応や酸化ストレス防止などに貢献することが知られ、食品として摂取した場合、人の健康増進にも有用であるフェノール由来成分であるフェルラ酸(FA)に注目し、蛍光法による同分子の定量を試みた。技術的留意点は、FA 濃度が変化するのに伴い蛍光特性が変化する点である。

FA は、細胞壁複合体における重要な化合物のひとつとして、多くの植物中で見られる単純なポリフェノールである。現在、米ぬか油などの食用油中の FA 結合脂質など FA や FA 派生物の定量分析には、分光光度計による簡便な定量や HPLC による詳細な分析が行われているが、非破壊的に野菜や青果物中の FA や FA 派生物を定量化するための手法として、固定波長の励起光照射下に認められる FA 特異的な蛍光の増加を利用した FA 関連化合物の検出に関する報告例がある（Meyer et al., 2003）。しかし、励起光の波長を固定して FA 蛍光を検出する場合、検出感度が低く、対応する濃度のレンジも限られてしまうことが明らかになった。本研究では、将来の幅広いレンジでの非破壊的 FA の検

出・定量に向けたモデル実験として、200 nm～400 nm までの紫外領域において変動させた励起波長に対する FA 特異的な蛍光帯（460 nm）におけるシグナル強度の変化を測定し、従来法よりも容易で正確な FA 定量法の開発を試みた。

第 7 章は、和文での研究の総括である。

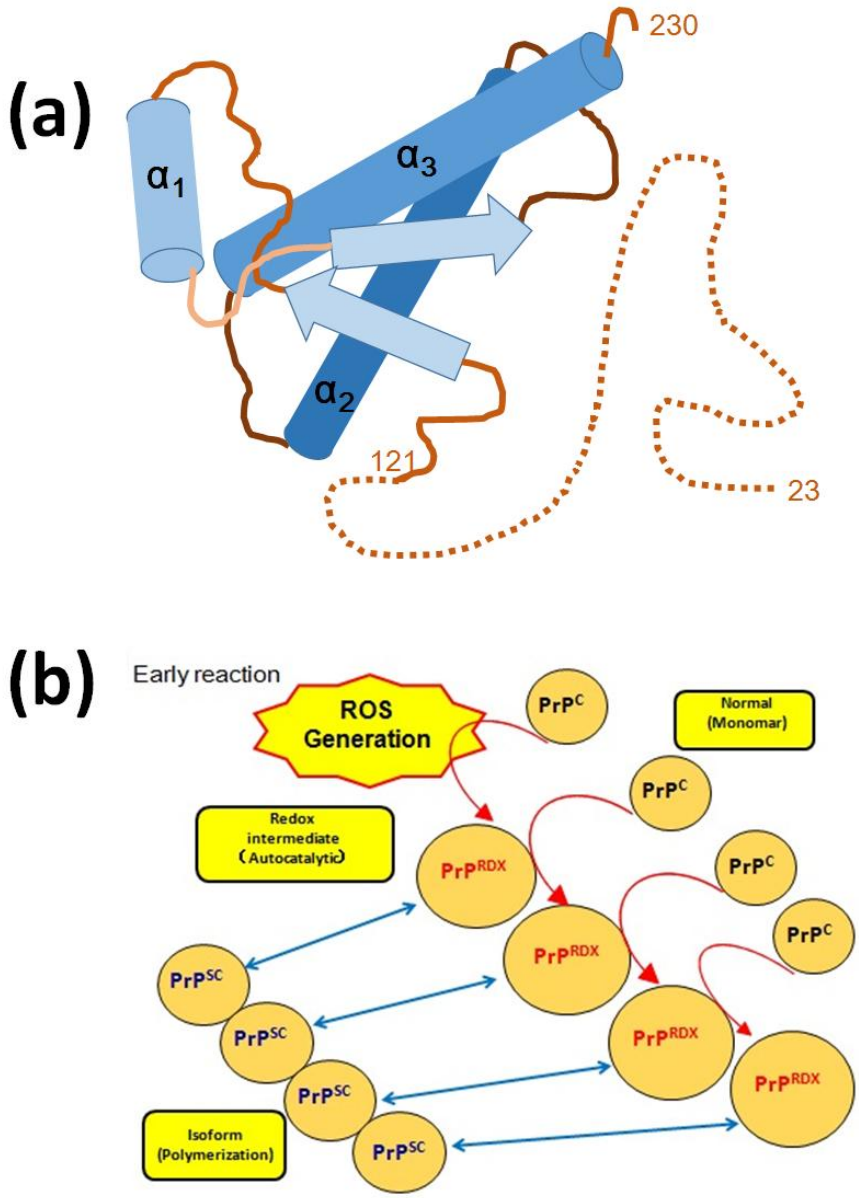

Fig. 1-1. Description of the prion protein (PrP). (a) Simplified structure of human PrP (Modified from Ralph Zahn et al., 2000). The helices are shown as cylindrical images, the β-strands are shown as arrows, the segments with nonregular secondary structure within the C-terminal domain are shown as lines, and the flexibly disordered "tail" of residues 23-121 is represented by dots. (b) Figure of changing normal PrP to isoform PrP (Modified from Furuichi, T. and Kawano, T., 2005).

CHAPTER 2

Proposed forms of biocatalysts: Production of Superoxide Anion Radical by Artificial Metalloenzymes

Recently, the group of Tomonori Kawano (who is the supervisor of the author) has summarized their effort on development of artificial metalloenzymes (Kawano et al., 2015; Yokawa et al., 2011a). In the aforementioned review articles, their recent approaches for understanding and modification of natural catalytic proteins/peptide and functional DNA sequences of mammalian and plant origins are covered, especially, focusing on the development of a novel classes of artificial redox-active biocatalysts involved in production and/or removal superoxide anion radicals ($O_2^{\bullet-}$). In their review articles, they introduced a novel concept on the category of biocatalysts as below.

Most of the cases, catalysts (*C*s) can be defined as the set of different types of elements/molecules/compounds:

$$\{C\text{s}\} = \{\{OC\text{s}\}, \{IC\text{s}\}, \{BC\text{s}\}\} \qquad (1)$$

In the above proposition, *OC*s, *IC*s, and *BC*s stand for organic catalysts, inorganic catalysts, and biocatalysts, respectively. Note that *OC*s can be represented by natured and bio-inspired organic molecules such as guanidine-type (as described by Nagasawa, 2003) or amino acid proline-type catalysts (as described by Jarvo and Miller, 2002), and *IC*s can be represented by inorganic molecules or complex such as metal-based catalysts (see Pardieck et al., 1992, etc.). In fact, the natures of *OC*s and *IC*s are clearly defined based on their chemical properties. In contrast, the category of *BC*s merely implies the origins but not the natures of these chemicals. Conventionally, it has been viewed that the set {*BC*s} can be divided into two subsets as follows (Kawano et al., 2015):

$$\{BC\text{s}\} = \{\{E\text{s}\}, \{N\text{s}\}\} \qquad (2)$$

where *E*s and *N*s are enzymes and nucleozymes, respectively.

In fact, *E*s and *N*s can be further confirmed as follows:

$$\{E\text{s}\} \in \{\{C\text{s}\} \cap \{\text{proteins} \cup \text{peptides}\}\} \qquad (3)$$

$$\{N\text{s}\} \in \{\{C\text{s}\} \cap \{\text{RNA} \cup \text{DNA}\}\} \qquad (4)$$

Moreover, the sets of {*E*s} and {*N*s} can be further divided into subsets as follows:

$$\{E\text{s}\} = \{\{E_n\text{s}\}, \{E_a\text{s}\}\} \quad (5)$$

$$\{N\text{s}\} = \{\{N_n\text{s}\}, \{N_a\text{s}\}\} \quad (6)$$

where E_ns and N_ns, are natural enzymes and nucleozymes, respectively, which can be found in or produced by living organisms; and E_as and N_as are artificial enzymes and nucleozyme, respectively, which are now newly designed or engineered in the laboratory.

Among the *E*s, many portion of both E_ns and E_as reportedly form the center of catalytic reactions within the molecules through binding of catalytically active metals directly or indirectly (by possessing prosthetic groups such as iron-centered hemes)(Rosati and Roelfes, 2010). Thus, catalytic activities of natural and artificial metal-binding enzymes can be largely attributed to the behaviors of bound metals. Therefore, it is natural to obtain the following proposition on the nature of enzymes, *P*(*E*s).

$$P(E\text{s}) = \exists \{E\text{s}\} \in \{IC\text{s}\} \quad (7)$$

This type of enzymes should be considered as metalloenzymes. According to recent reviews (Lu, et al., 2009; Rosati and Roelfes, 2010), an artificial metalloenzyme can be designed *de novo* by arranging the peptidic sequence composed of 20 natural amino acids. Basically, such *de novo* designs of metalloproteins can be achieved freely designing the amino acid sequences capable of binding metal ions (Rosati and Roelfes, 2010). In order to artificially design or modify the catalytic proteins or peptides, it is far easier to learn from the catalytically active peptidic motifs within the naturally existing active enzymes or proteins as the platforms of engineering (Kawano, 2011; Yokawa et al., 2011a).

Interestingly, Yeung *et al*. (2009) have reported that modification of myoglobin (Mb) is one of successful cases in engineering of semi-natural metalloenzyme. Accordingly, natural Mb was re-designed into an enzyme (a functional nitric oxide reductase), by newly forming a non-heme iron binding site in the distal pocket of Mb, suggesting that novel synthetic enzymes can be developped by desingning a non-heme metal binding motifs. Presence of such natural, semi-natural and artificial

metalloenzymes consists the elements of conceptual subset of bio-originated catalysts within the set of {*IC*s} fulfilling the proposition (7): $P(E\text{s}) = \exists \{E\text{s}\} \in \{IC\text{s}\}$.

Similarly to the cases of metalloenzymes, kawano's group have been seeking for the cases of metallonucleozymes, in which catalytic activities of natural and artificial metal-binding nucleic acids (DNAs and RNAs) can be attributed to the behaviors of bound metals. Then following proposition on the nature of catalytic nucleic acids, *P*(*N*s) can be obtained.

$$P(N\text{s}) = \exists \{N\text{s}\} \in \{IC\text{s}\} \qquad (8)$$

Two propositions listed above (7, 8) can be combined and generalized :

$$P(BC\text{s}) = \exists \{BC\text{s}\} \in \{IC\text{s}\} \qquad (9)$$

It could be assumed that catalytic actions of some *BC*s can be attributed to the catalytic mode of metal actions similar to *IC*s. In the chapter 3, 4 and 5, the auther enphasized the protocols to determine on detect the binding of metals such as Cu and Tb onto the petides of interest, in order to form the catalytic corpley belonging to *IC*-type *BC*s. Futhermore, some *BC*s can be categorized as part of *OC*s as proline, one of natural amino acids composing proteins, is now consider as an active catalyst (Jarvo and Miller, 2002). Thus, following proposition can be arisen.

$$P(BC\text{s}) = \exists \{BC\text{s}\} \in \{OC\text{s}\} \qquad (10)$$

This proposition implies that peptides rich in prolin may act as *OC*-types *BC*s.

The peptides we employed include prion-derived octarepeat sequence which contains Pro-residue. Role of this residue is discussed in the chapter 3.

Finding and defining the metal-binding and catalytic motifs within chicken prion proteins

There is a set of proteins which could not be defined by proposition (3)

$$\{E\text{s}\} \in \{\{C\text{s}\} \cap \{\text{proteins} \cup \text{peptides}\}\}$$

The case of prion proteins (PrPs) and derived small peptides could be one such example. Generally, PrPs and derived peptides are not considered as enzymes at present, although they are either proteins or peptides having catalytic nature (proposition 11).

$$\{PrPs\} \in \{\{\{Cs\} \cap \{\text{proteins} \cup \text{peptides}\}\} \setminus \{Es\}\} \qquad (11)$$

By admitting that there are proteins or peptides (both natural and artificial) with catalytic activity which can be considered as element of {*BC*s} in a broad sense as defined below (proposition 12), the phenomena observed with plant O_3-inducible (OI)-peptides and animal PrPs belonging to novel class of *BC*s can be compared with conventional *BC*s such as plant peroxidases (Yokawa et al., 2011b).

$$P(\text{novel } BCs) = \exists \{\text{proteins} \cup \text{peptides}\} \in \{\{BCs\} \setminus \{ Es \cup Ns \}\} \qquad (12)$$

Actually, the kingdoms of plants and animals are rich in such small peptidic metalloenzymes, belonging to *BC*s in a broad sense, catalyzing the generation of $O_2^{\bullet-}$ (Kagenishi et al., 2011).

The criteria for consisting a minimal peroxidase-like small peptides is the presence of His-rich motifs required for binding to metals (chiefly copper), and free and/or peptide-bound substrates (Yokawa et al., 2011a). Similarly, recent studies have shown that peptides derived from human PrP mediates the production of $O_2^{\bullet-}$ through oxidation of substrates such as aromatic monoamines or phenolics (mostly, neurotransmitters and their analogues) (Kawano, 2007). Upon binding to copper at four different putative copper-binding motifs (Fig.3-1b) , PrP and derived peptides may gain the catalytic activities as our earlier works have revealed that PrP-derived copper-binding peptides catalyze the generation of $O_2^{\bullet-}$ in peroxidase-like manner involving H_2O_2 as e^- acceptor and aromatic amines or phenols as the e^- donors (Kawano, 2007; Yokawa et al., 2009a).

Actions of Cu-bound PrPs are of great importance from the engineering point of view in order to design the novel peptidic metalloenzymes. Apart from engineering purpose, but viewing from the biological and medical points, the importance of metalloproteins in neurobiology has been suggested both as oxidant and antioxidant in neurodegenerative processes in animals (Opazo et al., 2003). Cu is an essential trace

element in most living organisms but its redox reactivity often leads to the risk of oxidative damage to the cells and tissues, as observed in the neurodegenerative diseases such as 'prion' disease and Alzheimer's, Menkes' and Wilson's diseases all occurring *via* disorders of Cu metabolism (Rotilio et al., 2000; Vassallo et al., 2003; Rossi et al., 2004). Especially, Alzheimer's disease and prion disease are two of known major conformational diseases, as documented to date.

Deposition of abnormal protein fibrils is a common pathological feature observed in "protein conformational" diseases, including prion dementias and Alzheimer's, Parkinson's and motor neuron diseases (Tabner et al., 2001). Generation of ROS is now considered as one of key events required for development of conformational diseases. In the cases of accumulation of α-synuclein in Parkinson's disease and accumulation of β-amyloid in Alzheimer's disease, the evidence for involvement of ROS, chiefly H_2O_2 and derived $HO^{\bullet}$, in the neurodegenerative mechanisms have been documented, suggesting that pathogenesis of such neurodegenerative diseases could be attributed to the generation and damaging impacts of ROS which eventually stimulates the formation of abnormal protein aggregates (Tabner et al., 2001; Allsop et al., 2008).

PrPs are the only known causative agents for transmissible spongiform encephalopathies in mammalian brains (Jeffray et al., 2000). A number of studies have shown that PrPs can form a group of Cu-binding proteins possibly involved in redox reactions (Aronoff-Spencer et al., 2000; Burns et al., 2003) as human PrP has four Cu-binding sites in the "octarepeats" region (PrP 60-91) in which amino acid sequence P-H-G-G-G-W-G-Q appears four times in tandem and each repeat possibly binds single Cu^{2+} at physiological neutral and basic range of pH (Bonomo et al., 2000). Similarly, in chicken PrP, the Cu-binding motif analogous to the octarepeats are known as hexa-repeats in which each repeat consist of the six amino acids, H-N-P-G-Y-P. In chicken PrP, His residues in hexa-repeat are considered to play a key role in anchoring of Cu (Stanczak et al., 2004).

Note that both His and Tyr residues can be found in the chicken PrP's hexa-repeat unit. As Tyr-containing peptides could be a target of the redox reaction catalyzed by metal-containing proteins or peptides involved in peroxidative and ROS generating

reactions, we synthesized six peptides corresponding to Cu-binding region (hexa-repeat) of chicken PrP and examined its catalytic activity for the generation of $O_2^{\bullet-}$. Each of six peptide synthesized (N-P-G-Y-P-H, P-G-Y-P-H-N, G-Y-P-H-N-P, Y-P-H-N-P-G, P-H-N-P-G-Y, and H-N-P-G-Y-P) contains both histidine residue possibly anchoring Cu ion and Tyr residue possibly behaving as a substrate were used for assessing the $O_2^{\bullet-}$ generating activity using the $O_2^{\bullet-}$-specific CL of CLA (Yokawa et al., 2010). As a results, the generation of $O_2^{\bullet-}$ was observed in the presence of hexapeptide, copper and H_2O_2 without addition of any phenolic substrate since tyrosine-residue on the hexapeptide possibly behaves as a substrate for the reaction.

To conclude that requirement of tyrosine residue on the peptides in H_2O_2-dependent generation of $O_2^{\bullet-}$, we also tested the mutation of Tyr resides into Phe residues in two model peptides (*i.e.* N-P-G-F-P-H and F-P-H-N-P-G). As expected, the Y-to-F substitution mutant peptides showed complete loss of H_2O_2-dependent generation of $O_2^{\bullet-}$. Furthermore, we confirmed that supplementation of free Tyr to the reaction mixture containing the Y-to-F mutant peptides results in production of $O_2^{\bullet-}$. It is conclusive that similarly to plant OI-peptide, both the presence and positions of His and Tyr residues in chicken PrP's hexa-repeat units are highly important for the catalytic modes leading to generation of $O_2^{\bullet-}$.

Catalytic activity in human prion-derived peptides

To date, key involvement of trace elements, chiefly of Cu, in prion disease has been well documented (Sauer et al., 1999; Wong et al., 2001; Watt et al., 2005). Until recently, two opposing roles for Cu-bound PrPs have been proposed and discussed, namely the role of bound copper as an anti-oxidant element and contrary as a pro-oxidant element enhancing the neurodegenerative process (Koga et al., 1992). In both cases, Cu-binding sequences highly preserved in PrPs play key roles in generation (Kawano, 2007) or removal of ROS (Wong et al., 2001).

A series of works conducted by our group suggested that 4 distinct peptide sequences corresponding to 7 putative copper-binding sites containing metal anchoring His residues (His61, His69, His77, His85, His96, His111, and His187) in human PrP

function as catalytic motifs active for $O_2^{\bullet-}$ generation through reactions with aromatic monoamines (Kawano, 2007). Furthermore, phenol-dependent $O_2^{\bullet-}$ generation catalyzed by several PrP-derived copper-binding peptides was recently assessed using various phenolics as substrates such as free phenolics and free Tyr (Kagenishi et al., 2011; Yokawa et al., 2008), solubilized polymers with phenolic groups (*i.e.* polyvinyl phenol which is a polymer with multiple phenolic groups, chain length, 12 - 58 mer; Yokawa et al., 2011b) and Tyr residues on peptide chains (Yokawa et al., 2009a). Since supplementation of H_2O_2 is required for oxidation of amines or phenols by these copper-centered peptides, the modes of reactions were considered to be peroxidase-like (Kawano, 2007; Yokawa et al., 2011b).

Among PrP-derived and related Cu-binding motifs ever examined, H_2O_2-dependent $O_2^{\bullet-}$-generating activity was most active in a truncated helical sequence (V-N-I-T-K-Q-H-T-V-T-T-T-T) which is highly analogous to original (wildtype) PrPs' helical sequence (Kawano, 2007; Yokawa et al., 2008).

Two distinct metal-binding motifs overlaid in the PrP octarepeat region

Our earlier studies have revealed that His residues (at least single His) are required for anchoring copper on PrP-derived peptides (Kawano, 2006, 2007), and consequently, the catalytically active copper-binding motif within PrP-derived peptides was determined to be X-X-H, where X can be any amino acids followed by His residue (Yokawa et al., 2011b; Kagenishi et al., 2009).

In human PrP, His96 is located between G-G-G-T and S-Q-W-N sequences. To examine the positional effect of His on the catalytic activity in the derived peptides, comparison of the His-started H-S-Q-W-N pentapeptide and the His-ended G-G-G-T-H pentapeptide was carried out (Kagenishi et al., 2011). While reaction with tyramine (given as model substrate) and G-G-G-T-H peptide resulted in robust production of $O_2^{\bullet-}$, the H-S-Q-W-N peptide showed no catalytic activity. By assuming that G-T-H motif within the G-G-G-T-H pentapeptide is one of X-X-H motif derivatives, experimental comparison of the catalytic activities among G-G-G-T-H pentapeptide and shorter derivatives (G-G-T-H and G-T-H) were performed and the data obtained clearly

suggested the importance of the *N*-terminal glycyl-chain elongation for manifesting the maximal redox activity in *C*-terminal His anchored peptides.

Example of artificial enzyme based on XXH motif was developed by Okobira et al. (2011), demonstrating that Cu-binding peptides with X-X-H motif conjugated to organic materials could form a novel class of biosensing and bioengineering tools. Accordingly, a tripeptide, Gly-Gly-His (G-G-H, one of X-X-H motif derivatives) was introduced onto the glycidyl methacrylate-grafted porous hollow fiber membrane made on the polyethylene platform by radiation-induced graft polymerization. After loading of Cu^{2+} on the membrane, CL assay was performed to testify the catalytic activity of the membrane, generating $O_2^{\bullet-}$ upon addition of H_2O_2 and tyramine as the paired substrates.

The author and her colleagues (Inokuchi et al., 2012) have studied the minimal motifs required for binding of metals within human PrP, by assessing (1) the peptide-dependent quenching of Tb^{3+} fluorescence and (2) the Cu^{2+}-dependent quenching of intrinsic fluorescence in human PrP octarepeat-derived peptides. Nobel assays based on the quenching of Tb-fluorescence by interacting peptides emphasized the role of His-ended peptides sharing X-X-H motif. The obtained data clearly supported the view that an intact X-X-H motif located at *C*-termini of peptides, is desirable as the site of metal chelation. In the case of human PrP's octarepeat unit, P-Q-H motif rather than *N*-terminal H-G-G-G-W motif was shown to be active in metal binding.

Empirically, *N*-terminal His-started oligo-peptides derived from human PrP have been used as models for Cu-binding in earlier *in vitro* studies. These study suggested that the actual least motif in the octarepeats necessarily required for binding of Cu consists of 5 amino acids H-G-G-G-W (Burns et al., 2002) or 4 amino acids H-G-G-G (Bonomo et al., 2000).

Interestingly, the role of His-started motif (H-G-G-G-W) was supported by the Cu-dependent peptide fluorescence quenching assay (Inokuchi et al., 2012). Among the octapeptide sequences examined, the P-H-G-G-G-W-G-Q peptide was shown to be the most sensitive to the low Cu concentration although this sequence lacks the presence of intact metal-binding X-X-H motif.

Taken together, in the mammalian PrP octarepeat regions, in which P-H-G-G-G-W-G-Q is repeated for four (human) to six (bovine) times, two distinct metal binding motifs, namely, X-X-H motif and H-G-G-G motif, could be overlaid by sharing common His residue and thus co-existed (Fig.3-6).

Role of Tyr residue within human PrP, the likely target of catalysis

Human PrP-derived catalytic model peptides all showed requirements for addition of aromatic substrates in order to produce $O_2^{\bullet-}$ in the presence of H_2O_2 (Kawano, 2007; Kagenishi et al., 2011) while the studies with the Cu-binging motifs in plant OI-peptides and chicken PrP are strongly indicating that Tyr residues presented on the peptide chains are likely target of redox relay eventually converting H_2O_2 into $O_2^{\bullet-}$ (Yokawa et al., 2010, 2011b). Since free Tyr (among the active phenolics examined) is a good substrates for human PrP-derived catalytic short peptides, we assume that the modes of catalytic actions among the plant-derived, chicken-derived and human-derived copper-binding peptides described above may not differ much.

In case of non-peptidic free Tyr given as a model substrate, the presence of phenolic moiety, but not the amino and carboxyl groups, was shown to be important in the interaction with Cu-bound PrP-derived peptide (Yokawa et al., 2009a). Therefore, it is tempting to testify if the Tyr residues flanking on peptidic chains or proteins function as putative targets of human PrP's copper-binding motifs.

In fact, human PrP possesses several Tyr-resides being exposed to the external media and events involving such Tyr residue may play a pivotal role in development of prion dementias, as recent reports suggested that helix H1 of human PrP and its two flanking loops (highly rich in Tyr residues) are subjected a transition into a β sheet-like structure during forced conformational conversion of the intrinsic cellular form of PrP (PrP^{C}) into the scrapie form of PrP (PrP^{SC}) (Bertho et al., 2008). By definition, conversion of the PrP^{C} into PrP^{SC} is a fundamental event observable upon onset of prion disease development.

Yokawa et al. (2009a) have reported an attempt to testify if the Tyr residues on PrP or derived peptides can be used as the substrate for a human PrP-derived Cu-bound catalytic peptide. In their experiments, the Cu-bound V-N-I-T-K-Q-H-T-V-T-T-T-T helical peptide was used as a model catalyst H_2O_2-dependently producing $O_2^{\bullet-}$. On the other hand, the tested putative substrates include (1) tyrosyl-tyrosyl-arginine tripeptide (Y-Y-R) which appears twice in the PrP's Tyr-rich region (DYEDR-YYR-ENMHRYPNQV-YYR-PMDEY) and (2) longer peptide sequences corresponding to the Tyr-rich region in human PrP (D-Y-E-D-R-Y-Y-R-E-N-M-H-R).

Compared to free Tyr, Y-Y-R tripeptide was shown to be much more active in production of $O_2^{\bullet-}$, confirming that both free form and peptide-integrated forms of Tyr can be recognized by the Cu-loaded catalytic peptide (Yokawa et al., 2009a). Although the reactivity of longer peptide sequences corresponding to the Tyr-rich region in human PrP (D-Y-E-D-R-Y-Y-R-E-N-M-H-R) was obviously lower than free Tyr, comparison with the Y-to-F substitution mutant (D-F-E-D-R-F-F-R-E-N-M-H-R) confirmed that Tyr-rich long peptides are favored for production of $O_2^{\bullet-}$. These data suggest that the Tyr residues presenting on the intra- and inter-PrP molecules could be the target of the Cu-bound PrP-catalyzed reaction.

Synthesis of novel metalloenzymes with peptides and their substrate preferences

Among human PrP-related Cu-binding model peptides, the octarepeat unit (P-H-G-G-G-W-G-Q) was shown to be active in aromatic monoamine (AMA)-dependent $O_2^{\bullet-}$ generation using phenylethylamine as model substrate (Kawano, 2007), by mimicking the plant AMA-utilizing enzymes sensitive to monoamine oxidase inhibitors (Kawano et al., 2000a). On the other hand, a helical motif V-N-I-T-K-Q-H-T-V-T-T-T-T undecapeptide and G-G-G-T-H pentapeptide, both derived from human PrP, showed negligible AMA-dependent activity while performing much greater phenol-dependent $O_2^{\bullet-}$ generating activities (Kawano, 2007; Yokawa et al., 2009a; Kagenishi et al., 2011). Based on above knowledge, substrate specificity of novel metalloenzymes can be properly designed. Based on the results with PrP-derived peptides, our group has designed a series of novel peroxidative biocatalysts as discussed below.

By analogy to G-G-G-T-H, a phenol-oxidizing catalytic pentapeptide derived from human PrP, we have designed a series of simplified model peptides (G_nH series peptides) which are composed of oligoglycyl chains ended with *C*-terminal His. To test the importance of the elongated *N*-terminal glycyl chain and anchoring His residue, both G_nH series peptides varied in *N*-terminal glycyl chain length (n = 2, 3, 4, 5 and 10) and oligoglycyl peptides lacking His (G_n series) were synthesized.

As expected, G_n series showed no catalytic activity since these sequence lack the motif for binding to catalytically important Cu^{2+}. Within the G_nH series, catalytic activity of the minimal Cu-binging motif (G_2H tripeptide) was hardly detected despite the report by Okobira et al. (2011). Probably, in the Okobira model, in addition to G-G-H sequence, supporting chains of glycidyl methacrylate on which G-G-H is grafted may playing a role similarly to *N*-terminal elongating oligo-Gly chain. In G_nH series, G_3H tetrapeptide showed a detectable increase in production of $O_2^{\bullet-}$, confirming the importance of *N*-terminal Gly elongation. It can be generalized that the catalytic performance in G_nH series can be *ca*. 3-fold enhanced by single amino acid elongation (addition of *N*-terminal Gly residue, allowing elongation from G_2H to G_3H, G_3H to G_4H, and G_4H to G_5H). However, further elongation from G_5H hexapeptide to $G_{10}H$ undecapeptide resulted in only *ca*. 3-fold of enhancement suggesting that the requirement for the *N*-terminal elongation is nearly fulfilled. These data suggest that the presence of the *C*-terminal His is the primary requirement for catalytic performance, and *N*-terminal elongation contributes to the enhancement of the catalytic activity.

Although involvement of Cu and generation of ROS are analogous to tyrosinase which oxidizes Tyr and polyphenols with concomitant release of $O_2^{\bullet-}$ (Opazo et al., 2003), the roles played by H_2O_2 are largely different in the G_nH series metalloenzymes. While H_2O_2 is often regarded as an inhibitor of the tyrosinase reaction (Wood et al., 1991), the G_nH series metalloenzymes require the presence of H_2O_2 as co-substrate. On the other hand, plant peroxidases are shown to be active in generation of $O_2^{\bullet-}$ upon oxidation of various phenolics and monoamines in the presence of H_2O_2 (Kawano, 2003a; Kawano and Muto, 2000), suggesting that the modes of reactions catalyzed by PrP-derived peptides and artificial G_nH series metalloenzymes are analogous to the modes of peroxidase reactions.

Among hydroxybenzoic acids (HBAs) and benzoic acid (BA), 2-HBA (salicylic acid) and BA were shown to be poor substrates for $O_2^{\bullet-}$-generating reactions catalyzed by G-G-G-T-H pentapeptide and G_nH series metalloenzymes (Kagenishi et al., 2011). In contrast, 3-HBA and 4-HBA were shown to be good substrates, suggesting that the presence of phenolic moieties with *m*- or *p*-positioned OH group is required for generation of $O_2^{\bullet-}$, notably differed from the plant peroxidase which favors 2-HBA (Kawano et al., 1998). When dihydroxybenzoic acids (DHBAs) were used as model substrates, inutility of *o*-positioned OH group was also observed using 2,6-DHBA. However, PrP-derived peptides (G-G-G-T-H and V-N-I-T-K-Q-H-T-V-T-T-T-T), plant OI-peptides, and G_nH series metalloenzymes showed $O_2^{\bullet-}$ generating activity upon addition of other DHBAs with *o*-positioned OH (2,3-DHBA, 2,4-DHBA, and 2,5-DHBA), indicating that the presence of *o*-positioned OH does not interfere with the roles for active OH groups at *m*- and *p*-positions (Yokawa et al., 2009a; Yokawa et al., 2011b; Kagenishi et al., 2011).

Organic catalyst-like biocatalysts

Propositions (1) to (6), (12) are merely definitive. Predictions by propositions (7) to (9), of the cases of biocatalysts acting upon binding to catalytically active metals, such as copper-centered metallo-enzymes, peptides and nucleic acids, were examined and proven through discussion up to here, thus confirming the generalized proposition (9).

Contrary, our knowledge on the cases fulfilling the proposition (10) is yet to be covered.

$$P(BC\text{s}) = \exists \{BC\text{s}\} \in \{OC\text{s}\} \qquad (10)$$

As this proposition predict that there could be biocatalysts showing catalytic activity due to the action of guanidine-like or amino acid Pro-like catalytic domains without involvement of the action of metals. In addition, the model presented in a series of classical works by Kunitake and his colleagues on imidazole-containing enzyme-like

catalytic polymers could be also considered (Kunitake et al., 1969; Shinkai and Kunitake, 1975).

Interestingly, Pro-containing octarepeat-peptides from human PrP shows self-catalytic generation of $O_2^{\bullet-}$, showing spiky CLA-CL upon mixture with media lacking metals. Since this phenomenon can be silenced by replacing Pro with other groups (Inokuchi et al., unpublished results), this topic may provide more clues to the development of OC-type BCs in the near future.

Here, the author (Inokuchi) wishes to contribute to the course of developing a novel type of biocatalysts in which catalytic activities are conferred or modulated by the metal-binding motifs and proline-rich motifs in the natural protein-derived short peptides selected. Therefore, the present study could be the basis for further studies on the action of biochatalysts predicted by two propositions

$$P(Es) = \exists \{Es\} \in \{ICs\} \qquad (7)$$

$$P(BCs) = \exists \{BCs\} \in \{OCs\} \qquad (10)$$

In the most works presented here, the author handled oligo-peptides sharing both or either proline-residue(s) and/or metal-binding motifs such as XXH motifs using fluorometric and chminometric approaches.

CHAPTER 3

Fluorescence measurements revealed two distinct modes of metal binding by histidine-containing motifs in prion-derived peptides

3-1 Abstract

PrPs are infectious agents causing transmissible spongiform encephalopathies in a misfolded protease-resistant form of protein. Human PrP possesses 7 potential copper-binding sites. Notably, four of putative copper-binding sites are located in the octarepeat region (PrP 60-91). Recent studies have shown that peptides derived from human PrP effectively bind Cu^{2+} to form the Cu-centered catalytic complex required for generation of superoxide by coupling the oxidation of neurotransmitters and their analogues. In this study, we have studied the minimal motifs required for binding of metals within human PrP, by assessing (1) the peptide-dependent quenching of Tb^{3+} fluorescence and (2) the Cu^{2+}-dependent quenching of intrinsic fluorescence in human PrP octarepeat-derived peptides. Assays with peptide-dependent quenching of Tb fluorescence supported the positive role for the His-ended X-X-H motif (in this case P-Q-H tripeptide sequence) rather than His-started H-G-G-G-W motif, as metal chelating motifs in short peptides. Controversially, the role of His-started motif was supported by the Cu-dependent peptide fluorescence quenching assay. Above data suggested that there are two distinct modes of metal binding to His residues in the octarepeat regions in PrP, possibly by co-ordinations of His-started and His-ended motifs around the target metals depending on the conditions given.

Keywords*:* Cu-binding, fluorescence, octarepeat, peptide, Prion

3-2 Introduction

PrPs are infectious agents causing transmissible spongiform encephalopathies (TSE) in a misfolded protease-resistant form known as PrP^{res} (Jeffray et al., 2000). In general, the protease-sensitive form known as PrP^{sen} represents the intrinsic cellular PrP (PrP^{C}) and PrP^{res} represents the infectious scrapie isoform of PrP (PrP^{Sc}).

Studies have shown that PrPs form a group of copper-binding proteins(Aronoff-Spencer et al., 2000; Burn et al., 2002). For an instance, human PrP has 7 potential copper-binding sites (Fig. 3-1). In the so-called "octarepeat" region (PrP 60-91) in human PrP, in which amino acid sequence "P-H-G-G-G-W-G-Q" repeatedly appears in tandem, each repeat unit possibly binds single Cu^{2+} at physiological neutral and basic range of pH (Bonomo *et al.*,2000; Shiraishi et al., 2000; Opazo et al., 2003). Similarly, bovine PrP sequence contains six octarepeats thus possessing at least six putative copper-binding sites with high affinity (Burn et al., 2002; Morante et al., 2004). In chicken, the copper-binding sites analogous to the octarepeats are known as hexa-repeats with each repeat consisting of H-N-P-G-Y-P sequence and here again His residues play a key role in anchoring of copper (Stanczak et al., 2004).

Morante et al. (Morante et al., 2004) showed that partial occupancy of copper on bovine PrP is manifested by binding of copper to PrP in the intermolecular or inter-octarepeat orientations while total occupancy of copper is manifested by intra-repeat binding of copper to the octarepeat region. *In vitro* studies have shown that the actual least motif in the octarepeats necessarily required for binding of copper consists of 4 amino acids H-G-G-G (Bonomo *et al.*,2000) or 5 amino acids H-G-G-G-W (Burn et al., 2002).

There are additional Cu-binding sites on PrP such as amino acid regions 92-96 (G-G-G-T-H) (Burn et al., 2002), 124-126 (K-H-M) (Belosi et al., 2004) and 180-193 (V-N-I-T-K-Q-H-T-V-T-T-T-T) (Brown et al., 2004). Importantly, all studies suggested that His residue in each region (or each repeat unit) plays a key role in anchoring the copper (Fig. 3-1b).

Many metalloproteins behave both as oxidants and as antioxidants in biological systems (Rotilio et al., 2000; Vassallo and Herms, 2003; Rossi et al., 2004; Yokawa et al., 2011a; Yokawa et al., 2011b). PrP-derived Cu-binding small peptides were shown to be active in both the enhancement of oxidative reactions targeting the cells and the protection of

biological components from the oxidative stress, both due to the metal-binding nature of the peptides, depending on the conditions given (Kawano, 2006; Kawano, 2007; Kawano, 2011; Kagenishi et al., 2009; Kagenishi et al., 2011; Yokawa et al., 2009; Yokawa et al., 2009; Yokawa et al., 2011d) . Therefore, the interaction between Cu^{2+} and PrP (binding of Cu^{2+}) should be carefully monitored for further studying the modes of actions of PrP behaving as a metalloprotein.

Accordingly (Jeffray et al., 2000; Safar et al., 2005) , several diagnostic approaches for detection of human prion disease based on the conformation-dependent immunoassay (CDI assay) were developed. These approaches aim to determine both the proteinase K-sensitive and resistant forms of PrP without the use of proteolytic digestion while all conventional immunoassays for PrP^{Sc} rely on the limited proteolysis to eliminate PrP^{C}. Such CDI technique with enhanced sensitivity is based on the detection of PrP bound on microtitre plates using lanthanide-conjugated monoclonal antibodies(Safar et al., 2005; Bellon et al., 2003). The dissociation-enhanced lanthanide fluoro-immunoassay designated as DELFIA, utilizes the intrinsic fluorescence of specific lanthanides such as europium (Eu), samarium (Sm) and terbium (Tb). In DELFIA, the fluorescent signals for lanthanides are designed to be enhanced in the presence of the fluorescence-enhancing chelates.

In some cases, the fluorescence of lanthanides could be largely altered without such chelates when reacting with metal-binding proteins or peptides. Thus, apart from DELFIA, fluorescent nature of lanthanides, chiefly of Tb^{3+}, has been used for assessing the mode of metal binding to proteins and peptides since such ions of lanthanides mimic the behavior of copper, zinc, manganese and magnesium, and binds to proteins (Blandl et al., 1997).

In this study, we have studied the minimal motifs required for binding of metals (chiefly copper) to the human PrP by assessing (1) the peptide-dependent quenching of Tb^{3+} fluorescence and (2) the copper-dependent quenching of intrinsic fluorescence in human PrP octarepeat-derived peptides.

3-3 Materials and Methods

3-3-1 *Peptides and Chemicals*

Peptides corresponding to Cu-binding sequence in PrP protein were synthesized to examine the behavior of such Cu-binding domains. The peptides were obtained from the custom peptide service department of Sigma Genosys Japan, Ishikari, Hokkaido, Japan. The amino acid sequences of the peptides chemically synthesized were purified on high pressure liquid chromatography prior to the experimental use.

Other chemicals including terbium (III) chloride hexahydrate, used in this study were of reagent grade purchased from Wako Pure Chemical Industries Ltd. (Osaka, Japan).

3-3-2 *Fluorometric analysis*

Terbium (Tb)-dependent florescence and intrinsic fluorescence from the peptides and from amino acids were detected in phosphate buffered saline using a fluorescence spectrophotometer (F-4500 Hitachi High-Technol. Co., Tokyo) as described (Kawano, 2006). The three-dimensional (3D) spectral measurement of fluorescence was carried out at the excitation wavelength between 200 and 600 nm with 5 nm intervals and emission wavelength between 200 and 600 nm with 5 nm intervals.

In the phosphate-buffered medium, the actual concentrations of free Tb^{3+} after addition of mM orders of $TbCl_3$ were expected to be as low as μM order due to interaction between phosphate and Tb ion. The observed Tb-fluorescence is likely due to free Tb^{3+}, and thus quenching of Tb-fluorescence can be achieved by μM ranges of peptides or chelaters as previously described (Kawano, 2006). Here, quenching of Tb-fluorescence by PrP-derived peptides was performed with 1 mM $TbCl_3$ dissolved in 50 mM potassium phosphate buffer (pH. 7.0) supplemented with and without peptides of interest (up to 30 μM). Intrinsic fluorescence in PrP-derived peptides and free amino acids up to 30 μM dissolved in 50 mM potassium phosphate buffer (pH. 7.0) were also assessed with a fluorescence spectrophotometer in the presence and absence of $CuSO_4$.

3-4 Results and Discussion

3-4-1 *Quenching of Tb-fluorescence by octarepeat peptides*

As previously reported (Kawano, 2006), free Tb^{3+} showed the peaks of fluorescence with excitation wavelength at 224 nm and emission wavelengths at 545 nm and 585 nm (Fig. 3-2a). The Tb-dependent fluorescence was drastically lowered in the presence of peptides of octarepeat series confirming the metal binding nature of the peptides used (Fig. 3-2b-d).

Due to fluorescent nature and similarity to behavior of Cu ion, Tb ion has been used as a model for studying the kinetic analysis of metallo-complex formation by short Cu-binding peptides such as a 17 amino acid-sized conatntokin-G (Blandl et al., 1997). In the present study, the peptide ending with His residue (GGGWGQPH) showed highest activity for quenching of the Tb-fluorescence among eight different octapeptides tested (Fig. 3-2e).

3-4-2 *Peptides showed intrinsic fluorescence in the absence of Tb*

In the absence of fluorescent REE ions such as Tb^{3+}, the PrP-derived peptides tested here showed intrinsic fluorescence (Fig. 3-3a). The fluorescent nature of octapeptide could be attributed to the presence of Trp residue. Among amino acids constituting the octarepeat, only tryptophan showed major (excitation at 280 nm, emission at 365 nm) and minor (excitation at 230 nm, emission at 365 nm) peaks of intrinsic fluorescence (Fig. 3-3b-g). Comparison of fluorescence between the Trp-containing peptides and free Trp suggested that fluorescence by Trp is largely lower by conjugation with other amino acids.

As expected, the PrP octarepeat-derived short peptides lacking Trp residue showed no fluorescence, further confirming the role of Trp residue for fluorescence (Fig. 3-4). Again, data suggested that Trp-residue is required for the fluorescent nature of the octarepeat peptides and that conjugation of longer chains to tryptophan lowers the intrinsic fluorescence.

3-4-3 *Quenching of peptide fluorescence by copper*

As the characteristics of fluorescence which is intrinsic to the human PrP-derived octarepeat peptides were spectroscopically determined above, the impact of Cu-binding to the peptide on the yield of fluorescence was tested (Fig. 3-5). The intrinsic fluorescence in the octarepeat sequence-derived peptides and free tryptophan was shown to be quenched in the presence of excess of $CuSO_4$. The presence of Cu^{2+} in the range of molar ratios (Cu^{2+}/peptide) between *ca*. 0.2 and 1.0 showed linear decrease in fluorescence from the most peptides tested, suggesting that the mode of interaction between the PrP-derived peptide and metal ions can be optically monitored.

Kinetic analysis revealed that fluorescence from the PrP octarepeat-derived octapeptides showed higher sensitivity to the presence of low concentration of Cu ion (Fig. 3-5). Among the octapeptide sequences tested, PHGGGWGQ peptide was shown to be most sensitive to the low Cu concentration although this sequence lack the presence of metal-binding motif X-X-H. In turn, the role or significance of another motif, namely, H-G-G-G-W was suggested. It must be noted that our discussion does not cover the behavior of shorter Cu binding motif H-G-G-G reported by Bonomo *et al.* (Bonomo *et al.*,2000). Since fluorometric analysis is based on the Trp-dependent fluorescence, Cu-mediated in the tetrapeptide HGGG could not be assessed by our approach.

3-4-4 *Two distinct metal-binding motifs overlaid in the PrP octarepeat region*

According to earlier studies, at least single His residue is required for binding of copper on PrP-derived peptides (Kawano, 2006; Kawano, 2007), and the catalytically active copper-binding motif within PrP-derived peptides was determined to be X-X-H (where X can be any amino acids followed by His) (Yokawa et al., 2011a; Kagenishi et al., 2009). Furthermore, our demonstrations have shown that the PrP-derived and related short peptides ended with X-X-H motif, effectively bind Cu in the biological media and thus prevent the damaging impacts of Cu ions against DNA degradation (Yokawa et al., 2011d) and living plant cells (Kagenishi et al., 2009). Okobira et al. (Okobira et al., 2011) has demonstrated that Cu-binding peptides with the X-X-H motif conjugated to organic materials could form a novel class of bioengineering tools. Accordingly, a

tripeptide, glycyl-glycyl-histidine (G-G-H, one of X-X-H motif derivatives) as Cu-binding domain, was introduced onto the glycidyl methacrylate-grafted porous hollow fiber membrane made on the polyethylene platform by radiation-induced graft polymerization.

On the other hand, *N*-terminal His-started oligo-peptides were also used as model for Cu-binding in earlier *in vitro* studies describing that the actual least motif in the octarepeats necessarily required for binding of Cu consists of 5 amino acids H-G-G-G-W (Burn et al., 2002) or 4 amino acids H-G-G-G (Bonomo *et al.*,2000). Therefore, in the mammalian PrP octarepeat regions, in which PHGGGWGQ is repeated for four (human) to six (bovine) times, both metal binding motifs could be overlaid by sharing common His residue and thus co-existed.

Our fluorescent assay with Tb-fluorescence quenching supported the positive role of His-ended peptides. The obtained data clearly supported the view that the peptides sharing an intact X-X-H motif (in this case PQH motif) located at *C*-termini rather than N-terminal H-G-G-G-W motif, is desirable as metal chelating peptides.

Controversially, the role of His-started motif (H-G-G-G-W) was supported by the Cu-dependent peptide fluorescence quenching assay. Among the octapeptide sequences examined, the PHGGGWGQ peptide was shown to be the most sensitive to the low Cu concentration although this sequence lacks the presence of intact metal-binding X-X-H motif.

The present study suggested that there are two distinct modes of metal binding to His residues in the octarepeat regions in mammalian PrP, possibly by co-ordinations of His-ended motif (Fig. 3-6a) or His-started motif (Fig. 3-6b) around the target metals depending on the conditions given. The proposed two-motif model must be further testified by future experiments.

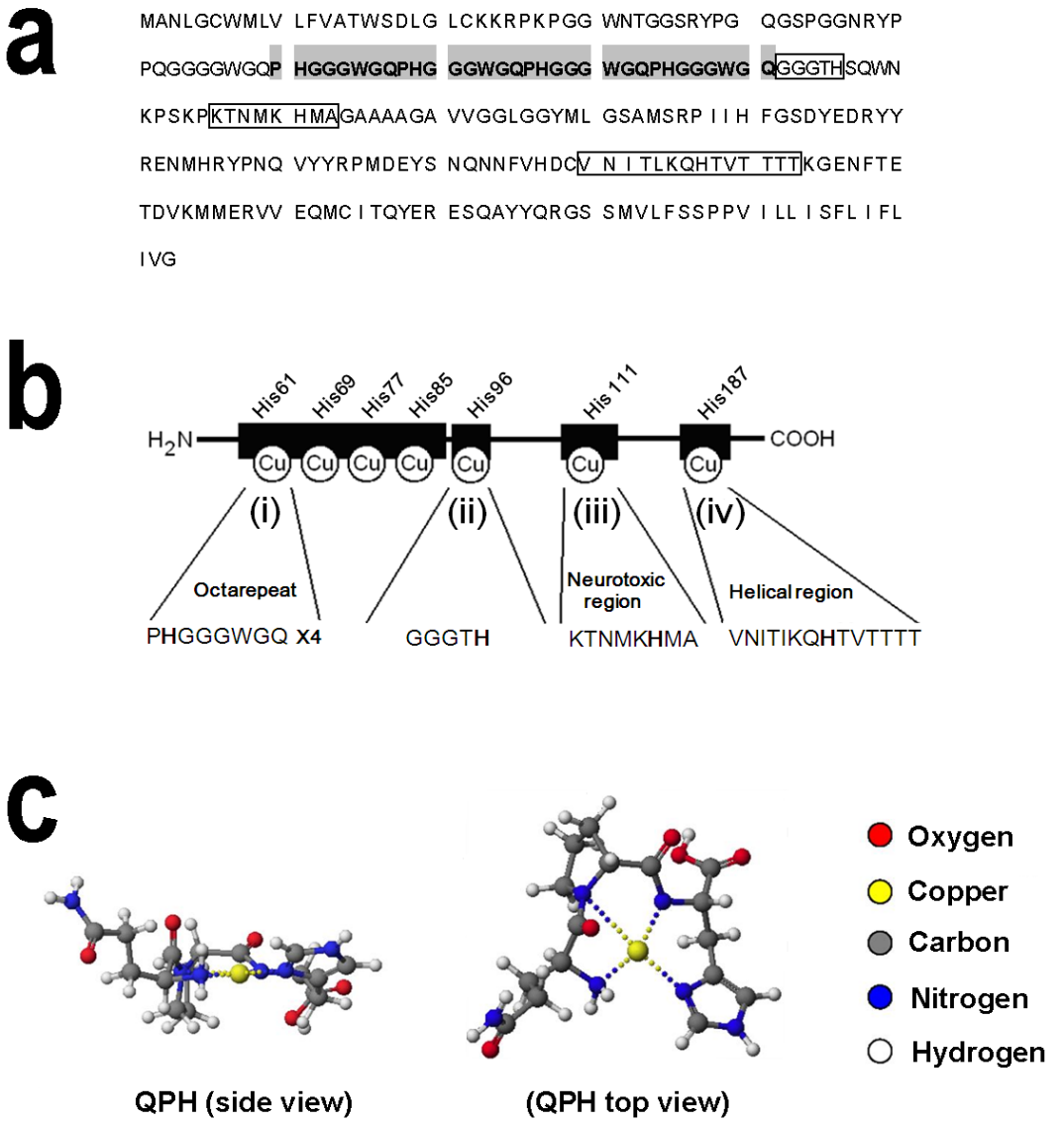

Fig. 3-1. The Cu-binding site and Cu-binding model of PrP. (a) Cu-binding site in PrP. (b) Amino acid sequence of octarepeat peptide. (c) Likely structure of peptide (QPH)-Cu complex.

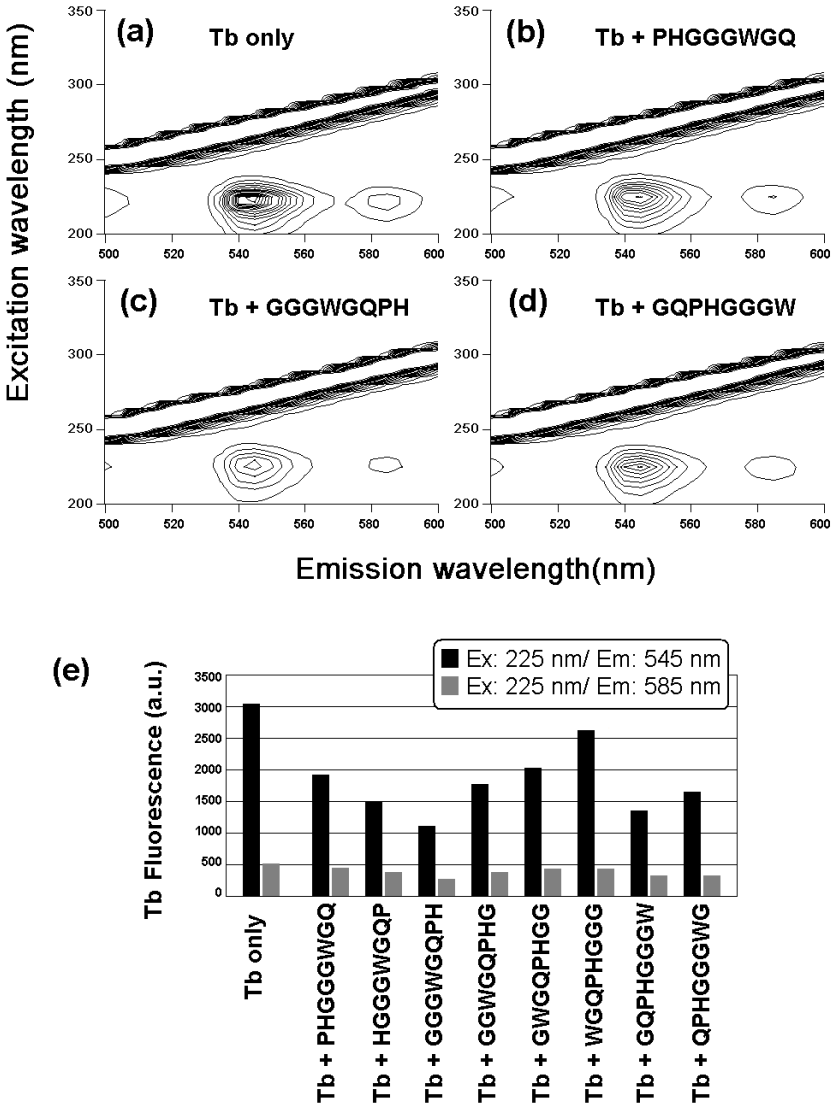

Fig. 3-2. PrP-dependet quenching of fluorescence in Tb solution. Typical 3D representations (contour plot) of the Tb-fluorescence spectra in the presence and absence of PrP-derived octapeptides are shown in (a) Tb alone, (b) Tb and PHGGGWGQ, (c) Tb and GGGWGQPH, and (d) Tb and GQPHGGGW. (e) Effects of eight different peptide sequences found in PrP octarepeat region on quenching of Tb-fluorescence are compared.

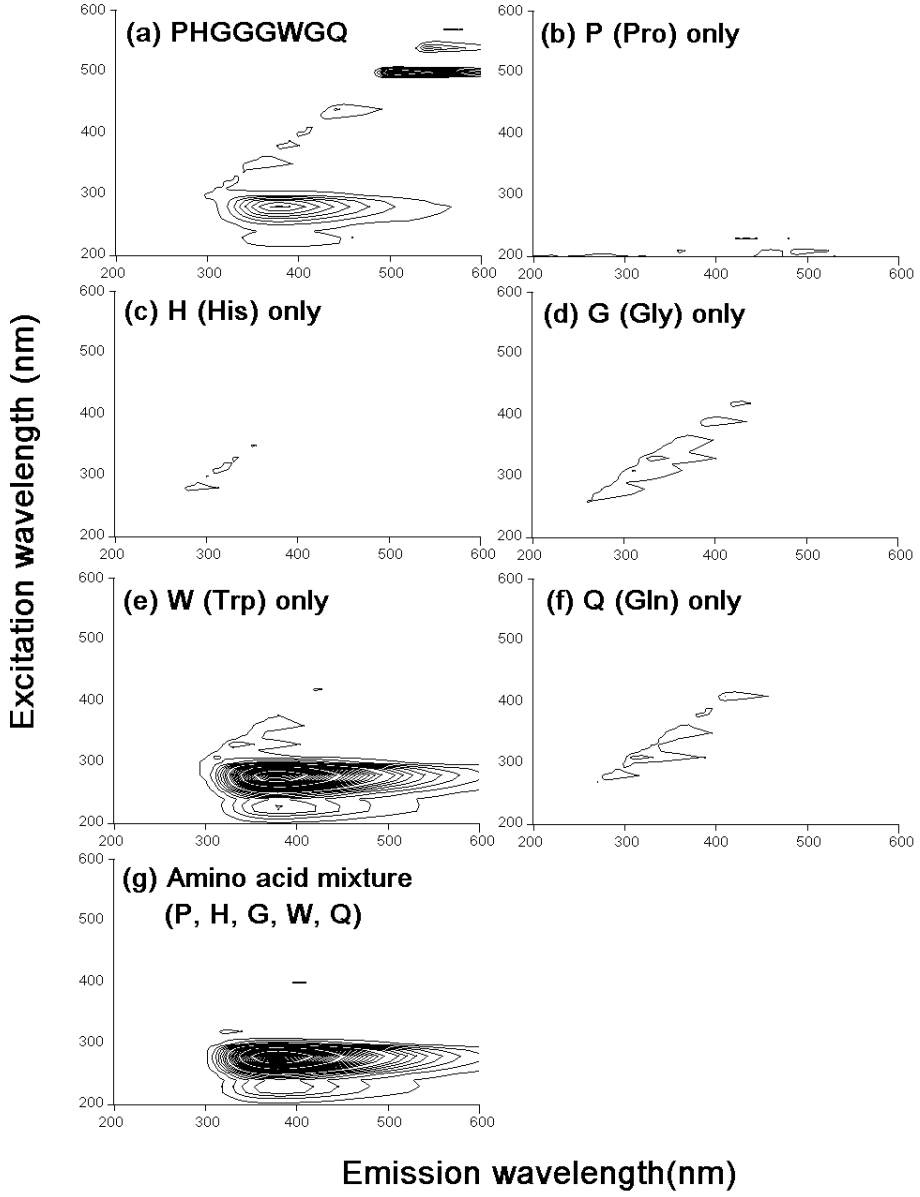

Fig. 3-3. Intrinsic fluorescence in octarepeat peptide and free amino acids.

Typical 3D-representations (contour plot) of the Peptide-FL and W-FL are shown. Typical results for octapeptide PHGGGWGQ (a), free proline (b), free histidine (c), free glycine (d), free tryptophane (e), free glutamine (f), and mixture of five amino acids (g). Concentration of the octapeptide and free proline, histidine, tryptophane, and glutamine were 30 µM. Concentrations of free glycine was 30 µM (d) or 90 µM (g).

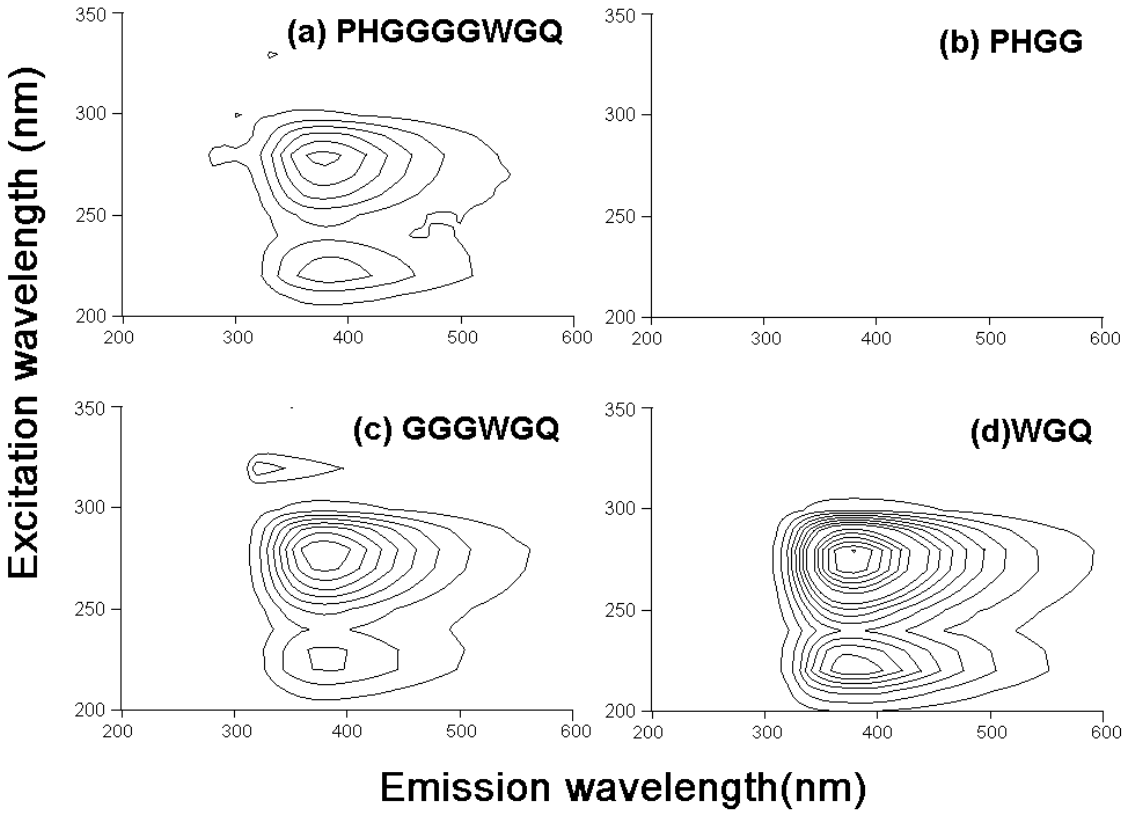

Fig. 3-4. Comparison of intrinsic fluorescence in PrP octarepeat-derived short peptides. (a) Octapeptide PHGGGWGQ, (b) tetrapeptide PHGG, (c) hexapeptide GGGWGQ, (d) tripeptide WGQ.

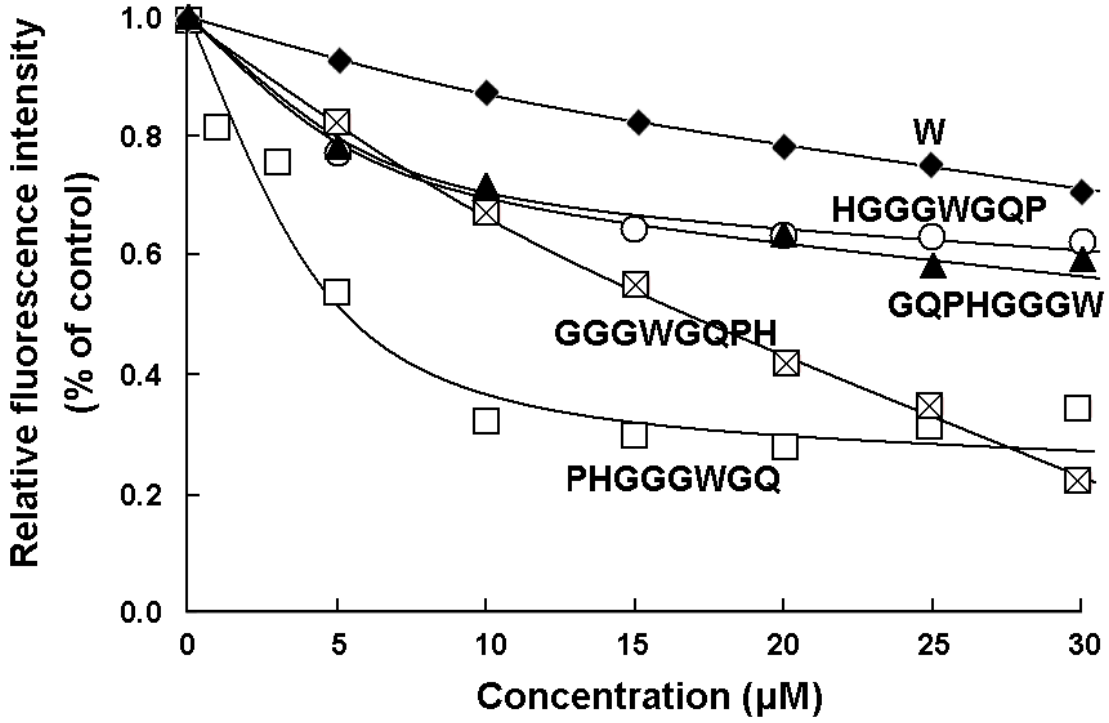

Fig. 3-5. In the presence of 30 μM peptides or tryptophan, fluorescence quenching action of copper at various concentrations (up to 30 μM) was examined.

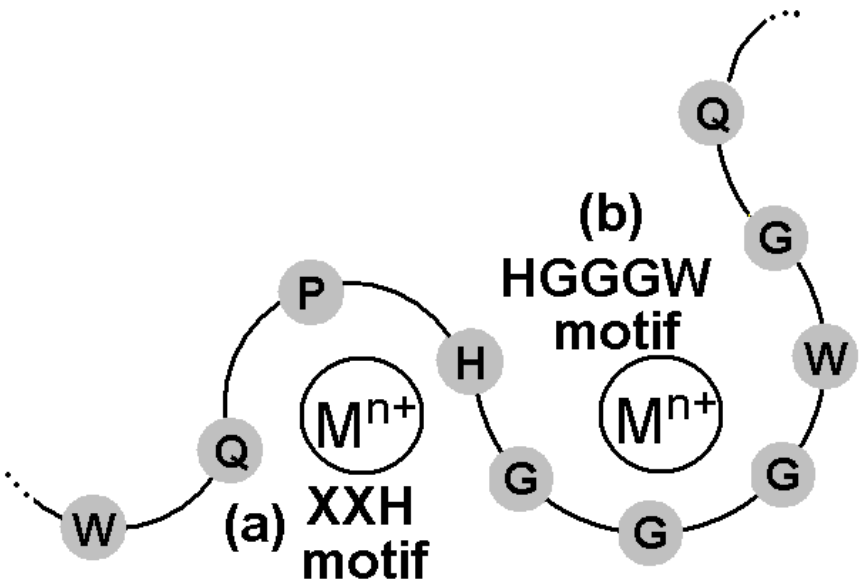

Fig. 3-6. Proposed involvement of overlapped two distinct motifs in the octarepeat region in binding to metal cations. (a) X-X-H motif (Yokawa et al.,2011; Kawano T, 2006; Kagenishi et al., 2009) suggested to bind Tb in the Tb-fluorescence assay. (b) H-G-G-G-W motif (Burns et al., 2002) suggested to bind Cu in the peptide-fluorescence assay. M^{2+}, metal cations.

CHAPTER 4

Fluorescent monitoring of copper-occupancy in His-ended catalytic oligo-peptides

4-1 Abstract

Controlled generation of reactive oxygen species (ROS) is widely beneficial to various medical, environmental, and agricultural studies. As inspired by the functional motifs in natural proteins, our group has been engaged in development of catalytically active oligo-peptides as minimum-sized metalloenzymes for generation of superoxide anion, an active member of ROS. In such candidate molecules, catalytically active metal-binding minimal motif was determined to be X-X-H, where X can be most amino acids followed by His. Based on above knowledge, we have designed a series of minimal copper-binding peptides designated as G_nH series peptides, which are composed of oligo-glycyl chains ended with *C*-terminal His residue such as GGGGGH sequence (G5H). In order to further study the role of copper binding to the peptidic catalysts sharing the X-X-H motif such as G5H-conjugated peptides, we should be able to score the occupancy of the peptide population by copper ion in the reaction mixture. Here, model peptides with Cu-binding affinity which show intrinsic fluorescence due to tyrosyl residue (Y) in the UV region (excitation at *ca*. 230 and 280 nm, and emission at *ca*. 320 nm) were synthesized to score the effect of copper occupancy. Synthesized peptides include GFP-derived fluorophore sequence, TFSYGVQ (designated as Gfp), and Gfp sequence fused to C-terminal G5H (Gfp-G5H). In addition, two Y-containing tri-peptides derived from natural GFP fluorophores, namely, TYG and SYG were fused to the G5H (TYG-G5H and SYG-G5H). Conjugation of metal-binding G5H sequence to GFP-fluorophore peptide enhanced the action of Cu^{2+} on quenching of intrinsic fluorescence due to Y residue. Two other Y-containing peptides, TYG-G5H and SYG-G5H, also showed intrinsic fluorescence which are sensitive to addition of Cu^{2+}. There was linear relationship between the loading of Cu^{2+} and quenching of fluorescence in these peptides was observed suggesting that Cu^{2+}-dependent quenching of Y-reside-derived fluorescence could be a measure of copper occupancy in the peptides. Lastly, the fate of Y residue in the Cu-loaded peptides under oxidative condition in the presence of H_2O_2 was discussed based on the Cu/H_2O_2-dependent changes in fluorescence spectra.

Key words: biocatalyst, copper, fluorescence, peptide, superoxide

4-2 Introduction

Controlled generation of reactive oxygen species (ROS) is widely beneficial to various medical, environmental engineering, and agricultural fields including clinically applied immunological modulations (Bogdan et al. 2000; Folkes et al., 2002), degradation of polluting organic compounds (Werner et al., 2005), inactivation of bacterial cells for the hygienic purpose (Laroussi and Leipold, 2004), activated sludge process (Sakai et al., 1997), and direct and indirect agricultural pest controls targeting pathogens and host plants, respectively (Yoshioka et al., 2008; Kawano and Bouteau, 2013).

In the last decade, our group has been engaged in development a novel classes of engineered biocatalysts including catalytic oligonucleotides (functional DNA sequences; Iwase et al., 2014) and peptides (Kagenishi et al., 2011), designed to catalyze the production and/or removal superoxide anion radicals ($O_2^{\bullet-}$) through understanding and modification of natural catalytic proteins and of animal and plant origins.

For examples, we found that peptides derived from human and mammalian PrPs (Kawano, 2007; Yokawa et al., 2009a,b) and plant stress-responsive peptides (Yokawa et al., 2011a) have catalytic nature although they are not considered as enzymes at present. Actually, the kingdoms of plants and animals are rich in such small peptides with high affinity to metal ions which might aid in catalysis. By mimicking such natural peptide, novel series of minimal-sized oligo-peptidic artificial enzymes catalyzing the generation of $O_2^{\bullet-}$ in peroxidase-like manner requiring hydrogen peroxide (H_2O_2) and electron donating substrates such as phenolics or amines were developed (Kagenishi et al., 2011; Okobira et al., 2011).

The first criterion for consisting such minimal peroxidase-like small peptides is the presence of His-containing motif(s) required for binding to metals (chiefly copper), and then, free-form and/or peptide-bound form of substrates fuels the reaction (Yokawa et al., 2011d). Our preliminary studies on PrP-derived peptides have pointed that His residues (at least single His) are required for anchoring of Cu onto PrP-derived peptides

(Kawano, 2006, 2007), and eventually, the catalytically active Cu-binding minimal motif was determined to be tri-peptidic sequence X-X-H, where X can be most amino acids followed by His (Kagenishi et al., 2009; Yokawa et al., 2011d). An engineering example of a catalytic peptide sequence sharing XXH motif for development of biosensing and bioengineering materials was reported (Okobira et al., 2011). Accordingly, one of X-X-H motif derivatives, Gly-Gly-His (G-G-H) sequence was introduced onto the glycidyl methacrylate-grafted on the polyethylene platform (porous hollow fiber membrane). Chemiluminescence assay reveled that loading of Cu^{2+} on the peptide-conjugated membrane conferred the catalytic activity to it, thus, catalyzing the generation of $O_2^{\bullet-}$ upon addition of a pair of substrates (H_2O_2 and tyramine).

In human PrP, His96 centered in G-G-G-T-H-S-Q-W-N sequences is considered as one of Cu-binding sites. Effect of His position on the catalytic activity in PrP-derived peptides were examined by comparing the H-S-Q-W-N (His-started pentapeptide) and the G-G-G-T-H (His-ended pentapeptide) (Kagenishi et al., 2011). While reaction with tyramine (given as a model phenolic substrate) and G-G-G-T-H peptide resulted in robust production of $O_2^{\bullet-}$, the H-S-Q-W-N peptide showed no catalytic activity, suggesting that G-T-H motif within the His-ended pentapeptide is one of X-X-H motif derivatives. As the catalytic activities among G-G-G-T-H and shorter derivatives (G-G-T-H and G-T-H) were compared and the importance of the *N*-terminal glycyl-chain elongation for maximal redox activity in *C*-terminal His anchored peptides was implied (Kagenishi et al., 2011). Furthermore, the likely common structure formed by Cu/X-X-X motif complex found in Cu-binding motifs in human PrP including octarepeat region (Inokuchi et al., 2012), helical region (Yokawa et al., 2011b), neurotoxic region (Kagenishi et al., 2009) was proposed to be semi-planar shape resembling the structure of metal-centered heme in which metallic element is coordinated by planarly arranged four nitrogen atoms, by analogy to the structure of Ni/X-X-H metallopeptides (Fang et al., 2004, 2006).

As inspired by the natural PrP-derived G-G-G-T-H sequence, we have designed a series of simplified model peptides designated as G_nH series peptides, which are composed of oligo-glycyl chains (G_n) ended with *C*-terminal His residue (Kagenishi et al., 2011). As expected, importance of the elongated *N*-terminal G_n chain with

anchoring His was confirmed by comparing the G_nH series peptides (n = 2, 3, 4, 5 and 10) and G_n series peptides lacking His. Notably, G_n series lacking the metal-binding motif showed no catalytic activity even in the presence of free Cu^{2+}. In G_nH series, G_3H tetrapeptide showed a detectable increase in production of $O_2^{\bullet-}$, and peptides with longer chain showed higher activity, confirming the importance of *N*-terminal G_n chain length. Data suggested that the requirement for the *N*-terminal G_n elongation is nearly fulfilled at between G_5 and G_{10} (Kagenishi et al., 2011), and amazingly, unlikely to conventional enzymes, the catalytic activity in these metal-binding peptides survive the heating treatment such as autoclaving and the repeated freeze and thaw cycles (Yokawa et al., 2009b).

Fluorometry often provides strong approaches for studying the molecular interaction. Inokuchi et al. (2012) assessed (1) the quenching of Tb^{3+} fluorescence by PrP-derived metal-binging peptides and (2) the Cu^{2+}-dependent quenching of intrinsic fluorescence in human PrP octarepeat peptide sequence. Quenching of Tb-fluorescence by interacting peptides implied the important role for His-ended peptidic sequence sharing X-X-H motif (in case of human PrP's octarepeat region, P-Q-H). On the other hand, quenching of intrinsic peptide fluorescence due to the presence of a tryptophan (W) residue by cupper ion suggested that classically known H-G-G-G motif in PrP (Burns et al., 2002) forms an active motif in metal binding. Taken together, in the mammalian PrP octarepeat regions, in which P-H-G-G-G-W-G-Q is repeated for four (human) to six (bovine) times, two distinct metal binding motifs, namely, X-X-H motif and H-G-G-G motif, could be overlaid by sharing common His residue and thus co-existed (Inokuchi et al., 2012).

In order to further study the role of copper binding to the biocatalysts sharing the X-X-H motif such as G_nH series catalytic peptides, we should be able to score the occupancy of the peptide population by copper ion in the reaction mixture. In the present study, we attempted to monitor the binding of copper to G_nH catalytic peptides by designing the chimeric molecule fusing fluorescent oligo-peptide sequence derived from green fluorescence protein (GFP) and G_5H sequence.

4-3 Materials and Methods

4-3-1 *Peptides and Chemicals*

Model peptides with Cu-binding affinity which show intrinsic fluorescence in the UV region were synthesized to score the effect of copper occupancy. The peptides were obtained from the custom peptide service department of Sigma Genosys Japan, Ishikari, Hokkaido, Japan. The amino acid sequences of the peptides chemically synthesized were purified on high pressure liquid chromatography prior to the experimental use. Other chemicals such as $CuSO_4$ and salts for buffer used in this study were of reagent grade purchased from Wako Pure Chemical Industries Ltd. (Osaka, Japan).

Synthesized peptides include GFP-derived fluorophore sequence, TFSYGVQ (designated as Gfp), and Gfp sequence fused to GGGGGH, thus, designated as Gfp-G5H. Note that the synthesized peptide sequences corresponding to GFP fluorophore do not show green fluorescence without post-translational process for developing the molecular rigidity in living cells. Instead, intrinsic fluorescence due to presence of the tyrosyl residue (Y) can be expected. Therefore, two Y-containing tri-peptide sequences found in natural GFP fluorophores, namely, TYG and SYG were fused to the Cu-binding GGGGGH sequence (thus, designated as TYG-G5H and SYG-G5H, respectively).

4-3-2 *Fluorometric analysis*

Intrinsic fluorescence from the 30 μM peptides with and without loading of copper ions were detected in potassium phosphate buffer (50 mM, pH 7.0) using a fluorescence spectrophotometer (F-4500 Hitachi High-Technol. Co., Tokyo). The three-dimensional (3D) spectral measurement of fluorescence was carried out at the excitation wavelength between 200 and 700 nm with 5 nm intervals and emission wavelength between 200 and 700 nm with 5 nm intervals.

4-4 Results and Discussion

4-4-1 *Enhanced Cu^{2+}-dependent changes in intrinsic fluorescence spectra of a GFP-fluorophore peptide conjugated with metal binding sequence*

GFP fluorophore-derived peptides tested here showed non-green intrinsic fluorescence at UV region (Fig. 4-1). Upon excitation at excitation at 230 nm (peak a) and 280 nm (peak b), both Gfp-G5H (TFSYGVQ-GGGGGH) and Gfp (TFSYGVQ) showed fluorescence emission at around 320 nm. Fluorescence signals at the peak a (230 nm excitation/320 nm emission) by 30 μM Gfp-G5H and Gfp showed tendency to be quenched in the presence of 30 μM Cu^{2+} by 61.6 % and 32.0 %, respectively. Under the same conditions, the fluorescence signals at the peak b (280 nm excitation/320 nm emission) by Gfp-G5H and Gfp showed Cu^{2+}-dependent quench by 48.5 % and 22.7 %, respectively. These data suggested that G5H-conjugated peptide showed twice greater sensitivity to addition of $CuSO_4$. Therefore, we can expect that Cu-dependent quenching of UVC-excited UVA fluorescence by Gfp-G5H can be used as a measure of Cu-occupancy in G5H domain.

4-4-2 *Intrinsic fluorescence in tyrosine-containing peptides showed sensitivity to Cu*

The intrinsic fluorescence signals (the peaks a and b) from the three G5H-conjugated GFP-derived peptides (30 μM of Gfp-G5H, TYG-G5H, and SYG-G5H) plotted on 3-dimentional contour graphs were compared. Data showed that the intrinsic fluorescence by all peptides can be quenched in the presence of $CuSO_4$ (10, 25 and 100 μM; Fig. 4-2). Among three peptides examined, SYG-G5H was most sensitive to lower range of $CuSO_4$ concentration (10 μM, molar ratio to peptide: *ca.* 0.17-0.33). The fluorescent signals from TYG-G5H also showed higher sensitivity to Cu as compared to the signals from Gfp-G5H.

4-4-3 *Linear relationship between loading of Cu^{2+} and quenching of fluorescence*

Among three peptides examined, only Gfp-G5H showed linear decrease in fluorescent signal along with occupancy with cupper in the range between 0.17 and 1.33 of molar ratios of Cu^{2+} over peptide (Fig. 4-3 and 4). Note that within this range of copper concentration, the squared correlation coefficients (r^2) for Cu-dependent quenching of fluorescence signals at the peaks a and b in Gfp-G5H were 0.982 and 0.989, respectively (Fig. 4-3 and 4, insets).

On the other hand, r^2 for Cu-dependent quenching of fluorescence signals by TYG-G5H and SYG-G5H ranged at relatively low scores between 0.700 and 0.906 (Fig. 4-3 and 4, insets). Therefore, we could conclude that the kinetics reported by Gfp-conjugated G5H peptide is most proportional to the copper occupancy in G5H sequence.

Previously, catalytic nature of G_5H hexapeptide was assessed (Kagenishi et al., 2011). It has been shown that catalytic activity in G5H peptide requires the binding of copper to it. Furthermore, Michaelis constant (K_m) for $O_2^{\bullet-}$ production using tyramine as a model substrate for Cu/G5H complex (0.15 mM) was determined to be 0.24 mM. Then, V_{max} at molar basis and weight basis were determined to be 52.91 mmol ($O_2^{\bullet-}$) mmol (peptide)$^{-1}$ min^{-1} and 0.12 mmol ($O_2^{\bullet-}$) mg (peptide)$^{-1}$ min^{-1}, respectively (Kagenishi et al., 2011). With molar-basis comparison, the catalytic activity looks week, however, due to its low molecular weight characteristics, weight-basis comparison of the catalytic activity reaches applicable range which is almost 1/6 of purified horseradish peroxidase (Kagenishi et al., 2011). It is obvious that this type of approach for creating heat-stable biocatalysts require further innovation. Therefore, we expect that the use of Gfp-fused G5H peptide for quantification of Cu-binding to G5H motif may contribute to further engineering of the G_nH-based catalytic peptides.

4-4-4 *Fate of tyrosine residue after oxidative reaction*

Up to here we mostly discussed the role of His-ended metal binding motif in novel class of catalytic peptides with aid by fluorescent signal which could be attributed to the

presence of Tyr residue. We view that Tyr residue has an additional important role in designing the peptidic $O_2^{\bullet-}$-generating catalysts (Kawano, 2011).

Reportedly, supplementation of structurally similar free catecholamine-related chemicals (tyramine or phenylethylamine), a free amino acid Tyr (Y), or Tyr-rich oligopeptides (such as tyrosyl-tyrosyl-arginine, YYR) as model substrates (instead of typical peroxidase substrates such as phenolics or amines) to the reaction mixture containing Cu-bound peptides sharing X-X-H motif such as Cu/VNITKQHTVTTTT (helical Cu-binding motif in mammalian PrP; Yokawa et al., 2009), Cu/GGGTH (short Cu-binding motif in human PrP; Kawano, 2007), Cu/GGGGGH (artificial catalyst; Kagenishi et al., 2011), Cu/GGGFGH (Yokawa et al., 2011a), or Cu/ NPGFPH (Yokawa et al., 2010) resulted in H_2O_2-dependent $O_2^{\bullet-}$-generation. Notably, Y residue-containing peptides with X-X-H motif including Cu/GGG**Y**GH (plant ozone-inducible peptide sequence; Yokawa et al., 2011a), Cu/NPG**Y**PH (chicken PrP hexa-repeat sequence; Yokawa et al., 2010), and Cu/FLTE**Y**VA-GGGGGH (Erk1/Erk2 MAP kinase substrate sequence fused with metal binding sequence designated as ErkG5H; Kawano, 2011) showed catalytic activity for H_2O_2-dependent $O_2^{\bullet-}$ generation without supplementation of any free phenolic substrates. These knowledges suggest that Y-residue mimics the role for free phenolics in H_2O_2-dependent $O_2^{\bullet-}$ generating reactions.

The above view was supported by Y-to-F mutation in chicken PrP sequence (Yokawa et al., 2009) and plant ozone-inducible peptide sequence (Yokawa et al., 2011a), by which Phe residues on catalytic peptides were replaced with Tyr residues. The difference was merely the presence and absence of the OH group on the aromatic ring. Moreover, masking of Y-residue (at OH group) in ErkG5H through tyrosyl phosphorylation in Erk1/Erk2 MAP kinase substrate moiety of ErkG5H peptide was performed, and catalytic activity for H_2O_2-dependent $O_2^{\bullet-}$ generation was largely lost in the resultant Y-phosphorylated peptide (Kawano, 2011). To date, ErkG5H is the only artificial catalyst which can be attenuated by phosphorylation event.

Involvement of free Y or Y residue in the Cu/peptide complex-catalyzed H_2O_2-dependent generation of $O_2^{\bullet-}$ suggests that a phenoxy radical derived from Y (tyrosyl radical, $Y^{\bullet}$) can be formed in aid of single electron reduction of molecular oxygen, by

analogy to plant enzymes H_2O_2-dependently generating $O_2^{\bullet-}$ by coupling to oxidation of phenolics (such as salicylic acid) to form phenoxy radicals (Kawano et al., 1998; Kawano and Muto, 2000).

There would be two distinct models for the fate of Y residue in model Cu/peptide complex. One likely model is that Y-residue is simply consumed and oxidized by the Cu-bound catalytic center in the presence of H_2O_2 as observed for various free phenolics (Kagenishi et al., 2011). Another likely model is that Y residue lasts longer by repeatedly participating the reaction as shuttle for transferring electron, by analogy to the putative intra-molecular substrate-like roles for Y residues within ribonucleotide reductases (Boal et al., 2010) and cyclooxygenase-2 (Li et al., 2010), in which corresponding reactions proceed *via* transient formation of $Y^{\bullet}$ and recycling of Y.

To obtain a clue to this view, we examined the fate of Y-dependent fluorescence in Gfp-G5H, TYG-G5H, and SYG-G5H peptides after addition of Cu and H_2O_2 (Fig. 4-5). Ratio of H_2O_2 concentration (1 mM) over Cu/peptide concentration (30 μM) was set at excess level since higher range of H_2O_2 concentration has been employed in the previous studies using G5H-based catalysts.

Addition of copper to three peptides largely lowered the fluorescence signals as described earlier in this report. Addition of H_2O_2 to SYG-G5H lowered the fluorescence signals. Contrary, addition of H_2O_2 enhanced the fluorescence at both peaks a and b in TYG-G5H and the peak a in Gfp-G5H. The reason why two peaks of Y fluorescence in different peptides showed different sensitivity to H_2O_2 should be attributed to the fact that even a monomer of phenolic compound often possesses multiple fluorophores within the molecule despite its simple structure as in the case of ferulic acid (Djikanović et al., 2007).

To combination of Cu and H_2O_2, three peptides responded differently. Response to Cu/H_2O_2 co-treatment in Gfp-G5H was almost identical to the response to Cu alone. Changes in SYG-G5H was less obvious. The fluorescence intensities at 230 nm excitation/320 nm emission and 280 nm excitation/320 nm emission corresponding to the peaks a and b in Cu/H_2O_2 co-treated TYG-G5H were seemed to be maintained at higher level compared to control. Note that the peak excitation wavelength at peak b

fluorescence slightly shifted from 280 to 290 nm, therefore the product of peptide-catalyzed redox reaction challenging Y-residue under Cu/H_2O_2 co-treatment must be no-longer intact Y residue. The case in TYG-G5H suggest that after possible formation of $Y^{\bullet}$ via Cu/peptide-catalyzed H_2O_2-dependent reaction, recycling of Y did not sufficiently occurred thus spectral changes (shift in the excitation peak) was observed.

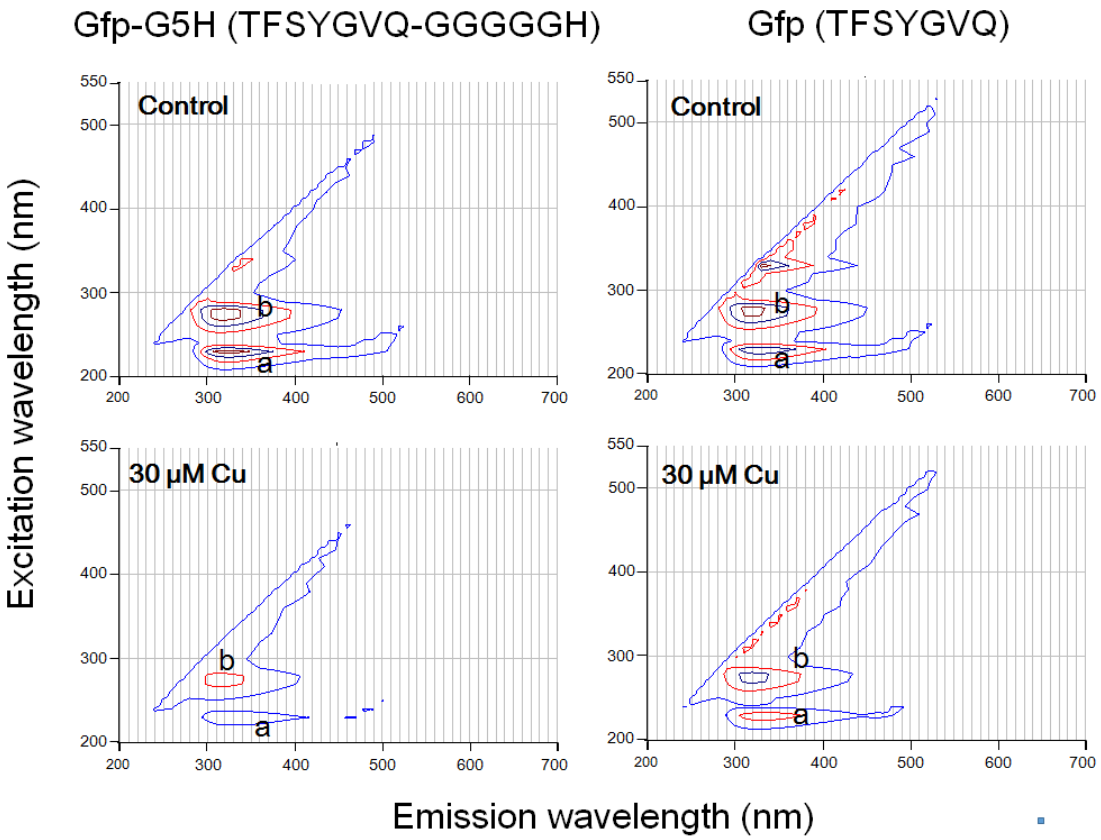

Fig.4-1. Different quenching action of copper ion against intrinsic tyrosine fluorescence in GFP-derived fluorophore sequence with and without fusing to copper binging sequence hexapeptide. Peptides (30 µM) used were Gfp-G5H (TFSYGVQ-GGGGGH) and Gfp (TFSYGVQ). Peaks of tyrosine fluorescence (emission at *ca*. 320 nm) were observed with excitation at 230 nm (a) and 280 nm (b). Quenching of fluorescence in the presence of 30 µM $CuSO_4$ was assessed.

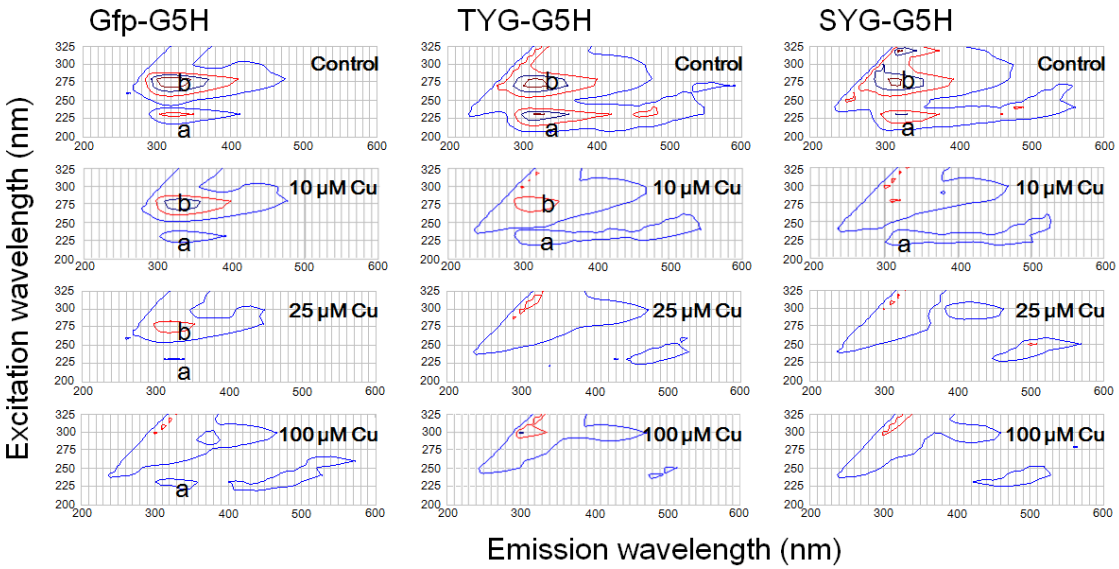

Fig. 4-2. Effect of copper ion on quenching of intrinsic fluorescence signals by three GFP fluorophore-derived oligo-peptides conjugated with copper-binding hexapeptide motif. Peptides (30 μM) used were Gfp-G5H (TFSYGVQ-GGGGGH), TYG-G5H (TYG-GGGGGH), and SYG-G5H (SYG-GGGGGH). In the absence of $CuSO_4$, two typical peaks of tyrosine fluorescence (emission at *ca*. 320 nm) were observed with excitation at 230 nm (a) and 280 nm (b). Quenching of fluorescence in the presence of 10, 25 and 100 μM $CuSO_4$ was assessed.

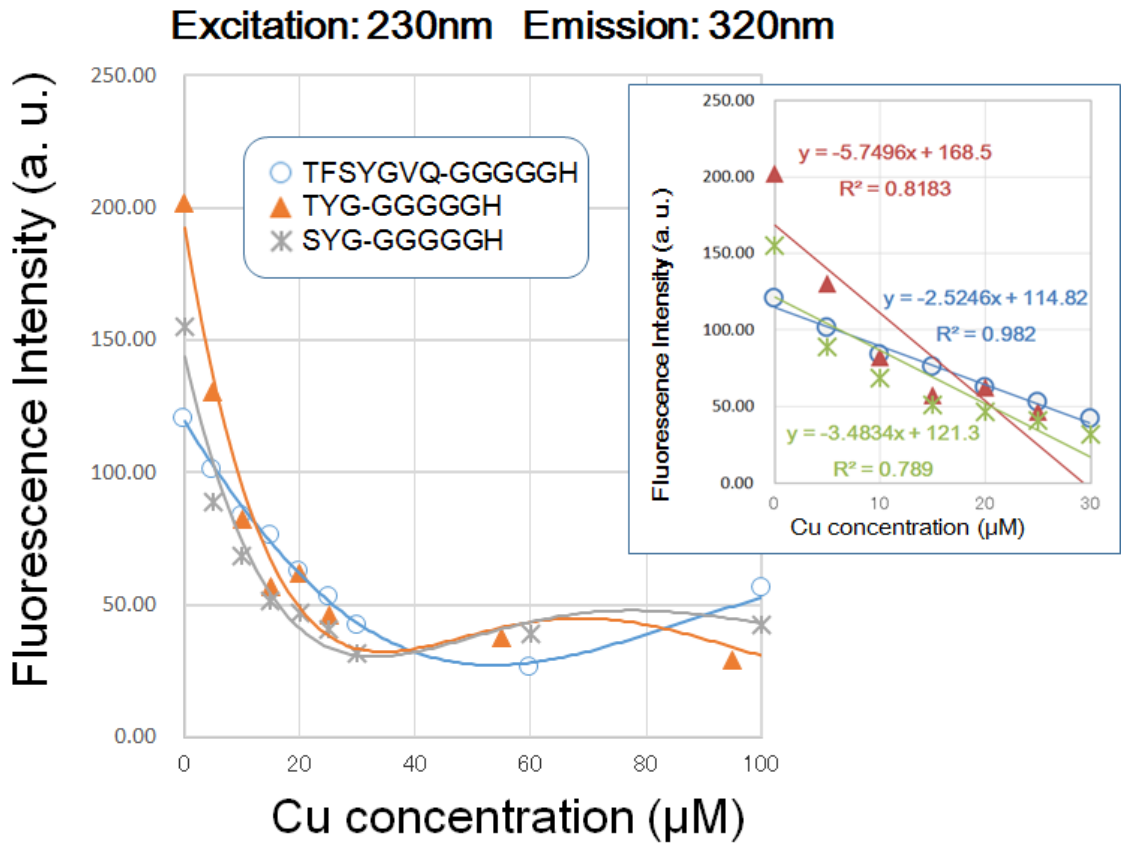

Fig. 4-3. Effect of copper concentration on quenching of 230 nm excitation/320 nm emission signals by three G5H-conjugated GFP fluorophore-derived oligo-peptides. Peptides (30 μM) used were as in Figure 2. Quenching of fluorescence was performed with 5-100 and 100 μM $CuSO_4$ was assessed. Three different symbols represent the data points obtained. Curves were merely approximation of the response (note that they are not regression curves). In the inset, linear relationships between the remitted range of Cu concentration (up to 40 μM) and the decrease in peptidic fluorescent signals are shown.

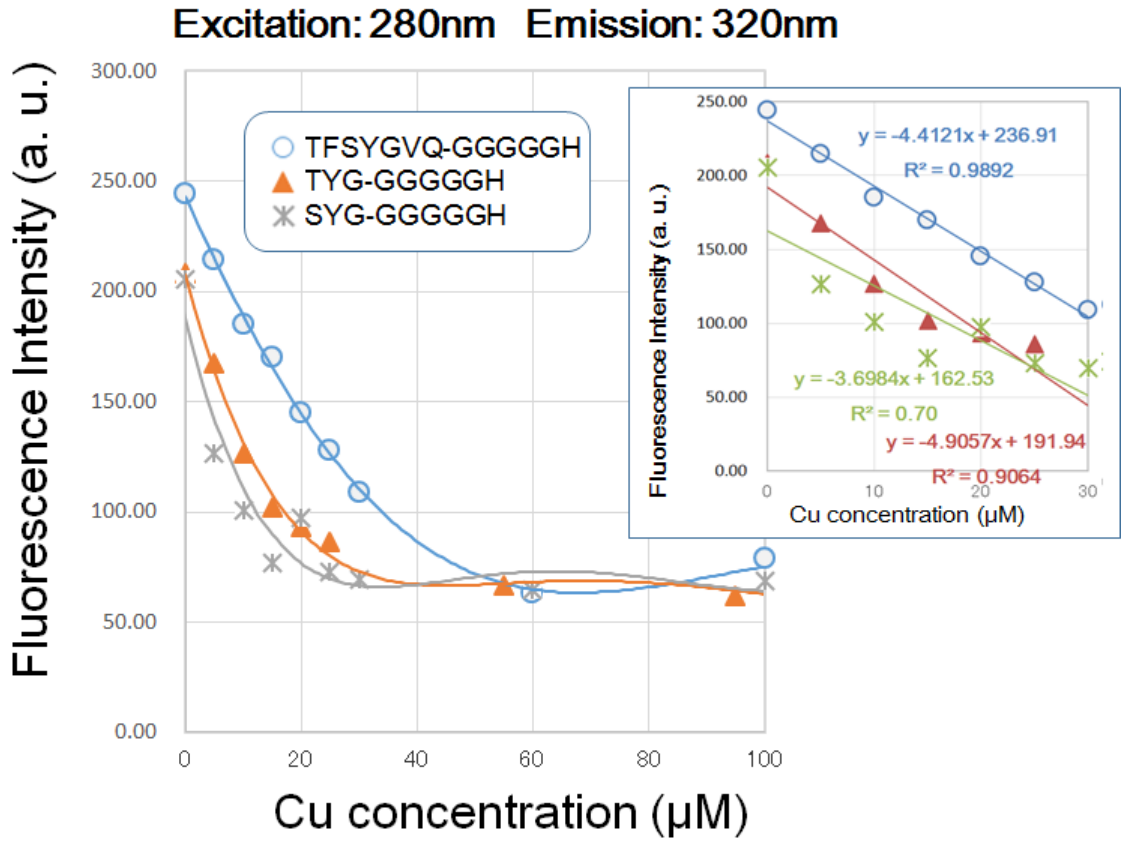

Fig. 4-4. Effect of copper concentration on quenching of 280 nm excitation/320 nm emission signals by three G5H-conjugated GFP fluorophore-derived oligo-peptides. Peptides (30 μM) used were as in Figure 2. Quenching of fluorescence was performed as in Figure 3. In the inset, linear relationships between the remitted range of Cu concentration (up to 40 μM) and the decrease in peptidic fluorescent signals are shown.

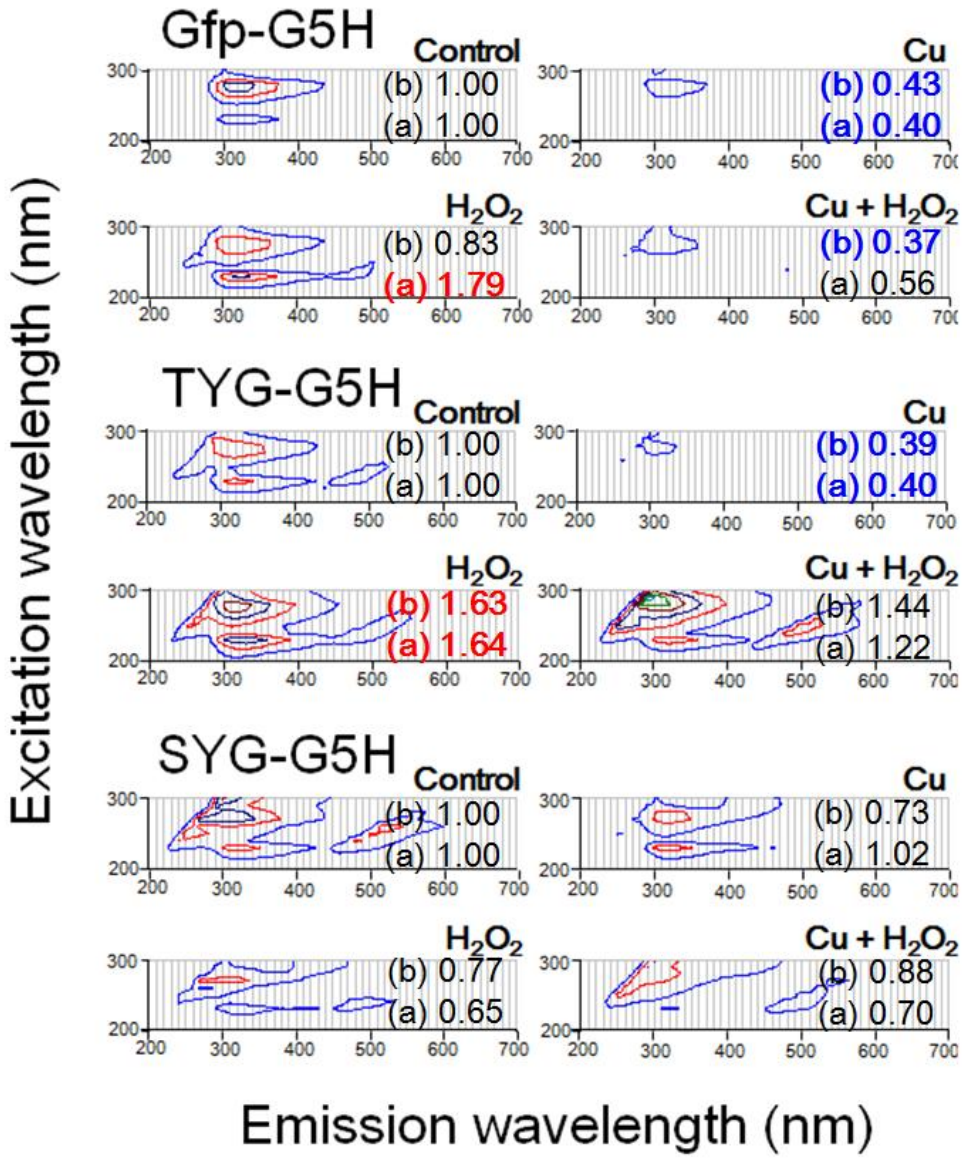

Fig. 4-5. Changes in UV-excited fluorescence contour spectra in three peptides after addition of copper and/or excess hydrogen peroxide. Peptides used were as in Figure 2, namely Gfp-G5H, TYG-G5H and SYG-G5H. Each peptide (30 μM) was treated with none, either or both of $CuSO_4$ (30 μM) or/and H_2O_2 (1 mM). Numbers after (a) and (b) shown with each spectrum represent the relative changes in fluorescence intensities at peaks a (230 nm excitation/320 nm emission) and b (280 nm excitation/320 nm emission), respectively.

CHAPTER 5

Monitoring of Copper Loading to Cationic Histidine-rich Short Salivary Polypeptides, Histatins 5 and 8, Based on the Quenching of Copper-sensitive Intrinsic Red Fluorescence

5-1 Abstract

Recent studies identified nearly 100 of high abundance salivary proteins/peptides, including a group of cationic histidine-rich short polypeptides known as histatins (Hsts). The most recognized roles for Hsts are anti-microbial activities, and the modes of action of Hsts (chiefly, Hst-5 and 8) have been subjected to intense debates. Since Hst-5 and 8 possess metal-binding motifs, analysis of Cu occupancy in Hsts is of great importance. Here, we conducted two distinct fluorescence-based assays, namely, the Hst-dependent quenching of Tb^{3+}-fluorescence and the Cu^{2+}-dependent quenching of intrinsic red fluorescence in Hsts. Notably, Cu-sensitive intrinsic red fluorescence from Hsts is documented for the first time. In addition, novel catalytic activities in Cu-loaded Hsts were demonstrated. Upon addition of H_2O_2, both Hsts catalyzed the generation of superoxide. The present study may provide key technical knowledge required for development of non-invasive fluorometric and chemiluminometric monitoring of metal binding to the peptides of interest.

Key words: Copper occupancy, Fluorescence quenching, Metal-binding motif, Peptide

Abbreviations: ATCUN, amino-terminal Cu/Ni binding motif; AU, arbitrary units; CL, chemiluminescence; FL, fluorescence; Hst-5, histatin 5; Hst-8, histatin 8; Hsts, histatins; ROS, reactive oxygen species.

5-2 Introduction

Saliva is a glandular secretion that is vital in the maintenance of healthy oral tissues (Huq et al., 2007). Recent proteomic and peptidomic studies have reported the identification of over 1,300 proteins and peptides in human saliva, including nearly 100 of high abundance salivary proteins/peptides (Huq et al., 2007). Historically, several research groups have documented the existence of a group of cationic histidine-rich short polypeptides which are now recognized as human salivary histatins (Hsts) (Bonilla, 1969; Azen, 1972; Holbrook and Molan, 1975; Baum et al., 1976). The most recognized biological functions proposed for Hsts are bactericidal action against *Streptococcus mutans* (MacKay et al., 1984) and antifungal activities against opportunistic yeast *Candida albicans* (Yoshida et al., 2001; Tsai, 1998), and *Cryptococcus neoformans* (Tsai et al., 1996), and are therefore potential therapeutic reagents against *Candida* species. Actions by Hsts are now considered as the first line of defense (primordial mechanism of immunity commonly observed in vertebrate and nonvertebrate organisms) against oral candidiasis caused by *Candida albicans* (Melino et al., 2014; Puri et al., 2015). Accordingly, fungal cells are killed by Hsts through their binding to the cell membrane and their internalizing, eventually disrupting the cellular volume regulatory mechanisms and mitochondrial function (Yoshida et al., 2001). As a consequence, production of reactive oxygen species (ROS) and non-lytic cell death.

Among salivary peptides, histatin 5 (Hst-5) consisted of 24 amino acids (DSHAKRHHGYKRKFHEKHHSHRGY), is the most potent molecule with regard to its fungicidal activity towards *C. albicans*(Puri et al., 2015; Pauri and Edgerton, 2014). Therefore, its use as a therapeutic reagent against *Candida* species is highly expected (Yoshida et al., 2001). In the C-terminal half of Hst-5, a sequence of a dozen amino acids (KFHEKHHSHRGY) corresponding to full sequence in histatin 8 (Hst-8) is conserved. Hst-8 is kwon to serve as hemagglutination-inhibiting peptide (Yoshida et al., 2001). A study using truncated fragments of Hst-8 revealed that last tripeptide (RGY) could be involved in effective inhibition of hemagglutination by *Porphyromonas gingivalis* (Murakami et al., 1992). In addition to the above listed effects of Hst-5 and

Hst-8 against oral pathogens, the effect of Hsts on mammalian host immune systems has also been studied (Yoshida et al., 2001). Reportedly, in the wide range of concentration spanning from nM to sub-mM, both Hst-5 and Hst-8 (with lesser extent) induce the release of histamine from rat peritoneal mast cells in a dose-dependent manner.

The mode of action of Hsts (chiefly, Hst-5) has been a subject of intense debate (Pauri and Edgerton, 2014). While most of classical host innate immune proteins act by membrane lysis or pore formation on microbial plasma membrane, the Hst-5 likely targets multiple proteins inside the microbial cells. In case of fungicidal action against *C. albicans*, Hit 5 firstly binds to fungal cell wall proteins (Ssa1/2) and glycans, then, Hst-5 is actively internalized (in an energy-dependent manner) by *C. albicans* cells with involvement of the polyamine transporters (Pauri and Edgerton, 2014; Murakami et al., 1992; Li et al., 2003).Once entering inside the fungal cells, Hst-5 may cause dysfunction in mitochondria, thus, leading to oxidative burst releasing ROS. Note that the last straw for dying fungal cells is osmotic stress accompanying the volume dysregulation and ion imbalance triggered (Vylkova et al., 2007).

Many predicted that His-residue-mediated high affinity to metals in Hst members could provide clues to understand the mechanism of Hst actions. In fact, Hst-5 binds various metals in saliva, *viz.*, Zn, Cu, Ni (Pauri and Edgerton, 2014), and Fe (Puri et al., 2015). It has been proposed that the metal binding by Hst-5 would be much more significant under limitation of nutrients as the metal binding by Hst-5 could potentially further limit the essential metals needed for microbial growth (Pauri and Edgerton, 2014). Apart from such a passive mechanism, metal-loaded Hst-5 may have active roles. As shown in Fig. 1, Hst-5 possesses an NH_2-terminal Cu/Ni binding (ATCUN) motif and a Zn(II)-binding motif (HEXXH) at the C terminus for binding of metals (Pauri and Edgerton, 2014).

In a number of proteins, the ATCUN motif is formed from a His residue in the third position, two preceding residues, and the free N-terminus (NH_2-XXH), therefore a peptide or protein maximally possesses only single ATCUN motif at its N-terminus (Sankararamakrishnan et al., 2005). According to the crystal structure of a small metal-

bound ATCUN peptide, four nitrogen atoms in the ATCUN motif (three residues with free amino-terminus) form a square semi-planar geometry (Sankararamakrishnan et al., 2005), thus, mimicking to the manner for allocating the nitrogen atoms around a single metal in the metal-centered tetrapyrroles such as heme. The likely metals potentially bound to ATCUN motif in Hst-5 are Cu, Ni and Fe. Especially, the interactions between Hst-5 and either of Cu or Fe reportedly contribute to generation of ROS members which eventually oxidize an array of key proteins in the mitochondria causing mitochondrial dysfunction leading to further oxidative burst and cell death in microbial cells (Sankararamakrishnan et al., 2005).

Presence of the HEXXH motif in C-terminal half of Hst-5 and center of Hst-8 suggests that these molecules have high affinity to Zn. According to an earlier study (Melino et al., 1999), binding to Zn may be required for fusing into the negatively charged phospholipid-based membranes or vesicles. However, Zn binding to Hst-5 shows only limited effects on Hst-5's fungicidal activity (Puri et al., 2015).

While the HEXXH motif can be found in both Hst-5 and Hst-8, the ATCUN motif can be found only in Hst-5 (Fig. 5-1). However, knowledge on peptide geometry predicts that even to Hst-8, copper can be bound due to the presence of the XXH motif where X can be most amino acids followed by His, therefore ATCUN can be one form of XXH motif concepts.

It has been revealed that the XXH motif has been shown to play key its role as one of Cu-binding motifs in mammalian PrPs (Kawano, 2007; Yokawa et al., 2009; Yokawa et al., 2009) and plant stress-responsive small peptides (Yokawa et al, 2011a). Interestingly, upon binding to Cu (II), natural (Kawano, 2007; Yokawa et al., 2009; Yokawa et al, 2011a) and engineered (Kawano, 2007; Kagenishi et al., 2011; Okobira et al., 2011) peptides containing XXH motif show catalytic activity for generation of superoxide anion radical ($O_2^{\bullet-}$) by coupling to oxidation of aromatic monoamines and phenolics in the presence of H_2O_2, thus, similarly to plant peroxidase reaction (Kawano and Bouteau, 2013; Yokawa et al., 2011b). Taken together, we can expect that both Hst-5 and Hst-8 might capture Cu to form functional or catalytic nature. Similarly to the fact that enzyme-like activity for H_2O_2-dependent substrate oxidation accompanying ROS

generation can be found in human prion-derived Cu (II)-bound peptides (Kawano, 2007; Yokawa et al., 2009) and mimicking engineered peptides (Kagenishi et al., 2011), the Cu (II)-bound form of Hst-5 also exhibits enzyme-like enzyme-like kinetics requiring (Tay et al., 2009).

As discussed above, analysis of Cu occupancy in Hsts is of great importance. Monitoring of metal-Hst-5 interaction can be performed by various techniques such as circular dichroism (Puri et al., 2015). Use of fluorescence (FL)-active rare earth element ions such as terbium ion (Tb^{3+}) as model metal ions is one of such approaches assessing the mode of metal-binding in Cu-binding peptides as performed for conantokin-G, a toxic metallo-peptide derived from a snail (Blandl et al., 1997) and human prion-derived Cu-binding peptides (Kawano, 2006; Inokuchi et al., 2012).

In the present study, we conducted two distinct FL-based assays, namely, (1) the Hst-dependent quenching of Tb^{3+}-FL and (2) the Cu^{2+}-dependent quenching of intrinsic FL in Hst-5 and Hst-8. We emphasized the latter study focusing on the intrinsic red-FL newly found in both Hst-5 and Hst-8, since the monitoring of intrinsic FL emitted by biological molecules of interest without using artificial FL probes has advantages to be applied to a variety of future assays including microscopic, flow-cytometric studies in intact cells and organisms.

5-3 Materials and Methods

5-3-1 *Peptides and Chemicals*

Model peptides sequences with metal-binding affinity which show intrinsic red-FL under irradiation by UV, corresponding to Hst-5 (DSHAKRHHGYKRKFHEKHHSHRGY) and Hst-8 (KFHEKHHSHRGY) were synthesized to score the effect of copper occupancy. Synthesis of the peptides was tailor-made through the custom peptide service department of Sigma Genosys Japan, Ishikari, Hokkaido, Japan. The chemically synthesized peptides were purified on high pressure liquid chromatography prior to the experimental use. *Cypridina* luciferin analog designated as CLA (2-Methyl-6-phenyl-3,7-dihydroimidazo[1,2-a]pyrazin-3-one) was obtained from Tokyo Chemical Industry, Tokyo. Other chemicals such as $CuSO_4$ and terbium (III) chloride hexahydrate used in this study were of reagent grade purchased from Wako Pure Chemical Industries Ltd. (Osaka, Japan).

5-3-2 *Terbium FL and Hsts' red intrinsic FL*

Using a FL spectrophotometer (F-4500 Hitachi High-Technol. Co., Tokyo), Tb-dependent FL was detected in in K phosphate buffer (50 mM, pH 7.0) as previously described (Kawano, 2007). The three-dimensional (3D) spectral analysis of FL was carried out by scanning through the excitation wavelength between 200 and 300 nm (interval, 5 nm) and emission wavelength between 500 and 600 nm (interval, 5 nm). In the phosphate-buffered reaction mixture, the actual concentrations of free Tb^{3+} after addition of 1 mM of $TbCl_3$ were expected to be as low as at µM order due to interaction between phosphate and Tb ion.[18)] Therefore, the FL due to free Tb^{3+} can be quenched by µM ranges of peptides or chelators as previously described (Kawano, 2006; Inokuchi et al., 2012).

Usually, tyrosine (Y)-containing peptides show two peaks in intrinsic FL in the UV regions (excitation at *ca*. 230 and 280 nm, and emission at *ca*. 320 nm) which is non-specific to the nature of proteins. In addition, in biological samples, FL signals in the

UV regions can be hardly distinguished from the background FL due to a variety of proteins, phenolics, catecholamines, and other aromatic molecules. Therefore, we focused on the intrinsic red-FL signals specific to Hst sequence commonly found in both Hst-5 and Hst-8.

Using a FL spectrophotometer, the intrinsic red-FL signals from the Hst-5 and Hst-8 (1, 3, 10, 30, and 100 μM) with and without loading of Cu^{2+} (5, 10, 15, 20, 25, 30, 60, and 100 μM) were detected in K phosphate buffer (50 mM, pH 7.0). The 3D spectral analysis of FL was carried out by scanning through the excitation wavelength between 200 and 350 nm (interval, 5 nm) and emission wavelength between 500 and 800 nm (interval, 5 nm).

5-3-3 *Detection of superoxide anion radical ($O_2^{\bullet-}$) with chemiluminescence (CL)*

To detect the generation of $O_2^{\bullet-}$, an $O_2^{\bullet-}$-specific CL agent, *Cypridina* luciferin analog (CLA) was used. The peptides (Hst-5 and Hst-8) and other chemicals were dissolved in 50 mM K-phosphate buffer adjusted at pH 7.0. The molar ratios among the components in the 200 μl of reaction mixture, the peptide, $CuSO_4$ and H_2O_2 were approximately 1:10:10 (0.15 mM peptides, 1.5 mM $CuSO_4$, 1.5 mM H_2O_2). Generation of $O_2^{\bullet-}$ was monitored by CLA-CL with a luminometer (Luminescensor PSN AB-2200-R, Atto, Tokyo), and the yield of CL was expressed as relative luminescence units (rlu).

5-4 Results and Discussion

5-4-1 *Quenching of Tb^{3+}-FL*

As previously documented (Kawano, 2006; Inokuchi et al., 2012), free Tb^{3+} showed intensive emission of FL signals upon irradiation by 224 nm UV light, dually peaking at 545 nm and 585 nm (Fig. 5-2). As expected, quenching of Tb^{3+}-FL by 30 μM of Hst-5 and Hst-8 was observed (Fig. 2). Interestingly, Hst-5 showed higher quenching activity compared to Hst-8. It is likely that the difference is possibly due to the presence of ATCUN motif in Hst-5, which is absent in Hst-8. Although limited at partial level, Hst-8 also showed quenching of Tb^{3+}-FL suggesting that HEXXH motif in Hst-8 which is considered as a Zn(II)-binding motif also do bind Tb^{3+}. As the Tb-based FL assay was originally proposed for assessing the metal-binding capacity in Cu-binding peptides (Blandl et al., 1997), we can assume that Hst-8 may interact with Cu.

5-4-2 *Cu-sensitive intrinsic red-FL*

Both Hst-5 and Hst-8 peptides (30 μM) showed intrinsic red-FL (at 610 nm) upon excitation by UV region (230 nm and 275 nm) as visualized in the contour (3D) plots of FL intensities (Fig.5-3). Fig. 4 shows the effect of peptide concentrations on the yield of red intrinsic FL by Hst-5 and Hst-8. Within the range of peptide concentration examined (up to 100 μM), both Hst peptides showed concentration-dependent increase in the yield of red intrinsic FL. The peak of FL under excitation at 230 nm showed much steeper and greater increase along with elevated concentrations of peptides.

5-4-3 *Linear relationship between loading of Cu^{2+} and quenching of FL*

As shown in Fig. 3, red-FL signals from both peptides showed tendency to be quenched in the presence of Cu^{2+}. Furthermore, effects of copper concentration on quenching of two distinct peaks of red intrinsic FL in Hst-5 and Hst-8 were examined (Fig. 5-5). Within the range of copper concentrations (up to 100 μM), curve for

quenching of intrinsic FL by 30 μM peptides were shown to be saturated. In the limited range of molar ratio of copper concentration over peptide concentration up to 2.0 (60 μM), there were linear relationships between the copper concentration and quenching of Hsts' red-FL. Compared to the 230 nm-excited FL from both Hst molecules, the 275 nm-excited fluorescent peak showed higher sensitivity to relatively low concentration of copper between 5 and 25 μM (Fig. 5-5 A,B). Notably, showed the squared correlation coefficients (r^2) for the regressions for the relationship between the copper concentration and the 230 nm-excited fluorescent peak in Hst-5 and Hst-8 were 0.9546 and 0.9684, respectively (Fig. 5-5B, insets), suggesting that changes in red-FL can be used as a measure of copper occupancy in these peptides.

5-4-4 *Catalytic activity in Cu-loaded peptides*

As discussed earlier in this report, binding of metals such as copper may confer specific functions to the peptides of interest sharing metal-binding motifs such as XXH motif (Kawano, 2007; Yokawa et al., 2009; Yokawa et al., 2009; Yokawa et al., 2011a; Kagenishi et al., 2011; Okobira et al., 2011). Accordingly, upon binding to Cu (II), these peptides containing XXH motif show $O_2^{\bullet-}$-generating catalytic activity in H_2O_2-dependent peroxidase-like manner with requirement for phenolic substrates or aromatic monoamines (Kawano and Bouteau, 2013; Yokawa et al., 2011b). As model substrates, an intermediate of neurotransmitters, tyramine (Kawano, 2007; Yokawa et al., 2009; Kagenishi et al., 2011; Okobira et al., 2011), and a structurally similar free amino acid, tyrosine (Yokawa et al., 2009; Kagenishi et al., 2011), are known to date. Our previous work on a Cu-binding peptide (GGGGGH hexapeptide designated as G_5H) demonstrated that the Cu-loaded peptide (0.15 mM) showed an enzyme-like $O_2^{\bullet-}$-generating catalytic activity (V_{max}, 52.91 mmol/ mmol peptide/ min) with Michaelis constant (K_m) 0.24 mM worked out for tyramine as a substrate, reaching the applicable range especially as the catalytic activity was evaluated by molecular weight-basis which is almost 1/6 of purified horseradish peroxidise (Kagenishi et al., 2011).By analogy, we view that Hst-5 and Hst-8 may show such catalytic activity.

In support of the above view, Tay et al. (Tay et al., 2009) have shown that Cu-bound form of Hst-5 catalyses the H_2O_2-dependent oxidation of catechol. However, $O_2^{\bullet-}$ could be hardly generated in the presence of catechol as Kagenishi et al. (Kagenishi et al., 2011) have thoroughly studied that phenol and the *m*-positioned benzenediol (resorcinol) were shown to be active as $O_2^{\bullet-}$-generating substrates by Cu-bound peptides, while *o*- and *p*-positioned benzenediols (catechol and hydroquinone) were shown to be inactive. Furthermore, natural frequency that Hst-5 meets catechol in salivary media should not be high unless suplemented with foods.

Interestingly, without supplementation of phenolics, catecholamines or related free molecules, tyrosine (Y) residue-containing oligopeptide sequences fused to Cu-binding XXH motif such as NPGYPH (chicken prion hexa-repeat sequence) (Yokawa et al, 2010), GGGYGH (plant ozone-inducible peptide sequence) (Yokawa et al, 2011a), and FLTEYVA-GGGGGH (Erk1/Erk2 MAP kinase substrate sequence fused to G5H peptide, thus designated as Erk-G5H) (Yokawa et al, 2010), showed catalytic activity for H_2O_2-dependent $O_2^{\bullet-}$ generation without supplementation of any free phenolic substrates. Involvement of Y-residue(s) in the Cu/peptide complex-catalyzed reactions suggests that a phenoxy radical derived from Y (tyrosyl radical, $Y^{\bullet}$) can be formed in aid of single electron reduction of molecular oxygen, by analogy to plant enzymes H_2O_2-dependently generating $O_2^{\bullet-}$ by coupling to oxidation of phenolics to form phenoxy radicals (Kawano, 2011; Kawano et al., 1998). In figure 5-6 (A andB), two distinct modes of H_2O_2-dependent generation of $O_2^{\bullet-}$ by Cu-bound catalytic peptides, which are differed in requirement for free electron-donating substrate molecules (chiefly phenolics), are illustrated for comparison.

Note that both Hst-5 and Hst-8 contain corresponding metal-binding domain(s) and Y-residue(s) as illustrated in Figure 1. Therefore, we can expect that Cu-bound Hst-5 and Hst-8 show H_2O_2-responsive $O_2^{\bullet-}$ generating activity without addition of phenolic substrates as similarly to previously engineered artificial enzymes such as Erk-G5H (Yokawa et al, 2010).

Lastly, we demonstrated the H_2O_2-induced generation of $O_2^{\bullet-}$ catalyzed by the copper-bound forms of Hst-5 and Hst-8 (Fig. 5-6). Upon addition of H_2O_2 to reaction

mixture containing Cu-loaded Hst-5 and Hst-8, immediate induction of $O_2^{\bullet-}$ generation was observed. The peak height of CLA-CL was almost identical (Fig. 5-6C), but the the reaction catalyzed by Hst-5 showed tendency to be long-lasted possibly due to the doubled number of metal-binding sites and Y-residues. Since depletion of copper, peptide, or H_2O_2 from the Hst-5-mediated reaction resulted in loss of oxidative burst (except for the initial spike observed in the absence of copper; Fig.5-6D), we can conclude that Hsts become reactive against H_2O_2 only after binding to Cu. Possible involvement of this hidden action of Cu-bound form of Hsts in antimicrobial action must be examined in the future study.

5-4-5 *Perspectives*

Recently, saliva-based therapeutic protocols using artificial salivas and antimicrobial agents are recently developed based on biochemical nature of Hsts and mucins (Huq et al., 2007). As the functions of Hsts largely depend on the loading of copper or related metal ions, protocol for functional evaluation of natural and supplemented Hsts in saliva or artificial media relating the binding of copper and/or other ions must be developed. The present study may provide key fluorometric and chemiluminometric knowledge supporting such approaches.

5-4-6 *Conclusion*

The most recognized roles for Hsts are anti-microbial activities, and the modes of action of Hsts (chiefly, Hst-5 and 8) have been subjected to intense debates. Since Hst-5 and 8 possess metal-binding motifs, analysis of Cu occupancy in Hsts is of great importance. FL-active rare earth element ions such as Tb^{3+} can be used for assessing the metal-binding capacity in Cu-binding peptides as previously performed for several Cu-binding peptides. In the present study, we conducted two distinct FL-based assays, namely, the Hst-dependent quenching of Tb^{3+}-FL and the Cu^{2+}-dependent quenching of intrinsic FL in Hsts. Compared to Hst-8, Hst-5 showed higher activity for quenching of Tb^{3+}-FL, possibly due to the presence of ATCUN in Hst-5, which is absent in Hst-8.

Hst-8 showed partial quenching of Tb^{3+}-FL suggesting that HEXXH motif contributes to binding of Tb^{3+}. Since the Tb-based assay was originally proposed for the study of Cu-binding peptides, we assumed that both Hsts interact with Cu. Both Hst-5 and 8 showed intrinsic red-FL at 610 nm upon excitation at 230 and 275 nm, which was shown to be quenched by Cu^{2+}. In the limited range of Cu/peptide molar ratio up to 2, there were linear relationships between the Cu^{2+} concentration and quenching of Hsts' red-FL. Therefore, the changes in red-FL can be used as a measure of Cu occupancy in these peptides.

Lastly, novel catalytic activity of Cu-loaded Hsts were demonstrated. Upon addition of H_2O_2, both Hsts catalyzed the generation of $O_2^{\bullet-}$. As the functions of Hsts largely depend on the binding of Cu or related metal ions, protocol for functional evaluation of Hsts relating the metal binding must be developed. The present study may provide key technical knowledge supporting such approaches.

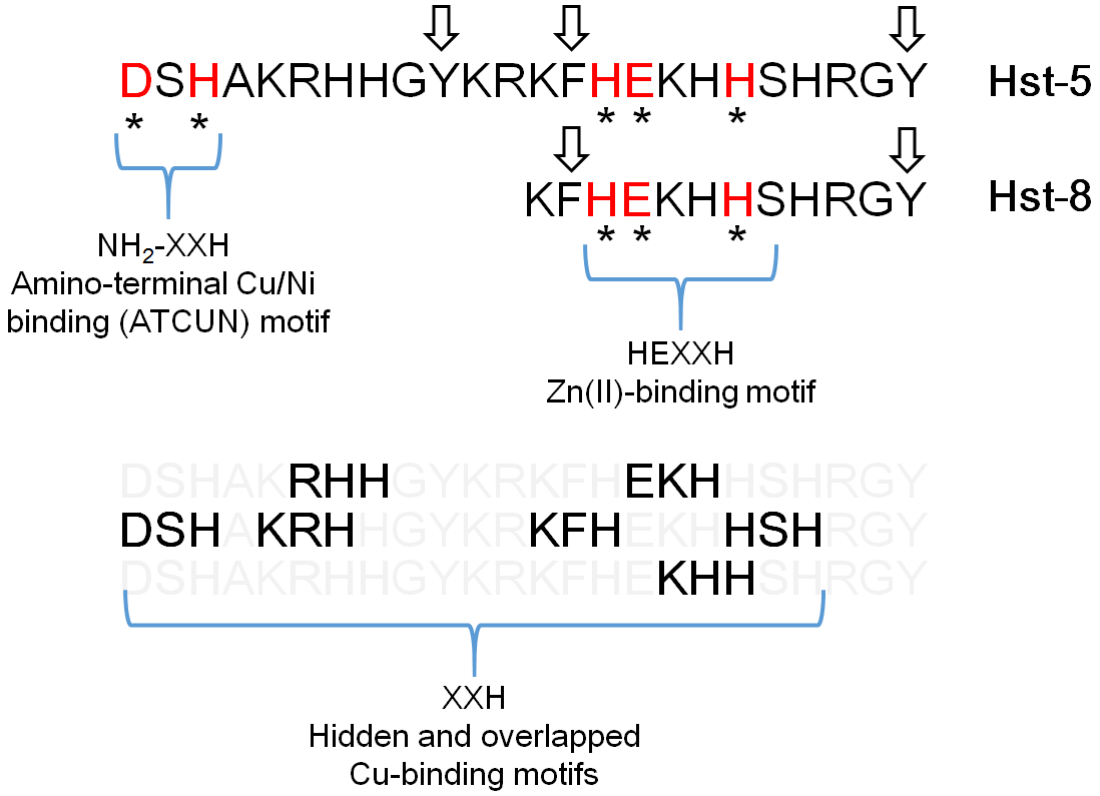

Fig. 5-1. Structures of Hst-5 and Hst-8 harboring multiple metal binding motifs.

Asterisks indicate the position of key amino acid in two typical metal binding motifs in Hsts, namely, the amino-terminal Cu/Ni binding (ATCUN) motif (NH_2-XXH) and Zn(II)-binding motif (HEXXH). In addition, overlapped presence hidden metal binding sites sharing the XXH motif known to bind a variety of metals chiefly, Cu (II), are shown. Arrows indicate the presence of aromatic amino acids which would contribute to the copper-sensitive FL signal.

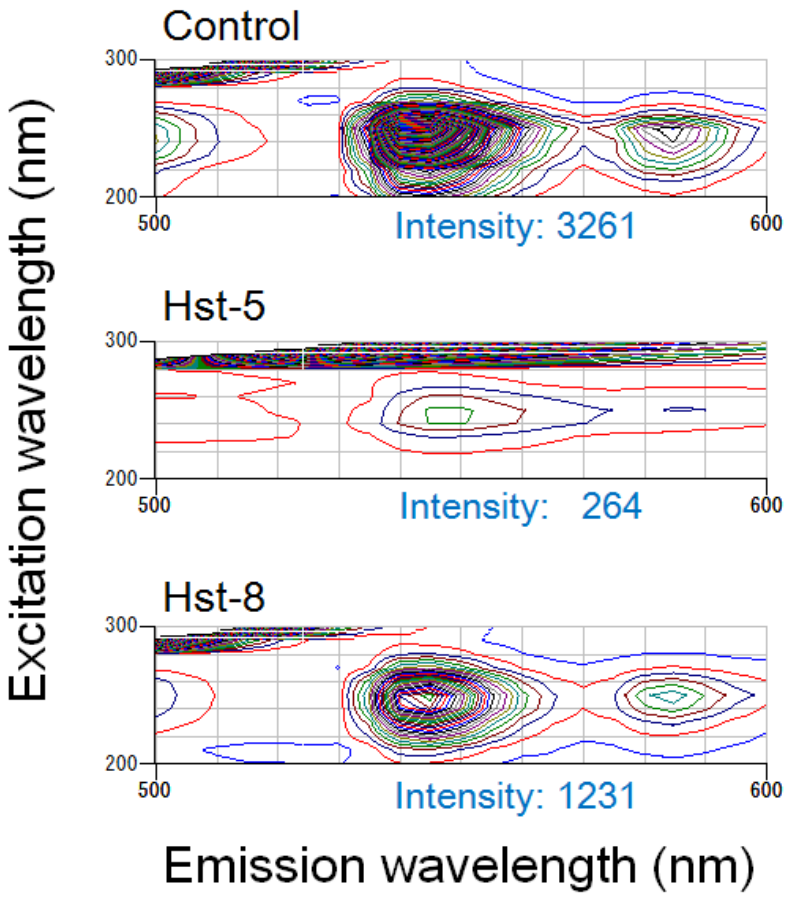

Fig. 5-2. Hst-dependent quenching of Tb FL. Typical 3D representations (contour plot) of the Tb^{3+}-FL spectra in the absence and presence of Hst-5 or Hst-8 (30 μM) are shown. Intensities of the FL signal peaking at 225 nm excitation and 545 nm emission are compared.

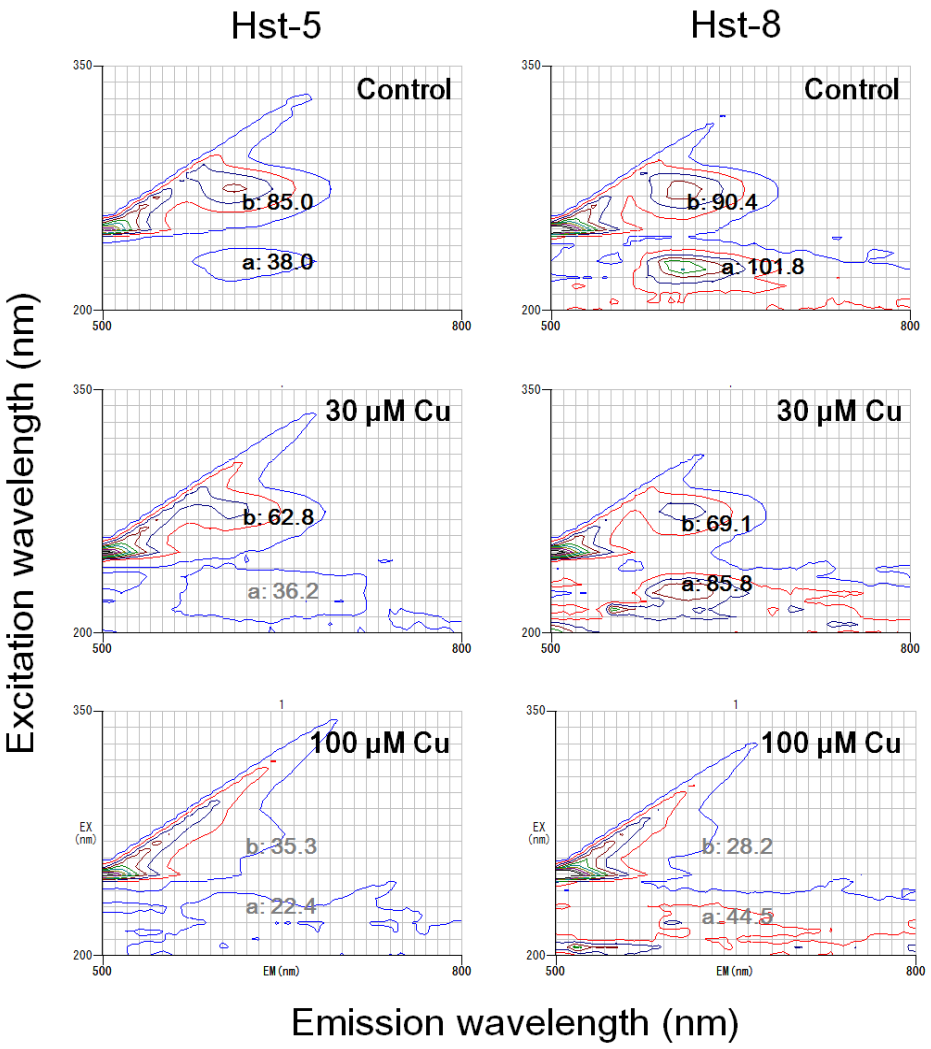

Fig. 5-3. Contour-plotted intrinsic red-FL signal from Hst-5 and Hst-8 in the presence and absence of $CuSO_4$. Peptides (30 μM) used were used. Two peaks of red-FL emission at *ca*. 610 nm were shown under excitation at 230 nm (peak a) and 275 nm (peak b). Quenching of intrinsic FL in the presence of 30 μM or 100 μM $CuSO_4$ was assessed and FL intensities at peaks (a) and (b) are shown.

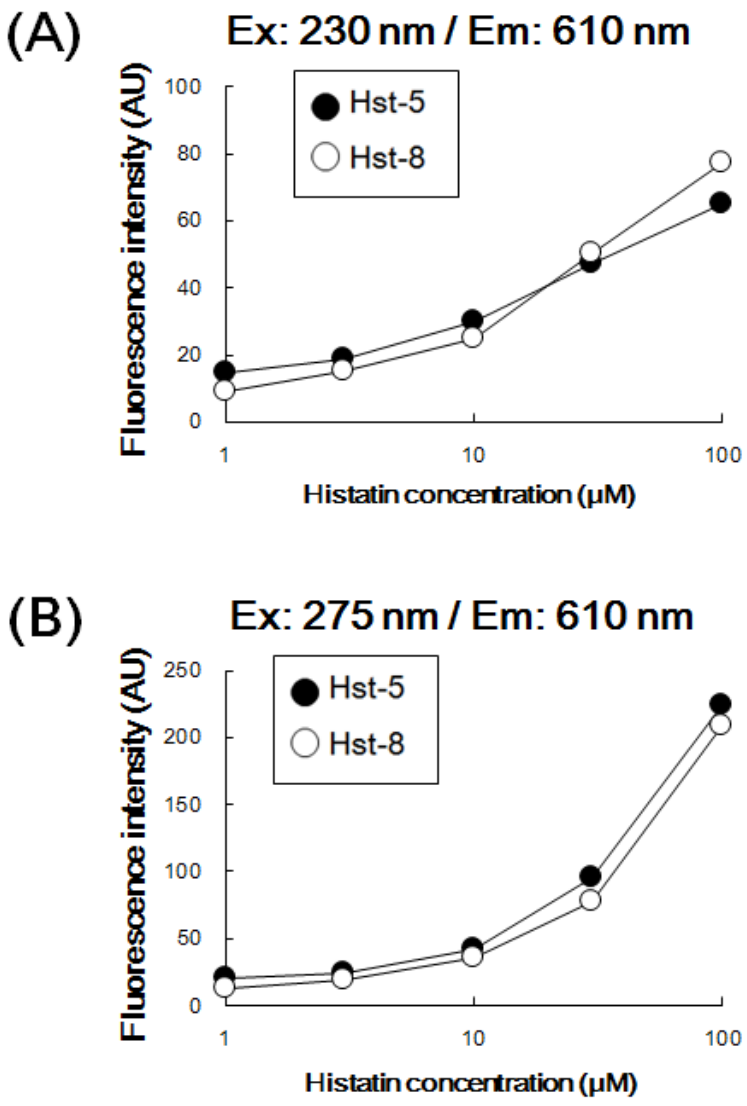

Fig. 5-4. Effect of peptide concentration on red intrinsic FL in Hst-5 and Hst-8.

(A) Effect of peptide concentrations on the yield of red-FL (610 nm) under excitation at 230 nm. (B) Effect of peptide concentrations on the yield of red-FL (610 nm) under excitation at 270 nm. AU stands for arbitrary units.

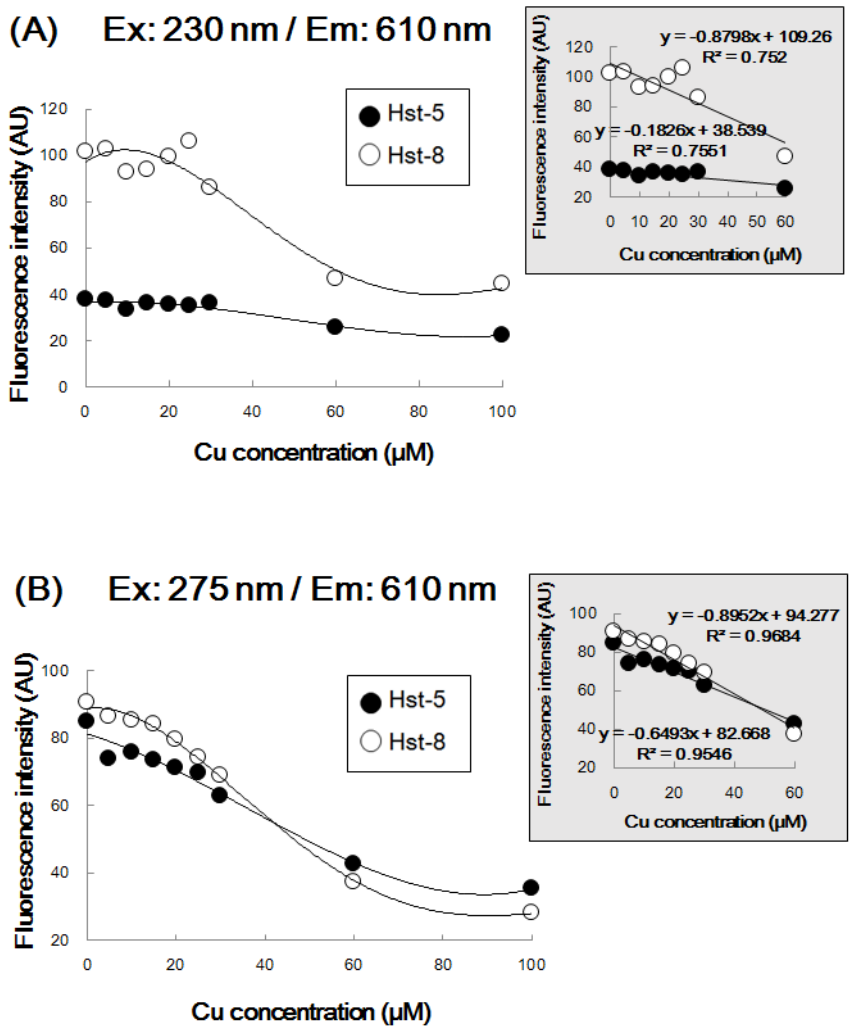

Fig. 5-5. Effect of copper concentration on quenching of red intrinsic FL in Hst-5 and Hst-8.(A) Effect of copper concentration on the quenching of red-FL (610 nm) under excitation at 230 nm. (B) Effect of copper concentration on the quenching of red-FL (610 nm) under excitation at 275 nm. Peptide concentration, 30 μM. AU stands for arbitrary units. Curves were merely for approximation of the response. In the insets, linear relationships (regressions) between the limited range of Cu concentration (up to 60 μM) and the decrease in fluorescent signals are shown.

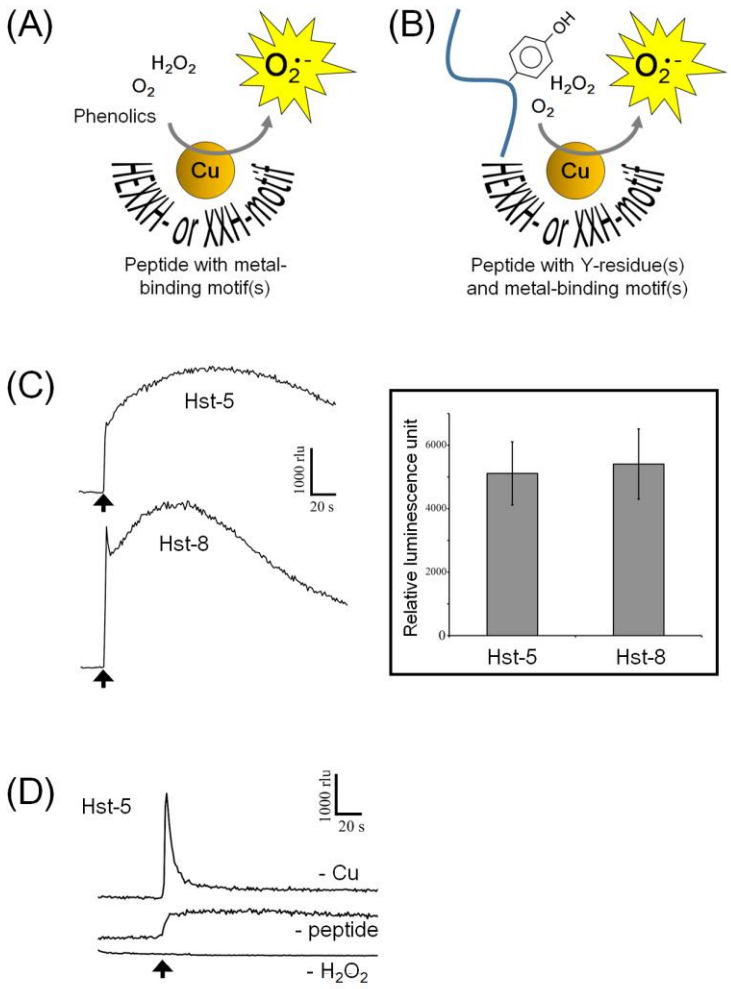

Fig. 5-6. H_2O_2-dependent $O_2^{\bullet-}$ generation catalyzed by Hst-5 and Hst-8. (A) Model mechanism for peroxidase-like H_2O_2-dependent $O_2^{\bullet-}$ generation catalyzed by Cu-bound oligo-peptides using phenolics as substrates. (B) Model mechanism for phenolics-free H_2O_2-dependent $O_2^{\bullet-}$ generation catalyzed by Cu-bound Y residue-containing oligo-peptides. (C) Typical traces of CLA-CL reflecting the generation of $O_2^{\bullet-}$. To 1.5 mM peptide (Hst-5 or Hst-8) was preincubated with 1.5 mM $CuSO_4$. Upon addition of 1.5 mM H_2O_2 (arrows), increase in CLA-CL was observed. Inset: comparison of H_2O_2-induced CLA-CL in reaction mixture containing Hst-5 and Hst-8. Error bars, Standard deviation (n=3). (D) Requirement for copper, H2O2 and a peptide for generation of $O_2^{\bullet-}$ catalyzed by Hst-5.

CHAPTER 6

Fluorometric quantification of ferulic acid concentrations based on deconvolution of intrinsic fluorescence spectra

6-1 Abstract

Ferulic acid (FA) is one of phenolics found in most higher plants. It is important to quantify the internal FA level in vegetables and fruits, since it was epidemiologically demonstrated and a number of study supported that consumption of fruits and vegetables rich in phenolic acids including FA is associated with the prevention of chronic diseases such as cancer and cardiovascular disease. In order to allow handling of the intact fresh produces, non-invasive methods are desired. Previously, 355 nm ultraviolet (UV) laser-induced fluorescence spectrum revealed that living plants contain fluorophore corresponding to blue-green fluorescence (shown to be FA). However, quantification of FA based on fluorescence in UV-excited leaves can be hardly achieved since FA fluorescence measured at fixed excitation and emission can be applied only to the limited range of FA concentration. Here, we report a model experiment for fluorometric quantification of FA in solution *in vitro* which may provide a series of useful information required for estimation of FA concentrations *in vivo* fluid inside the vegetables. Based on deconvolution of intrinsic fluorescence spectra, we observed that FA fluorescence signals can be deciphered to determine the concentration of FA. By viewing that the recorded FA fluorescence (*h*) is reflecting the primitive function (*f*) corresponding to FA concentrations and kernel function (*g*) determining the spike position in the spectra. Thus, *f* should be obtained as $f = h \times g^{-1}$. In practice, cumulative curves of fluorescence signals at fixed emission wavelength (460 nm) along with the changes in excitation wavelength (200-400 nm) were plotted and the midpoints (along the scale of excitation wavelength) in the resultant curves corresponding to different FA concentration were graphically determined. FA's concentration-specific changes in fluorescence profiles must be due to the fact that FA possesses multiple fluorophores within the molecule despite its simple structure. Lastly, simplified protocol for determination of FA concentration using dual UV excitation wavelengths was proposed. In this assay, ratio of 460 nm fluorescence intensities induced by two distinct excitation wavelengths (short, 260 nm; long, 330-380 nm) were shown to be highly correlated with FA concentration ranged from μM to mM orders.

Keywords: fluorescence, mathematical handling of spectra, plant phenolics, sensing protocol.

6-2 Introduction

In plants, biosynthesis of an array of phenolic compounds, associated with plant development, senescence and chemical or physical defense mechanisms against invasion by pathogens, proceeds from *trans*-cinnamic acid, the first metabolite in the phenylpropanoid pathway (Kawano et al., 2004). The compounds produced *via* phenylpropanoid pathway include lignin, flavonoids, phytoalexins and a variety of phenolics.

Ferulic acid (FA) is one of such plant-specific phenolics, which is a simple polyphenol found in most higher plants as one of key components in cell wall complex (Johnson et al., 1998; Lichtenthaler and Schweiger, 1998; Buschmann et al., 2000). In the cell-walls of higher plants, members of hydroxycinnamates including FA are known to be derived from feruloyl-CoA, coumaroyl-CoA and other intermediates in the phenylpropanoid pathway (Brett et al., 1999). FA and *p*-coumaric acid are also known to tightly bound to the epicuticular waxes of the leaves of *Prunus persica* and *Olea europaea* (Liakopoulos et al., 2001). It has been suggested that life-stage dependently increased FA content in young plants such as seedlings of winter triticale may prevent the damages to photosynthetic apparatus under strong sunlight (Hura et al., 2010).

There have been a number of studies relating the human and animal health cares and the actions of FA and its derivatives. Recent advancement in analytical techniques using dispersive solid phase extraction and high-performance liquid chromatography with tandem mass spectrometric detection methods (LC-MS/MS), enabled a sensitive detection of FA circulating in human blood after orally taking vegetables (Mülek and Högger, 2015). Today, medical or pharmacological uses of FA in chemotherapeutic strategies against cancer are intensively discussed. FA applied in combination with an inhibitor of poly(ADP-ribose)polymerase, ABT-888, may serve as an effective combination chemotherapeutic agent of nature and biological origins (Choi et al., 2015). A recent clinical investigation revealed that FA in the extract from the roots of *Angelica sinensis* effectively contributes to the nephroprotective action of this herbal medicine

against the damages induced by cisplatin, a chemotherapeutic drug targeting tumor, at least through reduction of apoptosis rate (Bunel et al., 2015).

Antipyretic, analgesic and anti-inflammatory drugs in Japanese traditional herbal medicine (known as Shoma, which is dried rhizoma of *Cimicifuga* sp.) contains FA and its isomer isoferulic acid as the main active components which can effectively suppress the inflammation in murine macrophage cell line, RAW264.7, through inhibitory effects on the production of macrophage inflammatory protein-2 known to be induced in response to respiratory syncytial virus (Sakai et al., 1999). It was epidemiologically demonstrated that consumption of fruits and vegetables rich in phenolic acids including FA is associated with the prevention of chronic diseases such as cancer and cardiovascular disease, most likely by induction of detoxifying cellular phase II enzymes (phenolsulfotransferases) which are associated with cancer preventive potentials (Yeh and Yen, 2005). Furthermore, for unknown reason, FA might act against the high-fat and high-fructose diet-induced metabolic syndromes as tested in rats (Wang et al., 2015).

A number of studies suggested that FA is highly reactive against the members of reactive oxygen species (ROS), thus, this molecule may prevent the oxidative damages in living cells and ROS-mediated denature of proteins (Sgarbossa and Lenci, 2013). Recent demonstration further confirmed that FA protects the cells of human challenged by oxidative stress, as H_2O_2-induced apoptotic cell death in human embryonic kidney 293 cells (HEK293) was inhibited by pretreatment with FA (Bian et al., 2015). In addition to direct action of FA, the likely mechanisms suggested include indirect action of FA in induction of catalase and superoxide dismutase (Bian et al., 2015). Therefore, in order to prevent the ROS-mediated damages in human body, it is highly recommended to take vegetables and fruits rich in FA content (Park et al., 2015).

As discussed above, it is important to quantify the internal FA level in vegetables and fruits, thus, non-invasive methods are desired in order to allow handling of the intact fresh produces. Conventionally, FA-specific spectroscopic analysis was performed with extracts from vegetables and fruits (Yeh and Yen, 2005) and FA-conjugated lipids in edible oils such as rice bran oil (Hara et al., 2016), but this method

cannot be extended to applications in non-invasive approach. In this point of view, fluorometric approach has some advantages and there have been several reports on quantification of FA based on its intrinsic fluorescence. Meyer et al. (2003) have reported that the intact leaves of vegetables such as leafy lettuce often emit both red and far-red fluorescence signals upon irradiation by chlorophyll-targeting UV radiation. Notably, blue-green fluorescence is also emitted upon irradiation by UV, since hydroxycinnamic acids chiefly, FA bound to cell wall are readily excited, therefore, FA is known as the main blue-green fluorescent component in various plants (Liakopoulos et al., 2001; Buschmann et al., 2000; Johnson et al., 2000).

According to Tanaka et al. (2009), 355 nm ultraviolet (UV) laser-induced fluorescence spectrum recorded with a single intact leaf attached to a street *Zelcova* tree suggested that blue-green fluorescence can be detected by application of remote-sensing technology such as laser-induced fluorescence (LIF) spectrometry. The blue-green range of fluorescence could be most likely attributed to the presence of FA in the leaf. In a number of plant samples including the leaves of spinach (Goulas et al., 1990) and sugar beet (Morales et al., 1996, 1998), on both the adaxial and the abaxial sides of leaves were dominated by blue-green fluorescence of epidermis, upon excitation under UV radiation, and FA was the only fluorophore that emitted fluorescence in a similar manner to epidermis, thus, it was concluded that FA as the main fluorophore of the epidermis in such plants listed above.

However, quantification of FA based on fluorescence in UV-excited leaves can be hardly achieved since FA fluorescence measured at fixed excitation (355 nm) and emission (450 nm) can be applied only to the highly limited range of FA concentration (Meyer et al., 2003).

Here, we report a model experiment for fluorometric quantification of FA in solution *in vitro* which may provide a series of useful information required for estimation of FA concentrations *in vivo* fluid inside the vegetables. Based on deconvolution of intrinsic fluorescence spectra, we observed that FA fluorescence spectra can be altered depending on the FA concentrations. Therefore, existing

fluorometric methods based on single band measurements should be subjected to reconsideration.

6-3 Materials and Methods

6-3-1 *Spectroscopic and Fluorometric analysis.*

FA (Fig. 1A) and all chemicals used in analytical procedures were purchased from Wako Pure Chemical Industries, Ltd. (Osaka, Japan). FA (0.1, 0.5, 1.0, 5.0, 10.0 mM) dissolved in 2 ml absolute ethanol was used for spectroscopic and fluorescence analyses using a spectrophotometer (Shimadzu UV-1800, Kyoto, Japan) and a fluorescence spectrophotometer (F-4500, Hitachi High-technologies, Tokyo, Japan), respectively. For fluorometric analysis of FA's intrinsic fluorescence, three-dimensional (3D) contour plot was performed as demonstrated elsewhere (Sergiel et al., 2014; Park et al., 2015). This approach is often performed for analyses of various plant pigments such as chlorophyll catabolites (Kawano et al., 1999).

6-3-2 *Deconvolution of fluorescent spectra reflecting the concentration of FA.*

By assuming that spectra of fluorescence measured in the presence of FA represents the mixture of (i) concentration-specific integrating patterns of intrinsic FA fluorescent signal which can be altered depending of the FA concentration, which should be expressed as the primitive function of FA concentrations, and (ii) opposing differential modification causing splitting of FA fluorescence signals which is considered as the kernel function determining the spike position in the recorded spectra. Therefore, intensity (h) of recorded signals can be considered as the composite function derived after conjunction of the primitive function (f) and the kernel function (g). Taken together, the primitive function (f) should be obtained as follows:

$$f = h \times g^{-1}$$

where g^{-1} is an integral kernel function allowing conversion of h into f. This can be practically performed simply through integral conversion of fluorescence spectra obtained at fixed emission wavelength (460 nm) along with the changes in excitation wavelength (200-400 nm).

6-4 Results and Discussion

6-4-1 *Spectroscopic and fluorescent profiles of FA*

We have confirmed that free FA shows absorption at 330 nm and linear relationship between the FA concentration and the changes in absorbance was obtained (Fig. 6-1B, C), suggesting that FA specifically absorbs UV radiation. On the other hand, due to the presence of FA, plant leaves reportedly exhibits a blue-green fluorescence, with emission peaking in the ranges between 405 and 475 nm (blue emission) and between 510 and 550 nm (green emission) upon excitation by UV radiation (Johnson et al., 2000). For analysis of FA intrinsic fluorescence, 3D contour plot was performed (Fig.6-2). When the concentration of FA was higher than 1 mM, only single area of fluorescence with sharp excitation maximum at 360-385 nm and broad emission maxima ranging from 400 nm to 650 nm was observed. Interestingly, this analysis suggested that there is two additional areas of intensive FA fluorescence which could be visualized only at relatively lower concentrations of FA (Fig. 2, see 0.1 mM and 0.5 mM). In these additional fluorescence bands, excitation maxima were shown to be at 260 nm or 300 nm and intensive but broad emission was shown to span from *ca*. 380 nm to 600 nm.

6-4-2 *Concentration-dependent changes in fluorescent profile*

As shown in Fig. 6-3, peaks of fluorescent signal (emission, 460 nm) are highly sensitive to the changes in FA concentration. At lowest concentration examined (0.1 mM), three major peaks (at 260, 300 and 340 nm of exciting) can be observed.

The peak of fluorescence induced by short wavelength UV (260 nm) disappeared as FA concentration was elevated to the mM range. The peak(s) induced by long-wavelength UV showed FA concentration-dependent tendency to shift from peaking at 340 nm of excitation (at 0.1 mM) towards peaking at 385 nm of excitation (at 10 mM) (Fig. 6-3). Above data strongly suggested that FA fluorescence profile is concentration-

sensitive, thus, fluorescence signal may tell us the clues for estimation or quantification of FA content in the fluid.

6-4-3 *Natural role and concentrations of FA in plants*

Not only as a ubiquitous building block for lignocelluloses in plant kingdom (Saulnier and Thibault, 1999), FA may has multiple roles. In case of wheat, major form of compounds derived from phenolics is insoluble bound FA and interestingly FA present in such form contribute to resistance to wheat fungal diseases (Gelinas and McKinnon, 2006). FA is naturally found in the seeds of apple, artichoke, peanut, orange, and coffee, and most commelinid cereals such as barley and rice. In commelinid seeds, FA is localized in the bran the hard outer layer of grain, therefore FA-cojugated oils can be readily extracted from the rice bran (Hara et al., 2016). The highest range of FA concentrations in the glucosilated form has been found in seed of flax (*Linum usitatissimum*) reaching 0.02% of total dry weight (Beejmohun and Fliniaux, 2007).

6-4-4 *Estimation of FA concentration based on fluorescent profiles*

In general, the blue-green fluorescence tends to be relatively more intensive than chlorophyll fluorescence in monocotyledonous plants but not in dicotyledonous plants, due to high contents of FA and related phenolics (Lichtenthaler and Schweiger, 1998). In leafy lettuce, Meyer et al. (2003) found that the decrease in chlorophyll fluorescence and the increase in FA-dependent blue-green fluorescence coincide along with aging of tissues, without altering the shape of excitation and emission spectra or the lifetime of fluorescence.

To date, the known factors altering the fluorescence intensities in plants are (1) the changes in the concentration of emitting substances (chiefly, FA and chlorophylls), (2) changes in internal optic nature in the leaves which determine the penetration of excitation radiation (and partial re-absorption of the fluorescent signal), and (3) distribution of energy between photosynthesis, heat production and chlorophyll fluorescence (Buschmann et al., 2000). However, changes in the shape of excitation and

emission spectra along with the change in FA concentration have not been documented to date.

6-4-5 *Deconvolution of scanned FA fluorescence: Correlation between geometric center of UV-excited (200-400 nm) FA fluorescence and FA concentration*

There have been a number of approaches for deciphering the fluorescent profile from biological molecules with and/or without aids with additional fluorescent probes. For example, fluorometric studies in living cells often employ the fluorophore showing altered fluorescence profile upon binding to target chemicals such as calcium ion (Tsien et al., 1985), or pair of molecules (one must be a fluorophore) showing FRET (fluorescence resonance energy transfer) effect (Adams et al., 1991). By analogy, we attempted simple and practical deconvolution approach here.

As stated in the Material and Method section, we assume that the spectra of FA fluorescence measured in ethanol is made up after compromised actions of (i) concentration-specific integral patterns of intrinsic FA fluorescent signal which can be altered depending of the FA concentrations, and (ii) opposing differential modification allowing splitting (peaking) of FA fluorescence signals at specific excitation wavelength.

Thus, former function should be expressed as the primitive function of FA concentrations and the later function is considered as the kernel function determining the spike position in the recorded spectra. Therefore, as shown in Fig.6-4 (A), intensity (h) of recorded FA fluorescence signals can be considered as composite function derived after conjunction of the primitive function (f) and the kernel function (g). By definition, f should be obtained as follows:

$$f = h \times g^{-1}$$

In practice, we can simply work out the curves for relative increase in f (where f = 1.0 is the maximal value), by integrating the fluorescence signal at fixed emission wavelength (460 nm) along with the changes in excitation wavelength (200-400 nm) (Fig. 6-4B). The resultant plot (x axis, excitation wavelength; y axis, f (0→1.0) of

relative signal increase) displays the effect of FA concentration on the rate of increase in *f*. By focusing on the *x*-axis value (excitation wavelength) corresponding to $f = 0.5$, we can evaluate the impact of FA concentration on the fluorescent patterning.

The reason why FA shows different profiles of fluorescence depending on its concentration should be attributed to the fact that even the monomer of FA possesses multiple fluorophores within the molecule despite its simple structure, unlike most natural fluorescent molecules of biological origins (Djikanović et al., 2007). This hypothetical view must be examined in the future studies.

For simplification, we viewed the curves of f_i (x), with *i* corresponding to FA concentrations, as S-shaped sigmoidal curves. As originally shown by Pierre François Verhulst (1838), a logistic function or logistic curve shows a common sigmoid "S-shaped" curve, with standard equation:

$$f_i(x) = \frac{L}{1+e^{-\alpha(x-x_0)}} = \frac{L}{1+\frac{1}{e^{\alpha(x-x_0)}}}$$

By definition, values of *x* range between $-\infty$ and $+\infty$ of real numbers but we need to limit and shift the range within the range of realistic FA concentrations, the midpoint in sigmoid curve is defined by x_0 (which might correspond to FA concentration), *L* is the maximum value (in case of above curves, 1.0), and α defines the curve's steepness. This type of simplified mathematic approach may help us developing a simulative model. Such simulations must be performed in the future studies.

6-4-6 *Simplified measure of FA concentration with dual UV excitation wavelengths*

Although, the approach described above (scanning the excitation wavelength against the fixed emission wavelength) could provide a powerful tool for quantification of FA, actual application in non-destructive remote sensing techniques is not realistic. Therefore, we further propose a simplified and practical approach, in which, instead of continuous scanning the excitation wavelength between 200 and 400 nm, a pair of fixed UV light sources are used. In this dual UV excitation protocol, reading of 460 nm blue emission at two distinct excitation wavelengths, namely, short (260 nm) and long (330-

380 nm) UV (expressed as Long/Short ratio) showed significant correlation with FA concentration covering from μM order to mM order (Fig. 6-5).

As showed in figure 4B, only limited range (0.1 mM and 0.5 mM) of FA concentration can be detected by the geometric center-based fluorimentic approach, therefore, in combination with quantification by long/short fluorescence index (applicable in lower concentration down to μM order), we can cover broader range of FA concentrations.

6-4-7 *Perspectives*

There is additional fluorometric topic in which FA is likely involved in. According to Sgarbossa and Lenci (2013), FA interacts with several proteins and modify the biological activities of these proteins. Furthermore, intrinsic fluorescence by proteins due to the presence of tyrosine residues can be quenched by binding of FA to proteins. The mechanism of the FA action against the tyrosine-dependent fluorescence is under investigation, and it is most likely that FA action is not specific but acting as inner filter to block the fluorescence from tyrosine-residue (Sgarbossa and Lenci, 2013).

Non-destructive monitoring of lettuce leaf fluorescence reflecting the FA content and chlorophyll contents have been performed using LIF technology (Ishizawa et al., 2002). However, determination of FA concentration by LIF was hardly performed. In fact, single-band LIF may face the difficulty of FA quantification as we brought about, in this report, the discussion on the problems associated with single-band excitation-based scoring of the FA fluorescence. Therefore, we propose the use of dual-band UV LIF for simple quantification of FA in growing plant tissues *in vivo* as model demonstration for determination of FA content with dual excitation bands were successfully performed (Fig. 6-5).

FA measurements by such dual LIF technology may help quantifying FA content not only in the living plants in the fields, but also in the products after harvesting, such as the grains of wheat (Pussayanawin et al., 1988; Saadi et al., 1998) and rice bran oil (Hara et al., 2006). In fact, in general, monocots are rich in FA and its derivatives, so

that leaves of monocots can be distinguished from those of dicots solely based on the intensity of FA fluorescence (Panneton et al., 2010).

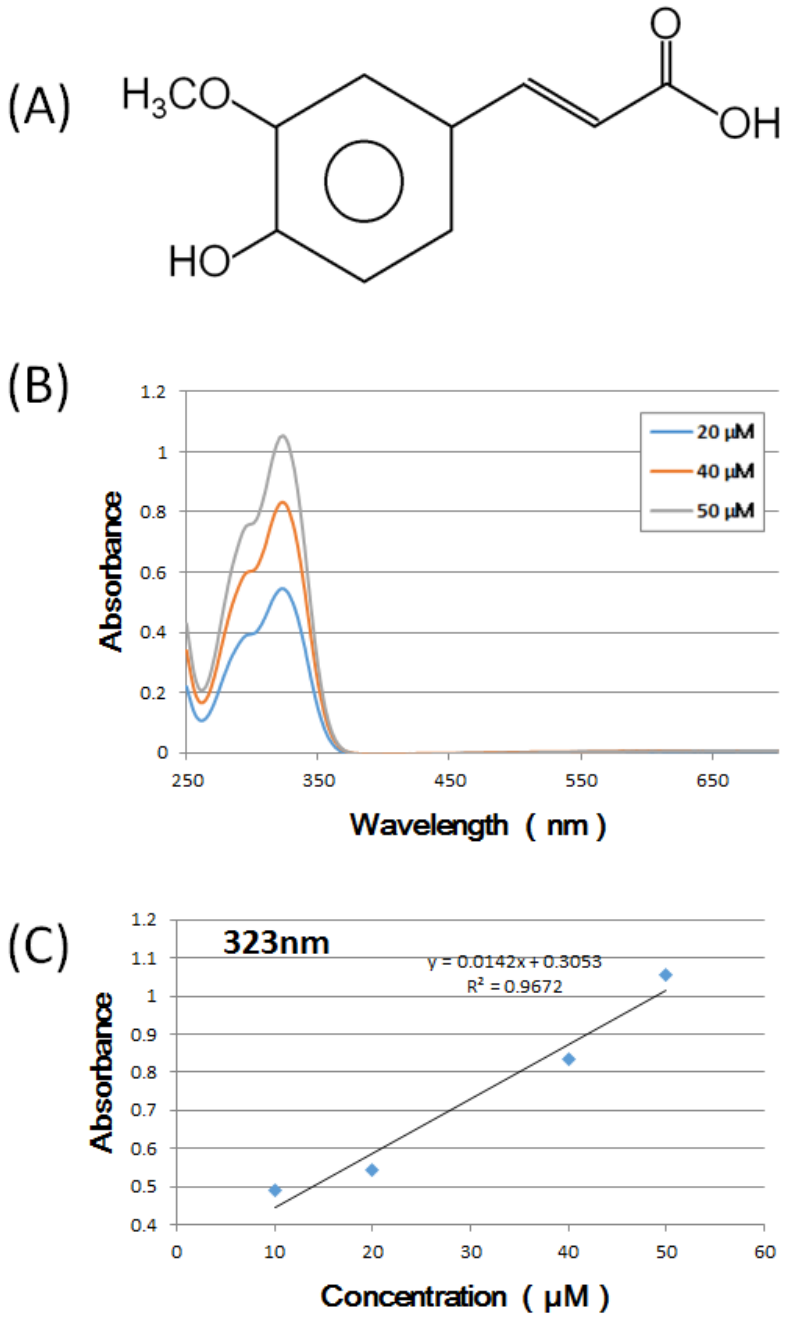

Fig. 6-1. Spectroscopic profile of feruric acid (FA). (A) Structure of FA. (B) Absorbance spectra of FA solutions (20, 40, and 50 μM dissolved in absolute ethanol) showing the peak of absorbance at 330 nm. (C) Relationship between FA concentration and absorbance at 323 nm.

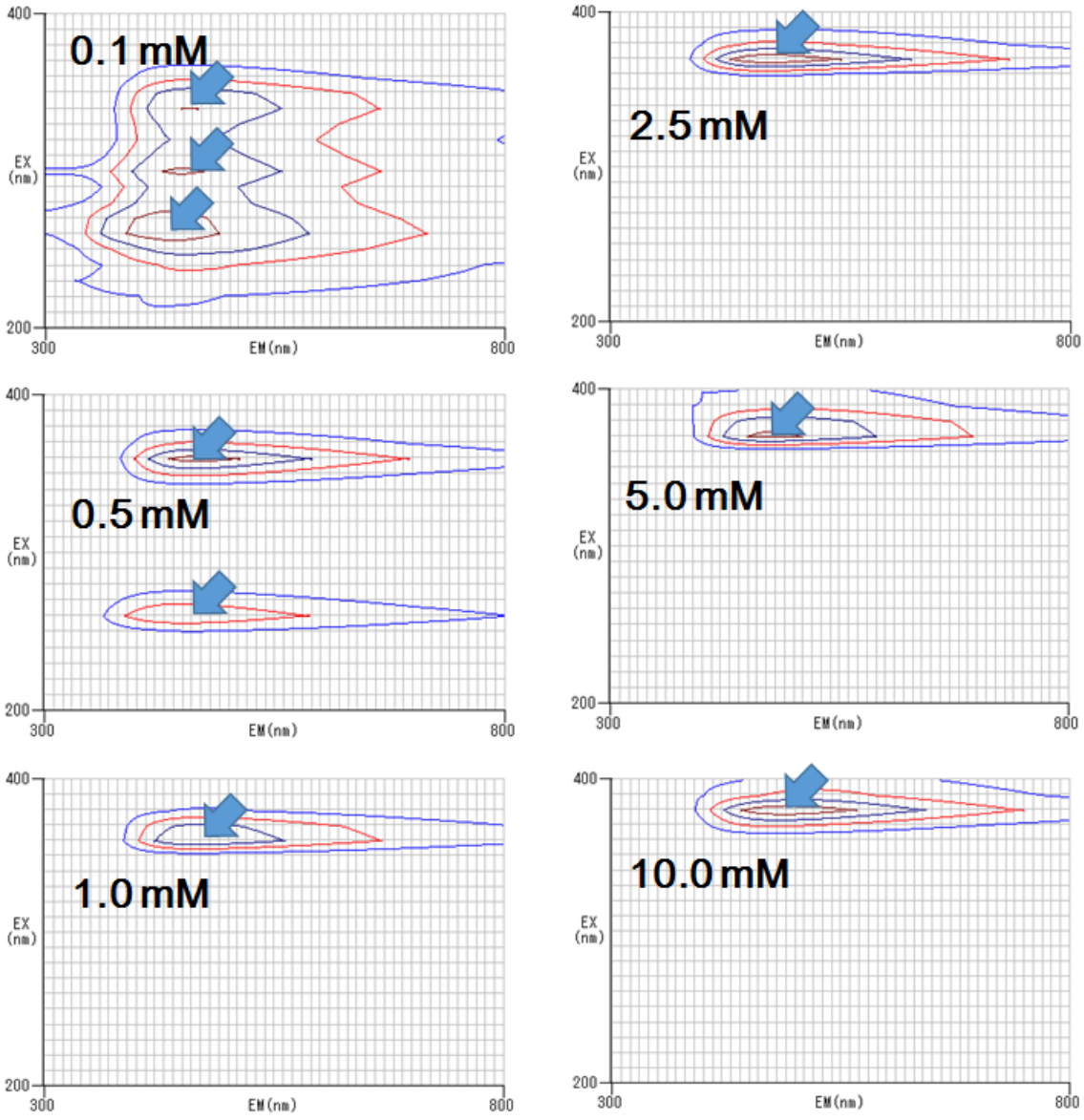

Fig. 6-2. Intrinsic fluorescence of FA. Typical 3D representations (contour plot) of fluorescence emitted by different concentrations FA. Contour-plot of FA-dependent fluorescence spectra were performed as described elsewhere (Kawano et al., 1998). FA concentrations; 0.1, 0.5, 1.0, 2.5, 5.0, 10.0 mM. Arrows indicate the peaks of fluorescence.

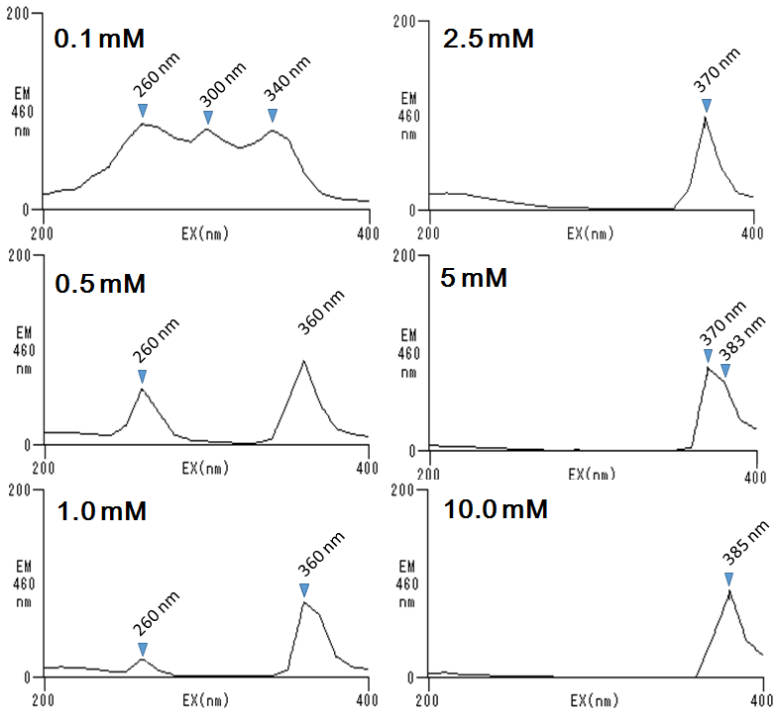

Fig. 6-3. Fluorescence spectra (emission at 460 nm) of FA at various concentrations examined under excitation by UV range (200-400 nm) of radiation.FA concentrations; 0.1, 0.5, 1.0, 2.5, 5.0, and 10.0 mM.

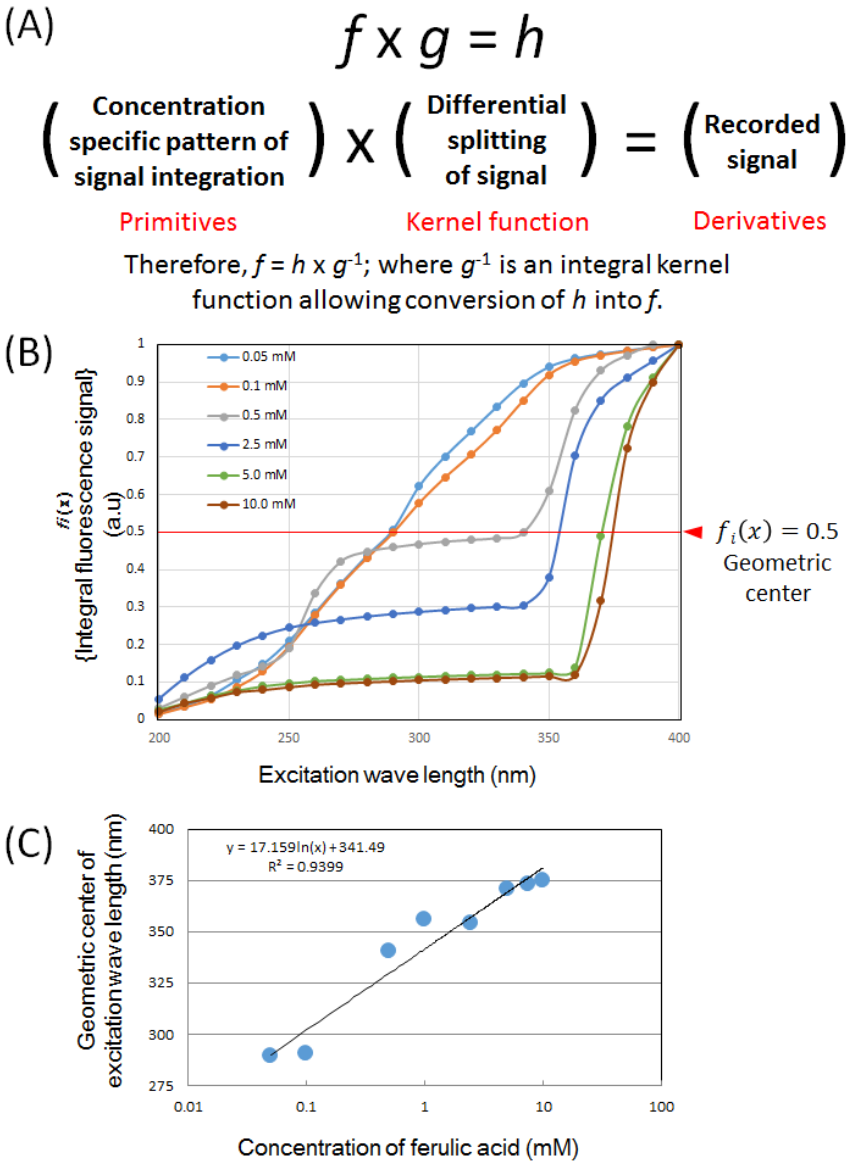

Fig. 6-4. Possible quantification of FA concentration in ethanol through deconvolution of intrinsic FA fluorescence spectra. (A) Concept on the deconvolution of intrinsic fluorescence spectra. (B) Concentration-dependent changes in integral patterns of FA fluorescence signal $\{f_i(x)\}$ and plotted against the increase in excitation wavelength. Geometric center of FA fluorescence spectra within UV excitation range (excitation wavelength required for achieving $f_i(x) = 0.5$) can be graphically identified. (C) Relationship between the geometric center of FA fluorescence spectra and FA concentration.

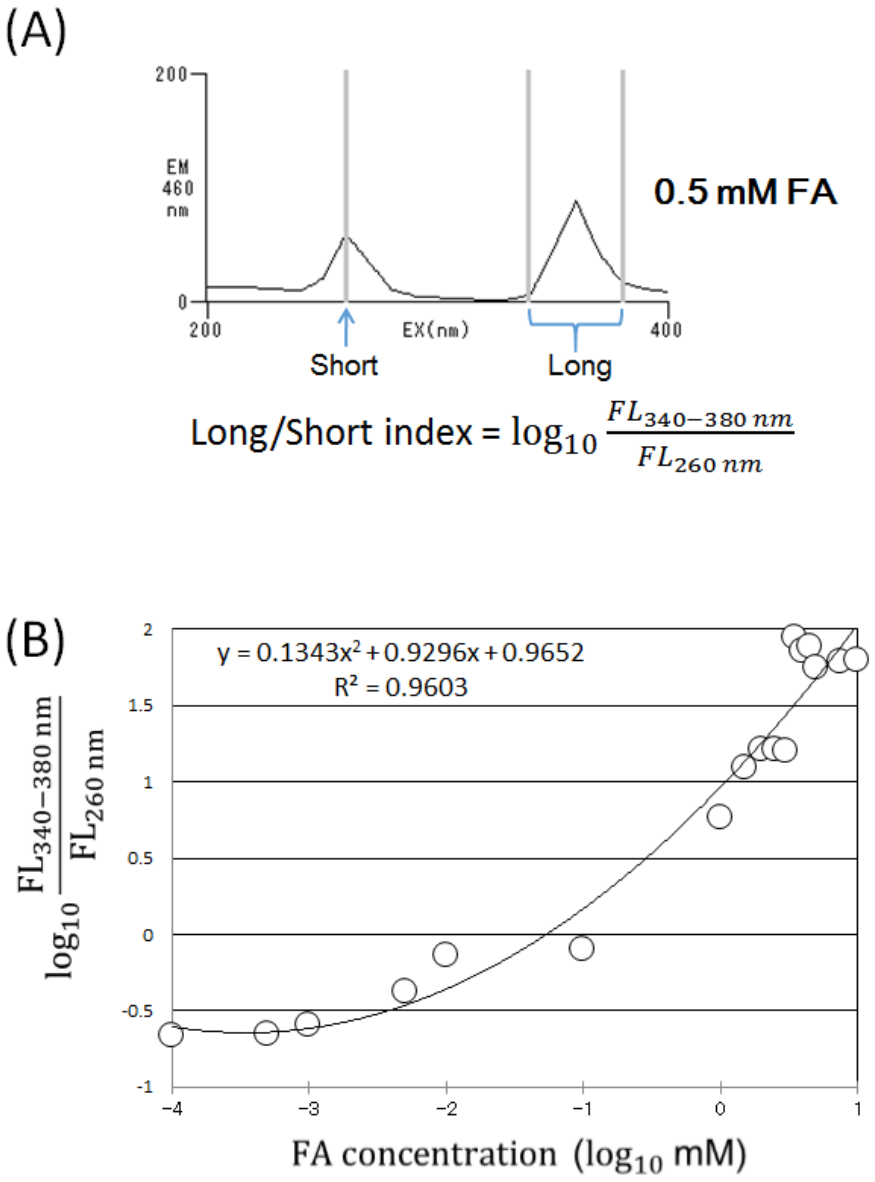

Fig. 6-5. Dual band ratio for quantification of FA. (A) Definition of Long/Short fluorescence index which is logarithm of the ratio of 460 nm fluorescence signal obtained under excitation by short wavelength UV radiation (260 nm) over that under excitation by long wavelength UV (340-380 nm). (B) Relationship between FA concentration and Long/Short fluorescence index.

CHAPTER 7

General Discussion

CHAPTER 3 Fluorescence measurements revealed two distinct modes of metal binding by histidine-containing motifs in prion-derived peptides

フリーの Tb^{3+}イオンは励起波長 225 nm、蛍光波長 545 nm, 585 nm の２ヶ所で自家蛍光のピークが得られることが判明した。また、Tb 由来蛍光の蛍光強度がオクタリピートペプチドと結合することで減少し、特に GGGWGQPH の配列をもつペプチドが、最も強い Tb 由来蛍光の消光能をもつことが判明した。

以上より、フリーの Tb^{3+}イオンは２ヶ所で自家蛍光のピークを持ち、オクタリピートペプチドと結合することで消光されることが判明した。Tb^{3+}イオンの蛍光特性と銅イオンの挙動との類似性のため、Tb^{3+}イオンは複数のアミノ酸から構成される銅結合ペプチドから成る、半金属複合構造体の挙動解析研究のモデルとして、用いることが可能であると考察される。

また、Tb 由来蛍光がオクタリピートペプチドと結合することで消光し、特に GGGWGQPH の配列をもつペプチドが、最も強い消光能をもつことが判明した。これより、C 末端が His で終わる X-X-H モチーフのペプチドが、金属との結合力が最も強いと考察される。

ヒト PrP・オクタリピート領域由来ペプチドである PHGGGWGQ を用いて実験を行った結果、このペプチドは自家蛍光を持つことが確認された。また、このオクタリピートペプチドの自家蛍光は Trp 由来のものであり、ペプチドを構成するアミノ酸(Pro, His, Gly, Trp, Gln)のなかで、Trp のみが自家蛍光の大きなピーク（ 励起波長 280 nm 蛍光波長 365 nm ）と小さなピーク（ 励起波長 230 nm 蛍光波長 365 nm ）を持つことが確認された。

オクタリピートペプチドおよび Trp の自家蛍光を銅の添加前後で比較した結果、両者の自家蛍光は銅添加後に消光していることが確認された。さらに、銅濃度が上昇するにつれて、ペプチドおよび Trp 由来の蛍光強度が減少していくことから、銅添加による両者由来蛍光の消光には銅濃度依存性があり、実験に

用いたオクタリピートペプチドの中で銅に対する感受性が最も強いのは、PHGGGWGQ であることが判明した.

以上より、オクタリピートペプチドの自家蛍光は Trp 由来のものであることが判明した。これより、オクタリピートペプチドの蛍光特性には Trp が必要不可欠であると考察される。

また、銅添加によるオクタリピートペプチドおよび Trp 由来蛍光の消光には銅濃度依存性があり、用いたオクタリピートペプチドの中で銅に対する感受性が最も強いのは、PHGGGWGQ であることが判明した。実験に用いた大半のペプチド由来の蛍光強度が、ペプチドに対する濃度比 0.2~1.0 の Cu^{2+}イオンが存在する条件下において、直線的に減少していることから、PrP 由来ペプチドと金属との相互作用は可視化できると考察される。

この挙動解析は、PrP・オクタリピート領域由来ペプチドの自家蛍光が、低濃度銅イオンの存在に対して高い感受性をもつことを示している。よって、低濃度銅イオンに対して最も強い感受性を示すペプチドは、PHGGGWGQ であることが考察される。

上記より、本研究で用いたオクタリピートペプチドにおいて、Tb 由来蛍光の消光能が最も高いのは GGGWGQPH、銅感受性が最も高いのは PHGGGWGQ であることが判明した。以上より、ヒト PrP・オクタリピート領域由来ペプチドには、異なる金属に対応する異なるモチーフが重複し、存在すると考察される。

CHAPTER 4 Fluorescent monitoring of copper-occupancy in His-ended catalytic oligo peptides

Gfp-GGGGGH(Gfp-G5H)、Gfp ともに、励起波長 230,280 nm、蛍光波長 320 nm の２ヶ所で自家蛍光のピークが得られることが判明した。また、Gfp-G5H,TYG-G5H,SYG-G5H への銅添加実験において、銅の添加前後で比較した結果、全てのペプチドの自家蛍光は銅添加後に消光していることが確認された。

さらに、銅濃度が上昇するにつれて蛍光強度が減少していくことから、銅添加による消光には銅濃度依存性があることが判明した。

化学発光法を用いた実験結果(Fig.4-5)より、実験に用いた全てのペプチドに H_2O_2 を添加した場合、各自家蛍光強度の増加が確認された。また、銅を添加した場合、蛍光強度の減少が確認された。以上より、これらのペプチド由来の自家蛍光強度は金属と結合すると消光して減少し、酸化剤と反応すると増加すると考察される。

CHAPTER 5 Monitoring of copper loading to cationic histidine-rich short salivary polypeptides, histatins 5 and 8, based on the quenching of copper-sensitive intrinsic red fluorescence

Tb への Hist-5,8 添加実験の結果(Fig.5-2)より、Hist-5,8 はともに Tb 由来自家蛍光を消光していることから、これらのペプチドは Tb 結合能をもつことが判明した。

Fig.5-3,4 より、Hist-5,8 は、励起波長 230, 275 nm、蛍光波長 610 nm の２ヶ所で自家蛍光のピークが得られることが判明した。また、両者とも濃度が高くなるにつれて自家蛍光強度が高くなっていることから、Hist-5,8 由来自家蛍光強度は濃度依存性を持つことが判明した。

Fig.5-3,5 より、Hist-5,8 の自家蛍光強度を銅の添加前後で比較した結果、両者ともに銅添加後に消光していることが確認された。これより、Hist-5,8 は銅結合能をもつことが判明した。さらに、銅濃度が上昇するにつれて、Hist-5,8 由来の自家蛍光強度が減少していくことから、銅添加による両者由来蛍光の消光には銅濃度依存性があることが判明した。

Fig.5-6 より、化学発光法を用いた実験において、PrP + 銅の条件下でスーパーオキシドの生成が確認されていること、PrP 内にはチロシン(Y)残基を含むこ

とから、H-E-X-X-H もしくは X-X-H モチーフをもつペプチドで、Y 残基をもつ場合、基質のフェノール類なしで、ペルオキシターゼ様スーパーオキシド生成活性を示すと考察される。

CHAPTER 6 Fluorometric quantification of ferulic acid concentrations based on deconvolution of intrinsic fluorescence spectra

実際にイネ葉を利用した蛍光分析による FA 濃度の検出結果は以下の通りである。まず、FA 濃度依存性の 323 nm 光の吸収が検出された。次に、FA 濃度が高くなるにつれて得られる蛍光のピーク数は減少することから、FA 濃度は分光法・蛍光分析法を用いて、非破壊的に定量することが可能であることが判明した。さらに、累積相対蛍光強度比の重心 f (x) = 0.5 を求めることにより、広範囲の FA 濃度の定量が可能であることが判明した。これにより、紫外領域を励起光とした蛍光スペクトルの重心点である f(x) = 0.5 に対応する励起波長が、FA 濃度に依存し増大することを利用し、広範囲の FA 濃度の定量が可能であることが判明した。

今回提案した蛍光スペクトル分析手法が、生組織からの蛍光検出にも適用可能であれば、新規の非破壊的 FA 定量法の確立に道を拓くことができるということが考察されており、今後の更なる実証試験が期待されている。

Fig.7-1,7-2 は実際にイネ葉を用いた実証実験の模式図である。また、得られた実験結果より、Fig.6-5 (B)中の式を利用して FA 濃度を算出し、Table.7-1 の結果を得た。

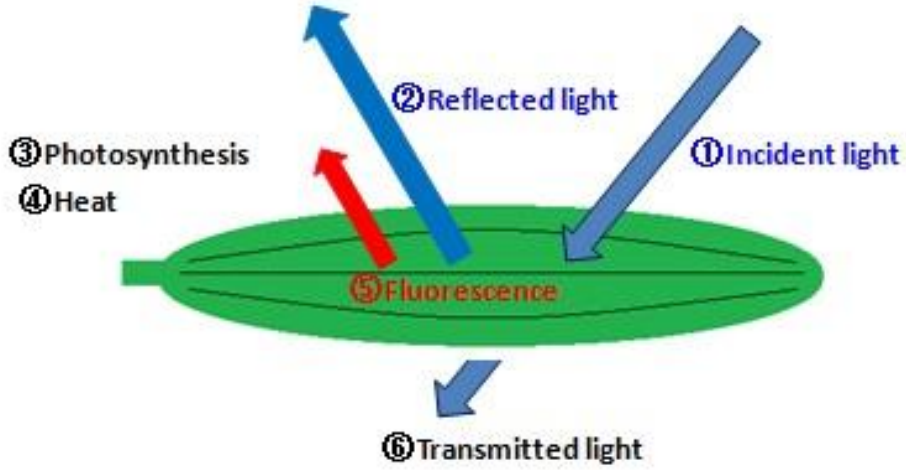

Fig.7-1. イネ葉への光照射図(Light irradiation of the rice leaf.)

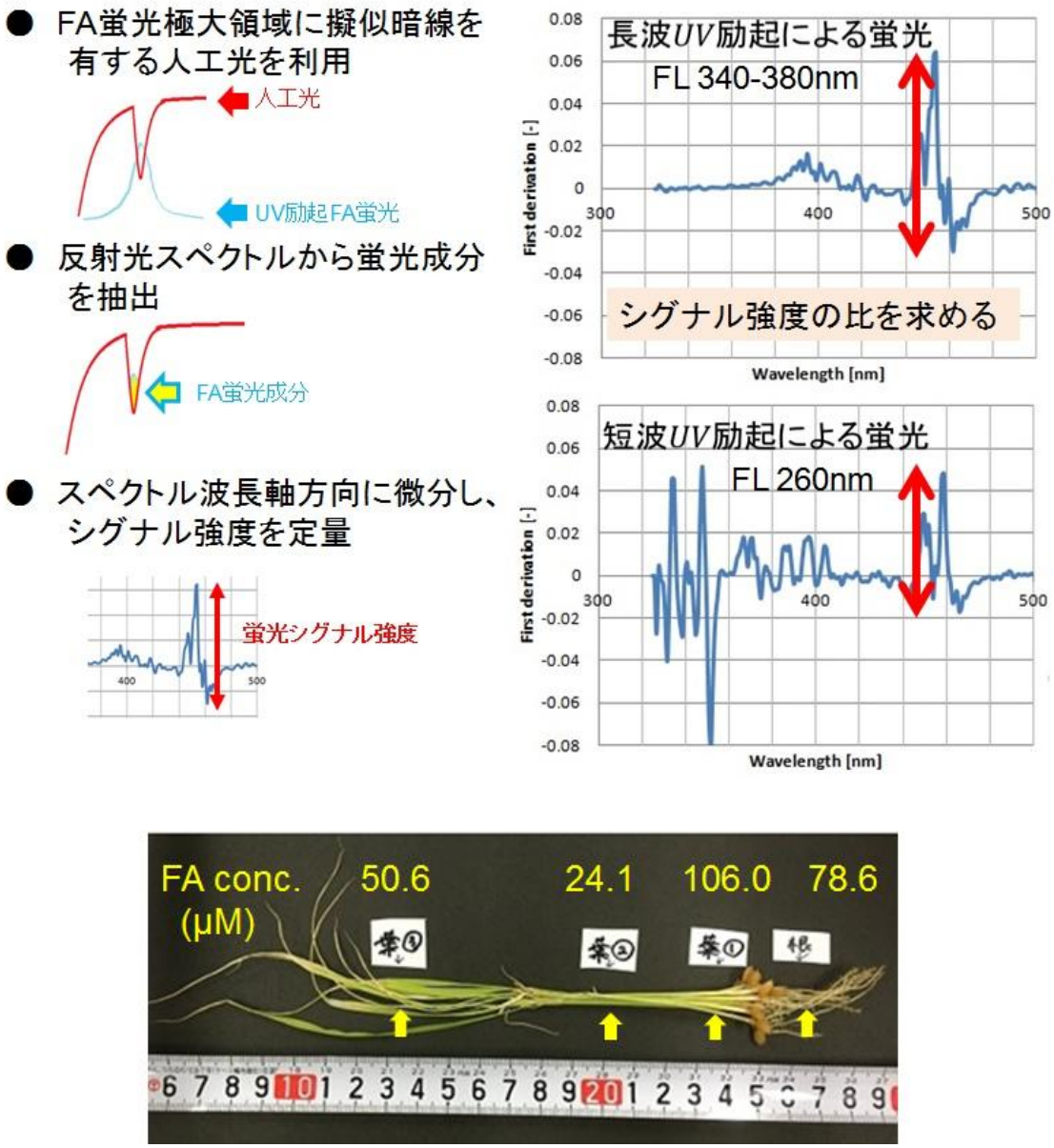

Fig.7-2. イネを用いた FA 実証実験

Table.7-1. Fig.6-5 (B)中の式を用いての FA 濃度算出

	$Log_{10}(FL_{350-380nm}/FL_{260nm})$	FA Conc. [Log_{10}mM]	FA Conc.[μM]
根	0.1021	−1.1048	78.6
葉①	0.1868	−0.9754	106.0
葉②	−0.1873	−1.6180	24.1
葉③	−0.0141	−1.2962	50.6

以上より、植物体に存在する FA 濃度は、光照射時に発生する一定波長の蛍光の強度を測定することにより、算出可能であることが示された。

Acknowledgement

本研究を進めるにあたり、河野研究室に配属されてから 6 年間、未熟者の私を叱咤激励し、成長させてくださった担当指導教官の河野智謙教授、また、蛍光分析機の基本操作や原理等を教えていただいただけでなく、参考資料として多くの論文を使用させていただいた陽川憲先輩、そして、実験時だけでなく、学校行事などにおいても互いに協力し、支えあった河野研究室の皆様に感謝します。

特に、本論文を作成するにあたり、指導教官の河野智謙教授からは、とても丁寧かつ熱心なご指導を賜りました。ここに感謝の意を表します。大学院生活も早３年と過ぎた頃、将来の不安と目標の消失から自己を見失ってしまい、大学へと向かう足が重く感じたとき、背中を押してくださり、ようやく一歩前に進むことができたことにはいくら感謝してもしきれないほどです。

この研究を博士論文として形にすることができたのは、担当していただいた河野智謙教授の熱心なご指導や、陽川憲先輩の蛍光分析機の基本操作や原理の教え、共に勉学に励んだ河野研究室の皆様の支えがあったおかげです。協力していただいた皆様へ心から感謝の気持ちと御礼を申し上げたく、謝辞にかえさせていただきます。本当に有難う御座いました

References

Adams, S.R., Harootunian, A.T., Buechler, Y.J., Taylor, S.S. and Tsien, R.Y. (1991) Fluorescence ratio imaging of cyclic AMP in single cells. Nature **349:** 694-697.

Allsop, D., Mayes, J., Moore, S., Masad, A., and Tabner, B. J. (2008) Metal-dependent generation of reactive oxygen species from amyloid proteins implicated in neurodegenerative disease. Biochem. Soc. Trans. **36:** 1293-2198.

Aronoff-Spencer, E., Burns, C. S., Avdievich, N. I., Gerfen, G. J., Peisach, J., Antholine, W. E., Ball, H. L., Cohen, F. E., Prusiner, S. B. and Millhauser, G. L. (2000) Identification of the Cu^{2+} binding sites in the N-terminal domain of the prion protein by EPR and CD spectroscopy. Biochem. **39:** 13760-13771.

Aruoma, O. I., Halliwell, B., Gajewski, E., and Dizdaroglu, M. (1991) Copper-ion-dependent damage to the bases in DNA in the presence of hydrogen peroxide. Biochem. J. **273:** 601-604.

Azen, E.A. (1972) Genetic polymorphism of basic proteins from parotid saliva. Science **176:** 673-674.

Ban C, Ramakrishnan B, Sundaralingam M. 1996. Crystal structure of the self-complementary 5'-purine start decamer d(GCGCGCGCGC) in the Z-DNA conformation. I. Biophysical Journal **71:** 1215-1221.

Baum, B.J., Bird, J.L., and Millar, D.B. and Longton, R.W. (1976) Studies on histidine-rich polypeptides from human parotid saliva. Arch. Biochem. Biophys. **177:** 427-436.

Beejmohun, V. and Fliniaux, O. (2007) Microwave-assisted extraction of the main phenolic compounds in flaxseed. Phytochem. Anal. **18:** 275–285.

Bellon, A., Seyfert-Brandt, W., Lang, W., Baron, H., Groner, A. and Vey, M. (2003) Improved conformation-dependent immunoassay: suitability for human prion detection with enhanced sensitivity. J. Gen. Virol. **84:** 1921-1925

Belosi, B., Gaggelli, E., Guerrini, R., Kozłowski, H., Łuczkowski, M., Mancini, F. M., Remelli, M., Valensin, D. and Valensin, G. (2004) Copper binding to the neurotoxic peptide PrP106-126: thermodynamic and structural studies. Chembiochem. **5:** 349-359.

Bian, Y.-Y., Guo, J., Majeed, H., Zhu, K.-X., Guo, X.-N., Peng, W. and Zhou, H.-M. (2015) Ferulic acid renders protection to HEK293 cells against oxidative damage and apoptosis induced by hydrogen peroxide. In Vitro Cell. Dev. Biol. Anim. **51:** 722-729.

Blandl, T., Zajicek, J., Prorok, M. and Castellino, F.J. (1997) Metal-ion binding properties of synthetic conantokin-G. Biochem. J. **328:** 777-783..

Boal, A.K., Cotruvo, J.A. Jr, Stubbe, J. and Rosenzweig, A.C. (2010) Structural basis for activation of class Ib ribonucleotide reductase. Science **329:** 1526-1530.

Bogdan, C., Röllinghoff, M. and Diefenbach, A. (2000) Reactive oxygen and reactive nitrogen intermediates in innate and specific immunity. Curr. Opin. Immunol. **12:** 64-76.

Bona E, Marsano F, Cavaletto M, Berta G. 2007. Proteomic characterization of copper stress response in *Cannabis sativa* roots. Proteomics **7:** 1121–1130.

Bonilla, C.A. (1969) Rapid isolation of basic proteins and polypeptides from salivary gland secretions by chromatography on polyacrylamide gel. Anal. Biochem. **32:** 522-529.

Bonomo, R. P., Imperllizzeri, G., Pappalardo, G., Rizzarelli, E. and Tabbi, G. (2000) Copper(II) binding modes in the prion octapeptide PHGGGWGQ: a spectroscopic and voltammetric study. Chemistry **6:** 4195-4202.

Brett, C.T., Wende, G., Smith, A.C. and Waldron, K.W. (1999) Biosynthesis of cell-wall ferulate and diferulates. J. Sci. Food Agric. **79:** 421-424.

Brown, D. R., Guantieri, V., Grasso, G., Impellizzeri, G., Pappalardo, G. and Rizzarelli, E. (2004) Copper (II) complexes of peptide fragments of the prion protein.

Conformation changes induced by copper (II) and the binding motif in C-terminal protein region. J. Inorg. Biochem. **98:** 133-143.

Bunel, V., Antoine, M.-H., Nortier, J., Duez, P. and Stévigny, C. (2015) Nephroprotective effects of ferulic acid, Z-ligustilide and E-ligustilide isolated from angelica sinensis against cisplatin toxicity in vitro. Toxic. in Vitro. **29:** 458-467.

Burns, C. S., Aronoff-Spencer, E., Dunham, C. M., Lario, P., Avdievich, N. I., Antholine, W. E., Olmstead, M. M., Vrielink, A., Gerfen, G. J., Peisach, J., Scott, W. G. and Millhauser, G. L. (2002) Molecular features of the copper binding sites in the octarepeat domain of the prion protein. Biochemistry **41:** 3991-4001.

Burns, C. S., Aronoff-Spencer, E., Legname, G., Prusiner, S. B., Antholine, W. E., Gerfen, G. J., Peisach, J., and Millhauser, G. L. (2003) Copper coordination in the full-length, recombinant prion protein. Biochemistry **42:** 6794-6903.

Buschmann, C., Langsdorf, G. and Lichtenthaler, H.K. (2000) Imaging of the blue, green, and red fluorescence emission of plants: An overview (Conference Paper). Photosynthetica **38:** 483-491

Caballero, L., Whitehead, K.A., Allen, N.S., and Verran, J. (2009) Inactivation of *E.coli* on immobilized TiO_2 using fluorescent light. J. Photochem. Photobiol. A **202:** 92-98.

Castilla, J., Saa, P., and Soto, C. (2005) Detection of prions in blood. Nat. Med., **11:** 982-985.

Choi, Y.E. and Park, E. (2015) Ferulic acid in combination with PARP inhibitor sensitizes breast cancer cells as chemotherapeutic strategy. Biochem. Biophys. Res. Com. **458:** 520-524.

Cobb, M. H., and Goldsmith, E. J. (1995) How MAP kinases are regulated. J. Biol. Chem. **270:** 14843-14186.

Dai, M., Liu. J., Chen, D-E., Rao, D-E., Tang, Z-J., Ho, W-Z., and Dong, C-Y. (2012). Tumor-targeted gene therapy using Adv-AFP-HRPC/IAA prodrug system

suppresses growth of hepatoma xenografted in mice. Cancer Gene Therapy **19:** 77-83.

Dietz KJ, Baier M, Krämer U. 1999. Free radicals and reactive oxygen species as mediators of heavy metal toxicity in plants. In: Prasad MNV, Hagemeyer J, ed. *Heavy metal stress in plants*. Berlin-Heidelberg, Springer-Verlag. 73-97.

Djikanović, D., Kalauzi, A., Jeremić, M., Mićić, M. and Radotić, K. (2007) Deconvolution of fluorescence spectra: Contribution to the structural analysis of complex molecules. Colloids Surfaces B: Biointerfaces **54:** 188-192.

Drążkiewicz M, Skórzyńska-Polit E, Krupa Z. 2004. Copper-induced oxidative stress and antioxidant defence in *Arabidopsis thaliana*. Biometals **17:** 379-387.

Fang Y.Y., Claussen C.A., Lipkowitz K.B. and Long E.C. (2006) Diastereoselective DNA cleavage recognition by Ni(II)Gly-Gly-His-derived metallopeptides. J. Am. Chem. Soc. **128:** 3198-3207.

Fang Y.Y., Ray B.D., Claussen C.A., Lipkowitz K.B. and Long E.C. (2004) Ni(II).Arg-Gly-His-DNA interactions: investigation into the basis for minor-groove binding and recognition. J. Am. Chem. Soc. **126:** 5403-5412.

Farahani, N., Kelly, P.J., West, G., Ratova, M., Hill, C., Vishnyakov, V. (2011) Photocatalytic activity of reactively sputtered and directly sputtered titania coatings. Thin Solid Films **520:** 1464-1469.

Folkes, L.K. and Wardman, P. (2001). Oxidative activation of indole-3-acetic to cytotoxic species as potential new role for plant auxins in cancer therapy. Biochem. Pharmacol. **61:** 129-136.

Folkes, L.K., Greco, O., Dachs, G.U., Stratfoed, M.R.L. and Wardman. P. (2002) 5-Fluoroindole-3-acetic acid: a prodrug activated by a peroxidase with potential for use in targeted cancer therapy. Biochem. Pharmacol. **63:** 265-272.

Fujishima, A., Rao, T.N., and Tryk, D.A. (2000) Titanium dioxide photocatalysis. J. Photochem. Photobiol. **C 1:** 1-21.

Furuichi, T. and Kawano, T. (2005) Possible Application of Electron Spin Resonance to Monitoring of Prion Diseases and Hypotheses on Oxidative Action and Propagation of Copper-bound Infectious Protein. Bull. Nippon sport sci. Univ. **35 :** 71-80.

Gazarian, I.G. and Lagrimini, L.M. (1998). Anaerobic stopped-flow studies of indole-3-acetic acid oxidation by dioxygen catalyzed by horseradish peroxidase C and anionic tobacco peroxidase at neutral pH: catalase effect. Biophys. Chem. **72:** 231-237.

Geierstanger BH, Kagawa TF, Chen SL, Quigley GJ, and Ho PS. 1991. Base-specific binding of copper(II) to Z-DNA. The 1.3-Å single crystal structure of d(m^5CGUAm^5CG) in the presence of $CuCl_2$. J. Biol. Chem. **266:** 20185-20191.

Gelinas, P. and McKinnon, C. M. (2006) Effect of wheat variety, farming site, and bread-baking on total phenolics. Int. J. Food Sci. Technol. **41:** 329-332

Gonzalez A, Vera J, Castro J, Dennett G, Mellado M, Morales B, Correa JA, Moenne A. 2010. Co-occurring increases of calcium and organellar reactive oxygen species determine differential activation of antioxidant and defense enzymes in *Ulva compressa* (Chlorophyta) exposed to copper excess. Plan, Cell Environ. **33:** 1627-1640.

Goulas, Y., Moya, I. and Schmuck, G. (1990) Time-resolved spectroscopy of the blue fluorescence of spinach leaves. Photosynth. Res. **25:** 299-307.

Gozzo, F. (2003). Systemic acquired resistance in crop protection: from nature to a chemical approach. J Agric Food Chem **5:** 4487-4503.

Hara, Y., Kikuchi, A., Noriyasu, A., Furukawa, H., Takaichi, H., Inokuchi R., Bouteau, F., Chin, S., Li X., Nishihama, S., Yoshizuka, K. and Kawano, T. (2016) Extraction of oil from lice bran by batch of liquefied low temperature dimethyl ether. Solvent Extr. Res. Dev. **23:** 87-99.

Higuchi, Y. (2003) Chromosomal DNA fragmentation in apoptosis and necrosis induced by oxidative stress. Biochem. Pharmacol. **66:** 1527-1535.

Holbrook, I.B. and Molan, P.C. (1975) The identification of a peptide in human parotid saliva particularly active in enhancing the glycolytic activity of the salivary microorganisms. Biochem. J. **149:** 489-492.

Huq, N.L., Cross, K.J., Ung, M., Myroforidis, H., Veith, P.D., Chen, D., Stanton, D., He, H., Ward, B.R. and Reynolds. E.C. (2007) A review of the salivary proteome and peptidome and saliva-derived peptide therapeutics. Int. J. Peptide Res. Therap. **13:** 547-564.

Hura, T., Hura, K. and Grzesiak, M. (2010) Early stage de-etiolation increases the ferulic acid content in winter triticale seedlings under full sunlight conditions. J. Photochem. Photobiol. B: Biol. **101:** 297-285.

Inokuchi, R., Yokawa, K., Okobira, T., Uezu, K. and Kawano, T. (2012) Fluorescence measurements revealed two distinct modes of metal binding by histidine-containing motifs in prion-derived peptides. Curr. Topics Peptide Protein Res. **13:** 111-118.

Ishizawa, H., Saito, Y., Amemiya, T. and Komatsu, K. (2002) Non-destructive monitoring of agricultural products (lettuce) based on laser-induced fluorescence. J. Japan. Soc. Agric. Machin. **64:** 89-94.

Iwase, J., Furukawa, H., Hiramatsu, T., Bouteau, F., Mancuso, S., Tanaka, K., Okazaki, T. and Kawano, T. (2014) Protection of tobacco cells from oxidative copper toxicity by catalytically active metal-binding DNA oligomers. J. Exper. Bot. **65:** 1391-1402

Jarvo, E. R., and Miller, S. J. (2002) Amino acids and peptides as asymmetric organocatalysts. Tetrahedron, **58:** 2481.

Jeffray, M., McGovern, G., Goodsir, C. M., Brown, K. L. and Bruce, M. E. (2000) Sites of prion protein accumulation in scrapie-infected mouse spleen revealed by immuno-electron microscopy. J. Pathol. **191:** 323-332.

Jiang, D., Zhang, S., and Zhao, H. (2007) Photocatalytic degradation characteristics of different organic compounds at TiO_2 nanoporous film electrodes with mixed anatase/rutile phases. Environ. Sci. Technol. **41:** 303-308.

Johnson, G.A., Mantha, S.V. and Day, T.A. (2000) A spectrofluorometric survey of UV-induced blue-green fluorescence in foliage of 35 species. J. Plant Physiol. **156:** 242-252

Kagenishi, T., Yokawa, K., Kadono, T., Uezu, K. and Kawano, T. (2011) Copper-binding peptides from human prion protein and newly designed peroxidative biocatalysts. Z. Naturforsch. **66c:** 182-190.

Kagenishi, T., Yokawa, K., Kuse, M., Isobe, M., Bouteau, F. and Kawano, T. (2009) Prevention of copper-induced calcium influx and cell death by prion-derived peptide in suspension-cultured tobacco cells. Z. Naturforsch. **64c:** 411-417.

Kagenishi, T., Yokawa, K., Lin, C., Tanaka, K., Tanaka, L. and Kawano, T. (2008) Chemiluminescent and bioluminescent analysis of plant cell responses to reactive oxygen species produced by newly developed water conditioning apparatus equipped with titania-coated photocatalystic fibers. In: Bioluminescence and Chemiluminescence, 2008 (Eds, Kricka, L.J., Stanley, P.E.), World Scientific Publishing Co. Pte. Ltd., Singapore. 27-30.

Kawano, T. (2003a). Roles of the reactive oxygen species-generating peroxidase reactions in plant defense and growth induction. Plant Cell Reports **21:** 829-837.

Kawano, T. (2003b). Possible use of indole-3-acetic acid and its antagonist tryptophan betaine in controlled killing of horseradish peroxidase-labeled human cells. Med. Hypotheses **60:** 664-666.

Kawano, T. (2006) Quenching and enhancement of terbium fluorescence in the presence of prion-derived copper-binding peptides. ITE Lett. **7:** 383-385.

Kawano, T. (2007) Prion-derived copper-binding peptide fragments catalyze the generation of superoxide anion in the presence of aromatic monoamines. Int. J. Biol. Sci. **3:** 57-63.

Kawano, T. (2011) Learning from prion-derived peptides for designing novel phosphorylation-sensitive peptide probes. Med. Hypotheses **77:** 159-161.

Kawano, T. and Bouteau, F. (2013) Crosstalk between intracellular and extracellular salicylic acid signaling events leading to long-distance spread of signals. Plant Cell Reports **32:** 1125-1138.

Kawano, T. and Muto, S. (2000) Mechanism of peroxidase actions for salicylic acid-induced generation of active oxygen species and an increase in cytosolic calcium in tobacco suspension culture. J. Exper. Bot. **51:** 685-693.

Kawano, T., Adachi, M., Kurata, H., Azuma, R. and Shimokawa, K. (1999) Calcium-dependent catabolism of pheophorbide a in tomato fruit. J. Japan. Soc. Hort. Sci. **68:** 810-816.

Kawano, T., Furuichi, T. and Muto, S. (2004) Controlled salicylic acid levels and corresponding signaling mechanisms in plants. Plant Biotechnol. **21:** 319-335.

Kawano, T., Hiramatsu, T., Yokawan, K., Tanaka, L. and Tanaka, K. (2008) Responses of living plants to increasing UV and ozone. Can we protect the crops and flora from environmental stresses through bioengineering approaches? Proceedings of 3rd Japan–Taiwan Joint International Symposium on Environmental Science and Technology 2008. 116-122.

Kawano, T., Kagenishi, T., Kadono, T., Bouteau, F., Hiramatsu, T., Lin, C., Tanaka, K., Tanaka, L., Mancuso, S., Uezu, K., Okobira, T., Furukawa, H., Iwase, J., Inokuchi, R., Baluška, F. and Yokawa, K. (2015) Production and removal of superoxide anion radical by artificial metalloenzymes and redox-active metals. Commun. Integr. Biol. **8:** e1000710.

Kawano, T., Kagenishi, T., Kadono, T., Bouteau, F., Hiramatsu, T., Lin, C., Tanaka, K., Tanaka, L., Mancuso, S., Uezu, K., Okobira, T., Furukawa, H., Iwase, J., Baluška, F., and Yokawa, K. (2015) Production and removal of superoxide anion radical by artificial metalloenzymes and redox-active metals. Commun. Integr. Biol. (in press).

Kawano, T., Kawano, N., and Lapeyrie, F. (2002) A fungal auxin antagonist, hypaphorine prevents the indole-3-acetic aciddependent irreversible inactivation of

horseradish peroxidase: inhibition of Compound III-mediated formation of P-670. Biochem. Biophys. Res. Commun. **294:** 553-559.

Kawano, T., Kawano, N., Hosoya, H., and Lapeyrie, F. (2001) Fungal auxin antagonist hypaphorine competitively inhibits indole-3-acetic acid-dependent superoxide generation by horseradish peroxidase. Biochem. Biophys. Res. Commun. **288:** 546-551.

Kawano, T., Pinontoan, R., Uozumi, N., Miyake, C., Asada K., Kolattukudy, P.E., and Muto, S. (2000a) Aromatic monoamine-induced immediate oxidative burst leading to an increase in cytosolic Ca^{2+} concentration in tobacco suspension culture. Plant Cell Physiol. **41:** 1251-1258.

Kawano, T., Pinontoan, R., Uozumi, N., Morimitsu, Y., Miyake, C., Asada, K., and Muto, S. (2000b) Phenylethylamine-induced generation of reactive oxygen species and ascorbate free radicals in tobacco suspension culture: mechanism for oxidative burst mediating Ca^{2+} influx. Plant Cell Physiol. **41:** 1259-1266.

Kawano, T., Sahashi, N., Takahashi, K., Uozumi, N. and Muto, S. (1998) Salicylic acid induces extracellular superoxide generation followed by an increase in cytosolic calcium ion in tobacco suspension culture: The earliest events in salicylic acid signal transduction. Plant Cell Physiol. **39:** 721-730.

Kawano, T., Tanaka, S., Kadono, T. and Muto, S. (2004) Salicylic acid glucoside acts as a slow inducer of oxidative burst in tobacco suspension culture. Z. Naturforsch. **59c:** 684-692.

Kimura, M., Umemoto, Y. and Kawano, T. (2014) Hydrogen peroxide-independent generation of superoxide by plant peroxidase: Hypotheses and supportive data employing ferrous ion as a model stimulus. Front. Plant Sci. **5:** article 285

Kitamoto, T. 2005, Food and Drug Safety. Springer-Verlag, Tokyo, **1**.

Koga, S., Nakano, M., and Tero-Kubota, S. (1992) Generation of superoxide during the enzymatic action of tyrosinase. Arc. Biochem. Biophys**. 292:** 570-575.

Kumar, M., Kumar, S., and Kaur, S. (2012) Role of ROS and COX-2/iNOS inhibition in cancer chemoprevention: a review. Phytochem. Rev. **11:** 309-337.

Kunihiro S, Hiramatsu T, Kawano T. 2011. Involvement of salicylic acid signal transduction in aluminum-responsive oxidative burst in *Arabidopsis thaliana* cell suspension culture. Plant Signal. Behav. **6:** 611-616.

Kunitake, T., Shumada, F., Aso, C. (1969) Imidazole catalyses in aqueous systems. I. The enzyme-like catalysis in the hydrolysis of phenyl ester by imidazole-containing copolymers. J. Amer. Chem. Soc. **91:** 2716-2723.

Laroussi, M. and Leipold, F. (2004) Evaluation of the roles of reactive species, heat, and UV radiation in the inactivation of bacterial cells by air plasmas at atmospheric pressure. Int. J. Mass Spectrom. **233:** 81-86.

Li, W., Wu, S., Ahmad, M., Jiang, J., Liu, H., Nagayama, T., Rose, M.E., Tyurin, V.A., Tyurina, Y.Y., Borisenko, G.G., Belikova, N., Chen, J., Kagan, V.E. and Graham, S.H. (2010) The cyclooxygenase site, but not the peroxidase site of cyclooxygenase-2 is required for neurotoxicity in hypoxic and ischemic injury. J. Neurochem. **113:** 965-977.

Li, X.S., Reddy, M.S., Baev, D. and Edgerton, M. (2003) Candida albicans Ssa1/2p is the cell envelope binding protein for human salivary histatin 5. J. Biol. Chem. **278:** 28553–28561.

Liakopoulos, G., Stavrianakou, S. and Karabourniotis, G. (2001) Analysis of epicuticular phenolics of prunus persica and Olea europaea leaves: Evidence for the chemical origin of the UV-induced blue fluorescence of stomata (Article). Ann. Bot. **87:** 641-648.

Lichtenthaler, H.K. and Schweiger, J. (1998) Cell wall bound ferulic acid, the major substance of the blue-green fluorescence emission of plants. J. Plant Physiol. **152:** 272-282

Lin C, Kadono T, Suzuki T, Yoshizuka K, Furuichi T, Yokawa K, Kawano T. 2006. Mechanism for temperature-shift-responsive acute Ca^{2+} uptake in suspension-cultured tobacco and rice cells. Cryobiology and Cryotechnology **52:** 83-89.

Lin, C., Tanaka, K., Tanaka, L. and Kawano, T. (2008) Chemiluminescent and electron spin resonance spectroscopic measurements of reactive oxygen species generated in water treated with titania-coated photocatalytic fibers. In: Bioluminescence and Chemiluminescence, 2008 (Eds, Kricka, L.J., Stanley, P.E.), World Scientific Publishing Co. Pte. Ltd., Singapore. 225-228.

Lu, Y., Yeung, N., Sieracki, N., and Marshall, N. M. (2009) Design of functional metalloproteins. Nature **460:** 855-862.

Luo, Y., Henle, E. S., and Linn, S. (1996) Oxidative Damage to DNA Constituents by iron-mediated Fenton reactions: The Deoxycytidine family. J. Biol. Chem. **271:** 21167-21176.

MacKay, B.J., Denpitiya, L., Iocono, V.J., Krost, S.P. and Pollock, J.J. (1984) Growth-inhibitory and bactericidal effects of human parotid salivary histidine-rich polypeptides on Streptococcus mutans. Infect. Immun. **44:** 695-701.

Melino, S., Rufini, S., Sette, M., Morero, R., Grottesi, A., Paci, M. and Petruzzelli, R. (1999) Zn^{2+} ions selectively induce antimicrobial salivary peptide histatin-5 to fuse negatively charged vesicles. Identification and characterization of a zinc-binding motif present in the functional domain. Biochemistry **38:** 9626-9633.

Melino, S., Santone, C., Di Nardo, P. and Sarkar, B. (2014) Histatins: salivary peptides with copper (II)- and zinc (II)-binding motifs. Perspectives for biomedical applications. FEBS J. **281:** 657-672.

Meyer, S., Cartelat, A., Moya, I. and Cerovic, Z.G. (2003) UV-induced blue-green and far-red fluorescence along wheat leaves: A potential signature of leaf ageing. J. Exper. Bot. **54:** 757-769.

Miao, L., Tanemura, S., Kondo, Y., Iwata, M., Toh, S., and Kaneko, K. (2004) Microstructure and bactericidal ability of photocatalytic TiO_2 thin films prepared by rf helicon magnetron sputtering. Appl. Surf. Sci. **238:** 125-131.

Morales, F., Cerovic, Z.G. and Moya, I. (1998) Time-resolved blue-green fluorescence of sugar beet leaves. Temperature-induced changes and consequences for the

potential use of blue-green fluorescence as a signature for remote sensing of plants. Aust. J. Plant Physiol. **25:** 325-334.

Morales, F., Cerovic, Z.G., and Moya, I. (1996) Time-resolved blue-green fluorescence of sugar beet (Beta vulgaris L.) leaves. Spectroscopic evidence for the presence of ferulic acid as the main fluorophore of the epidermis. Biochim. Biophys. Acta – Bioenerg. **1273:** 251-262.

Morante, S., Gonzalez-Iglesias, R., Potrich, C., Meneghini, C., Meyer-Klaucke, W., Menestrina, G. and Gasset, M. (2004) Inter- and intra-octarepeat Cu(II) site geometries in the prion protein: implications in Cu(II) binding cooperativity and Cu(II)-mediated assemblies. J. Biol. Chem. **279:** 11753-11739.

Mülek, M. and Högger, P. (2015) Highly sensitive analysis of polyphenols and their metabolites in human blood cells using dispersive SPE extraction and LC-MS/MS. Ana. Bional. Chem. **407:** 1885-1899.

Murakami, Y., Tamagawa, H., Shizukuishi, S., Tsunemitsu, A. and Aimoto, S. (1992) Biological role of an arginine residue present in a histidine-rich peptide which inhibits hemagglutination of Porphyromonas gingivalis. FEMS Microbiol. Lett. **98:** 201-204.

Nagasawa K. (2003) Total synthesis of marine cyclic guanidine compounds and development of novel guanidine type asymmetric organocatalysts. Yakugaku Zasshi **123:** 387-398.

Nakano, M., Sugioka, K., Ushijima, Y., and Goto, T. (1986) Chemiluminescence probe with *Cypridina* luciferin analog, 2-methyl-6-phenyl-3,7-dihydroimidazo[1,2-a]pyrazin-3-one, for estimating the ability of human granulocytes to generate O_2^-. Anal. Biochem.**159:** 363-369.

Okobira, T., Kadono, T., Kagenishi, T., Yokawa, T., Kawano, T. and Uezu, K. (2011) Copper-binding peptide fragment-containing membrane as a biocatalyst by radiation-induced graft polymerization. Sens. Mater. **23:** 207-218.

Opazo, C., Inés-Barría, M., Ruiz, F. H. and Inestrosa, N. C. (2003) Copper reduction by copper binding proteins and its relation to neurodegenerative diseases. Biometals. **16:** 91-98.

Panneton, B., Guillaume, S., Roger, J.-M. and Samson, G. (2010) Improved discrimination between monocotyledonous and dicotyledonous plants for weed control based on the blue-green region of ultraviolet-induced fluorescence spectra. Appl. Spectrosc. **64:** 30-36.

Pardieck, D.L., Bouwer, E.J., Stone, A.T. (1992) Hydrogen Peroxide Use to Increase Oxidant Capacity for In Situ Bioremediation of Contaminated Soils and Aquifers: A Review. J. Contam. Hydrol. **9:** 221-242.

Park, Y.-S., Cvikrová, M., Martincová, O., Ham, K.-S., Kang, S.-G., Park, Y.-K., Namiesnik, J., Rombolà, A.D., Jastrzebski, Z. and Gorinstein, S. (2015) In vitro antioxidative and binding properties of phenolics in traditional, citrus and exotic fruits. Food Res. Int. **74:** 37-47.

Passardi, F., Cosio, C., Penel, C., and Dunand, C. (2005) Peroxidases have more functions than a Swiss army knife. Plant Cell Reports **24:** 255-265.

Paul D. Ray, Bo-Wen Huang, Yoshiaki Tsuji. (2012) Reactive oxygen species (ROS) homeostasis and redox regulation in cellular signaling. Cell. Signal. **24:** 981-990.

Pauri, S. and Edgerton, M. (2014) How does it kill?: Understanding the candidacidal mechanism of salivary histatin 5. Eukaryot Cell. **13:** 958-964.

Puri, S., Li, R., Ruszaj, D., Tati, S. and Edgerton, E. (2015) Iron Binding Modulates Candidacidal Properties of Salivary Histatin 5. J. Dent. Res. **94:** 201-208.

Pussayanawin, V., Wetzel, D.L. and Fulcher, R.G. (1988) Fluorescence detection and measurement of ferulic acid in wheat milling fractions by microscopy and HPLC. J. Agric. Food Chem. **36:** 519-520.

Ralph Zahn, Aizhuo Liu, Thorsten Luhrs, Roland Riek, Christine von Schroetter, Francisco Lopez Garcia, Martin Billeter, Luigi Calzolai, Gerhard Wider, and Kurt Wuthrich. (2000) NMR solution structure of the human prion protein. Proc Natl Acad Sci U S A. **97:** 145-150.

Rosati, F., and Roelfes, G. (2010) Artificial Metalloenzymes. ChemCatChem **2:** 916-927.

Rossi, L., Lombardo, M. F., Ciriolo, M. R. and Rotilio, G. (2004) Mitochondrial dysfunction in neurodegenerative diseases associated with copper imbalance. Neurochem. Res. **29:** 493-504.

Rotilio, G., Carr, M. T., Rossi. L. and Ciriolo, M. R. (2000) Copper-dependent oxidativestress and neurodegeneration. IUBMB Life **50:** 309-314

Saadi, A., Lempereur, I., Sharonov, S., Autran, J.C. and Manfait, M. (1998) Spatial distribution of phenolic materials in durum wheat grain as probed by confocal fluorescence spectral imaging. J. Cereal Sci. **28:** 107-114.

Safar, J. G., Geschwind, M. D., Deering, C., Didorenko, S., Sattavat, M., Sanchez, H., Serban, A., Vey, M., Baron, H., Giles, K., Miller, B. L., Dearmond, S. J. and Prusiner, S. B. (2005) Diagnosis of human prion disease. Proc. Natl. Acad. Sci. USA **102:** 3501-3506

Sakai, S., Kawamata, H., Kogure, T., Mantani, N., Terasawa, K., Umatake, M. and Ochiai, H. (1999) Inhibitory effect of ferulic acid and isoferulic acid on the production of macrophage inflammatory protein-2 in response to respiratory syncytial virus infection in RAW264.7 cells. Mediators of Inflammation **8:** 173-175.

Sakai, Y., Fukase, T., Yasui, H. and Shibata, M. (1997) An activated sludge process without excess sludge production. Water Sci. Technol. **36:** 163-170.

Sankararamakrishnan, R., Verma, S. and Kumar, S. (2005) ATCUN-like metal-binding motifs in proteins: identification and characterization by crystal structure and sequence analysis. Proteins **58:** 211-221.

Sauer, H., Dagdanova, A., Hescheler, J., and Wartenberg, M. (1999) Redox-regulation of intrinsic prion expression in multicellular prostate tumor spheroids. Free Radic Biol Med. **27:** 1276-1283.

Saulnier, L. and Thibault, J. F. (1999) Ferulic acid and diferulic acids as components of sugar-beet pectins and maize bran heteroxylans". J. Sci. Food Agric. **79:** 396-402

Savitsky, P.A., Gazaryan, I.G., Tishkov, V.I., Lagrimini, L.M., RuzGas, T., Gorton, L. (1999). Oxidation of indole-3-acetic acid by dioxygen catalyzed by plant peroxidases: specificity for the enzyme structure. Biochem J **340:** 579-583.

Sergiel, I. , Pohl, P., Biesaga, M. and Mironczyk, A. (2014) Suitability of three-dimensional synchronous fluorescence spectroscopy for fingerprint analysis of honey samples with reference to their phenolic profiles. Food Chem. **145:** 319-326.

Sgarbossa, A. and Lenci, F. (2013) A study for the cause of ferulic acid-induced quenching of tyrosine fluorescence and whether it is a reliable marker of intermolecular interactions or not. J. Fluorescence **23:** 561-567.

Shinkai, S. and Kunitake, T. (1975) Imidazole catalyses in aqueous systems. X. Enzyme-like catalytic hydrolyses of phenyl esters by polymers containing imidazole and other anionic functions. Polymer J. **7:** 387-396.

Shiraishi, N., Ohta, Y. and Nishikimi, M. (2000) The octapeptide repeat region of prion protein binds Cu(II) in the redox-inactive state. Biochem. Biophys. Res. Commun. **267:** 398-402.

Stanczak, P., Luczkowski, M., Juszczyk, P., Grzonka, Z. and Kozlowski, H. (2004) Interactions of Cu^{2+} ions with chicken prion tandem repeats. Dalton Trans. **14:** 2102-2107.

Stülke, J. (2010) More than just activity control: phosphorylation may control all aspects of a protein's properties. Mol. Microbiol. **77:** 273-275.

Tabner, B. J., Turnbull, S., El-Agnaf, O., and Allsop, D. (2001) Production of reactive oxygen species from aggregating proteins implicated in Alzheimer's disease, Parkinson's disease and other neurodegenerative diseases. Curr. Top. Med. Chem. **1:** 507-517.

Tajmir-Riahi, H.A., Langlais, M., and Savoie, R. (1988) A laser Raman spectroscopic study of the interaction of calf-thymus DNA with Cu(II) and Pb(II) ions: metal ion binding and DNA conformational changes. Nucleic Acids Res. **16:** 751-762.

Takayama, A., Kadono, T., and Kawano, T. (2012) Heme redox cycling in soybean peroxidase: hypothetical model and supportive data. Sensors and Materials **24:** 87-97.

Tanaka, H., Saito, Y., Kanayama, T., Kobayashi, F. and Kobayashi, K. (2009) Imaging system of solar-induced plant fluorescence for monitoring of plant living status. Geoscience and Remote Sensing Symposium, 2009 IEEE International, IGARSS 2009, **3:** 577-580.

Tanemura, S., Miao, L., Wunderlich, W., Tanemura, M., Mori, Y., Toh, S., and Kaneko, K. (2005) Fabrication and characterization of anatase/rutile-TiO_2 thin films by magnetron sputtering: A review. Sci. Technol. Adv. Mater. **6:** 11-17.

Tay, W.M., Hanafy, A.I., Angerhofer, A. and Ming, L.J. (2009) A plausible role of salivary copper in antimicrobial activity of histatin-5-metal binding and oxidative activity of its copper complex. Bioorg. Med. Chem. Lett. **19:** 6709-6712.

Tewari RK, Kumar P, Sharma PN. 2006. Antioxidant responses to enhanced generation of superoxide anion radical and hydrogen peroxide in the copper-stressed mulberry plants. Planta **223:** 1145-1153.

Tran D, El-Maarouf-Bouteau H, Rossi M, Biligui B, Briand J, Kawano T, Mancuso S, Bouteau F. (2013b). Post-transcriptional regulation of GORK channels by superoxide anion contributes towards increases in outward rectifying K^+ currents. New Phytologist **198:** 1039-1048.

Tran, D., Kadono, T., Meimoun, P., Kawano, T., and Bouteau, F. (2010) TiO_2 nanoparticles induce ROS generation and cytosolic Ca^{2+} increases on tobacco cells: A chemiluminescence study. Luminescence **25:** 140-142.

Tsai H, Raj PA. and Bobek LA. (1996) Candidacidal activity of recombinant human salivary histatin-5 and variants. Infect. Immun. **64:** 5000-5007.

Tsai, H. (1998) Human Salivary histatins: Promising anti-fungal therapeutic agents. Crit. Rev. Oral Biol. Med. **9:** 480-497.

Tsien, R.Y., Rink, T.J. and Poenie, M. (1985) Measurement of cytosolic free Ca^{2+} in individual small cells using fluorescence microscopy with dual excitation wavelengths. Cell Calcium. **6:** 145-157.

Vassallo, N. and Herms, J. (2003) Cellular prion protein function in copper homeostasis and redox sinnalling at the synapse. J. Neurochem. **86:** 538-544.

Verhulst, P.-F. (1838) Notice sur la loi que la population poursuit dans son accroissement. Correspondance Mathématique et Physique **10:** 113-121.

Vylkova, S., Jang, W.S., Li, W., Nayyar, N. and Edgerton, M. (2007) Histatin 5 initiates osmotic stress response in Candida albicans via activation of the Hog1 mitogen-activated protein kinase pathway. Eukaryot. Cell **6:** 1876-1888.

Wang, O., Liu, J., Cheng, Q., Guo, X., Wang, Y., Zhao, L., Zhou, F. and Ji, B. (2015) Effects of ferulic acid and γ-oryzanol on high-fat and high-fructose diet-induced metabolic syndrome in rats. PLoS ONE **10:** e0118135.

Watt, N. T., Taylor, D. R., Gillott, A., Thomas, D. A., Perera, W. S., and Hooper, N. M. (2005) Reactive oxygen species-mediated beta-cleavage of the prion protein in the cellular response to oxidative stress. J. Biol. Chem. **280:** 35914-35921.

Werner, J. J., McNeill. K. and Arnold, W. A. (2005) Environmental photodegradation of mefenamic acid. Chemosphere **58:** 1339-1346.

Wong, B. S., Brown, D. R., Pan, T., Whiteman, M., Liu, T., Bu, X., Li, R., Gambetti, P., Olesik, J., Rubenstein, R., and Sy, M. S. (2001) Oxidative impairment in scrapie-infected mice is associated with brain metals perturbations and altered antioxidant activities. J. Neurochem. **79:** 689-698.

Wood, J. M., and Schallreuter, K. U. (1991) Studies on the reactions between human tyrosinase, superoxide anion, hydrogen peroxide and thiols. Biochim. Biophys. Acta **1074:** 378-385.

Yeh, C.-T. and Yen, G.-C. (2005) Effect of vegetables on human phenolsulfotransferases in relation to their antioxidant activity and total phenolics. Free Rad. Res. **39:** 893-904.

Yeung, N., Lin, Y. W., Gao, Y. G., Zhao, X., Russel, B. S., Lei, L., Miner, K. D., Robinson, H., and Lu, Y. (2009) Rational design of a structural and functional nitric oxide reductase. Nature **462:** 1079-1082.

Yokawa K, Kagenishi T, Goto K. and Kawano T. (2009a) Free tyrosine and tyrosine-rich peptide-dependent superoxide generation catalyzed by a copper-binding, threonine-rich neurotoxic peptide derived from prion protein. Int. J. Biol. Sci. **5:** 53-63.

Yokawa K, Kagenishi T. and Kawano, T. (2011a) Superoxide generation catalyzed by the ozone-inducible plant peptides analogous to prion octarepeat motif. Plant Signal. Behav. **6:** 477-482.

Yokawa, K., Kagenishi, T. and Kawano, T. (2008) Use of *Cypridina* luciferin analog for assessing the monoamine oxidase-like superoxide-generating activities of two peptide sequences corresponding to the helical copper-binding motif. In: Bioluminescence and Chemiluminescence, 2008 (Eds, Kricka, L.J., Stanley, P.E.), World Scientific Publishing Co. Pte. Ltd., Singapore. 83-86.

Yokawa, K., Kagenishi, T. and Kawano, T. (2009b) Thermo-stable and freeze-tolerant nature of aromatic monoamine-dependent superoxide-generating activity of human prion-derived Cu-binding peptides. Biosci. Biotechnol. Biochem. **73:** 1218-1220.

Yokawa, K., Kagenishi, T. and Kawano, T. (2010) *Cypridina* luciferin analog, CLA as a probe for the enzymatic reaction of superoxide generation catalyzed by copper-binding hexapeptide found in chicken prion protein. Luminescence **25:** 139.

Yokawa, K., Kagenishi, T., and Kawano, T. (2009b) Thermo-stable and freeze-tolerant nature of aromatic monoamine-dependent superoxide-generating activity of human prion-derived Cu-binding peptides. Biosci. Biotechnol. Biochem. **73:** 1218-1220.

Yokawa, K., Kagenishi, T., and Kawano, T. (2011d) Prevention of oxidative DNA degradation by copper-binding peptides. Biosci. Biotechnol. Biochem. **75:** 1377-1379.

Yokawa, K., Kagenishi, T., Furukawa, H. and Kawano, T. (2011b) Comparing the superoxide-generating activities of plant peroxidase and the action of prion-derived metallopeptides: towards the development of artificial redox enzymes. Curr. Topics Peptide Protein Res. **12:** 35-50.

Yokawa, K., Kagenishi, T., Kawano, T., Mancuso, S., and Baluška, F. (2011c) Illumination of *Arabidopsis* roots induces immediate burst of ROS production. Plant Signal. Behav. **6:** 1457-1461.

Yoshida, M. Kimura, T., Kitaichi, K., Suzuki, R., Baba, K., Matsushima, M., Tatsumi, Y., Shibata, E., Takagi, K., Hasegawa, T. and Takagi, K. (2001) Induction of histamine release from rat peritoneal mast cells by histatins. Biol. Pharm. Bull. **24:** 1267-1270 .

Yoshioka, H., Bouteau, F. and Kawano, T. (2008) Discovery of oxidative burst in the field of plant immunity: looking back at the early pioneering works and towards the future development. Plant Signal. Behav. **3:** 153-155.